Dissertation for the Degree of Master of Science in Bioengineering
Major in Molecular Biotechnology

Faculdade de Engenharia da Universidade do Porto
Instituto de Ciências Biomédicas Abel Salazar

THE EFFECTS OF NANOSYSTEM-DELIVERED ANTI-INFLAMMATORY AND ANTI-PROTEOLYTIC COMPOUNDS ON THE INFLAMMATORY MICROENVIRONMENT OF CARTILAGE LESIONS

Alexandra Azevedo Freitas

Supervisors: Cecília Juliana Alves, PhD
Daniela Vasconcelos, PhD

July 2021

ACKNOWLEDGMENTS

I address this work to my parents and my sister for all the caring, for always believing in me, for always being proud and celebrating my accomplishments, for encouraging me to try giving my best and to being the main reason why this was made possible.

There are no enough thanks to my supervisor Dr. Juliana Alves. I am enormously grateful to her for always being so supportive, available, full of comprehension and with unseen ability to simplify any problem.

I also I would like to thank all the members of the NeSk group, to its leader Dr. Meriem Lamghari, to my co-supervisor Dr. Daniela Vasconcelos and to Marina Couto for all the help provided over the period of this work.

I address a special thank you to all my friends and all the teachers that have contributed to my personal and academic growth over these years.

I would to acknowledge the Restore's Partners that provided the nanomaterials used in this work. Specifically, the INEB groups Nanomedicine & Translational Drug Delivery Group and Microenvironments for New therapies Group for the ibuprofen-loaded PLGA nanoparticles and ibuprofen-loaded chitosan/PGA nanoparticles, respectively, and the CIDETEC for the nanoemulsions.

This work was financially supported by the European Union's Horizon 2020 research and innovation program under the RESTORE Project, grant agreement Nº 814558.

RESUMO

O tratamento de lesões na cartilagem é um grande desafio na Medicina, essencialmente porque a cartilagem articular tem uma capacidade limitada de reparação ou cura intrínseca. Quando este tecido é danificado, ocorre um aumento dos processos catabólicos concomitantemente com a diminuição dos processos anabólicos e das tentativas de reparo, pois os condrócitos são muito sensíveis a estímulos externos e intrínsecos.

Lesões não tratadas, juntamente com o seu microambiente inflamatório associado, podem causar um aumento de tamanho do dano, e, em última instância, desenvolvimento de doenças articulares, nomeadamente a osteoartrite. Esta doença é a comorbilidade musculoesquelética mais comum e a principal causa de incapacidade em todo o mundo devido à dor causada e comprometimento da função articular. Primeiramente, os condrócitos são expostos a estímulos extracelulares anormais, induzindo a produção excessiva de citocinas pró-infamatórias e enzimas que degradam a matriz, levando à degradação progressiva de colagénio e agrecano. A libertação destes fragmentos da matriz para o fluído articular pode ativar as células sinoviais, aumentando a produção de mediadores inflamatórios, contribuindo, assim, para a perpetuação da doença.

Nos estadios mais avançados da osteoartrite, o procedimento mais comum é a substituição total da articulação do joelho, condicionando uma redução na mobilidade e qualidade de vida. Uma intervenção precoce que impeça a progressão da doença poderia evitar situações de dor incapacitante, permitindo uma vida ativa apesar dos danos detetados. Assim, propõe-se uma nova estratégia para enfrentar este obstáculo médico, cobrindo o local da lesão com um scaffold nanoativado com compostos anti-inflamatórios e anti-proteolíticos. Neste trabalho estão descritos estudos *in vitro* que são necessários para a posterior tradução desta possível solução para a prática clínica. Neste estudo, condrócitos primários humanos foram estimulados com IL-1β previamente à aplicação de nanopartículas/nanoemulsões para avaliar os efeitos terapêuticos após o tratamento. O ambiente proteolítico que ambicionou mimetizar o ambiente do local das lesões condrais nas culturas 3D dos condrócitos foi induzido pela estimulação com 100 ng/mL de IL-1β. Os efeitos condroprotetores das nanopartículas de PLGA carregas com ibuprofeno e quitosano/PGA, e nanoemulsões carregadas com BB-94 e tricombinadas após tratamento de condrócitos articulares humanos estimulados com IL-1β, foram posteriormente estudados.

Globalmente, as nanopartículas de PLGA carregadas com 15 e 30 μg/mL de ibuprofeno e nanopartícula de quitosano/PGA carregadas com 15 μg/mL de ibuprofeno parecem induzir efeitos condroprotetores, sendo benéfico para os condrócitos articulares humanos primários cultivados em pellets. Adicionalmente, o

COPLA® Scaffold aparenta ser uma estrutura promissora para a produção de matriz extracelular e, ainda, ter propriedades anti-inflamatórias intrínsecas.

ABSTRACT

The treatment of cartilage injuries is a major medical challenge essentially because articular cartilage has a limited ability for intrinsic repair or healing. When this tissue is damaged, an increase in catabolic processes occurs concomitantly with a decrease in anabolic processes and in repair attempts, as chondrocytes are very sensitive to both external and intrinsic stimuli.

Untreated lesions, along with their associated inflammatory microenvironment, may lead the damage to increase in size and ultimately leading to the development of joint diseases, namely osteoarthritis. This is the commonest musculoskeletal disease and the leading cause of disability worldwide due to pain and impaired joint function. At first, chondrocytes, which are exposed to extremely abnormal extracellular stimuli, are induced to overproduce pro-inflammatory cytokines and matrix-degrading enzymes, leading to the progressive breakdown of collagen and aggrecan. The release of these matrix fragments into the joint fluid may ultimately activate synovial cells, increasing by far the production of inflammatory mediators and thus contributing to the perpetuation of the disease.

At advanced stages of osteoarthritis, the most common procedure is to perform a total joint replacement, reducing patients' mobility and quality of life. An early intervention to halt the damage progression would avoid patients to experience disabling pain and allow them to have a normally active life as the damage was detected. Herein is proposed a novel strategy to tackle this medical obstacle, by covering the lesion site with a scaffold nanoenabled with anti-inflammatory and anti-proteolytic compounds. In this work are described the *in vitro* experiments that are needed for the further translation of this possible solution into the clinical practice.

In this study, primary human chondrocytes were stimulated with IL-1β prior to nanoparticles/nanoemulsions application to evaluate the therapeutic effect of the post-treatment. The proteolytic environment that aimed to mimic the one at the chondral lesions' site in the 3D cultures of chondrocytes was induced by the stimulation with 100 ng/mL of IL-1β. The chondroprotective effects of ibuprofen-loaded PLGA and chitosan/PGA nanoparticles, and BB-94-loaded and tricombinatory nanoemulsions post-treatment to IL-1β-stimulated hACs were studied afterwards.

Overall, PLGA nanoparticles loaded with 15 and 30 μg/mL of ibuprofen and chitosan/PGA nanoparticles loaded with 15 μg/mL of ibuprofen appear to induce beneficial chondroprotective effects to primary human articular chondrocytes cultured in pellets, and COPLA® Scaffold seem to be a promising structure to support ECM production and to possess intrinsic anti-inflammatory properties.

CONTENTS

LIST OF FIGURES

LIST OF TABLES

ACRONYMS AND ABBREVIATIONS

2D	Two-Dimensional
3D	Three-Dimensional
ACAN	Protein coding gene for Aggrecan
ACT	Autologous Chondrocyte Transplantation
ADAM	A Disintegrin And Metalloproteinase
ADAMTS	A Disintegrin And Metalloproteinase with Thrombospondin Motifs
BB-2516	Matimastat
BB-94	Batimastat
B2m	Beta2-Microglobulin
bFGF	Basic Fibroblast Growth Factor
BMAC	Bone Marrow Aspirate Concentrate
BSA	Bovine Serum Albumin
cDNA	Complementary Deoxyribonucleic Acid
COL2A1	Protein coding gene for Collagen Type II Alpha 1 Chain
COX	Cyclooxygenase
DAPI	4',6-Diamidino-2-Phenylindole
dNTPs	Deoxyribonucleotide Triphosphates
DMEM	Dulbecco's Modified Eagle's Medium
ECM	Extracellular Matrix
EMA	European Medicine Agency
ELISA	Enzyme-Linked Immunosorbent Assay
FDA	Food and Drug Administration
GAG	Glycosaminoglycan
hAC	human Articular Chondrocyte
HEPES	N-2-Hydroxyethylpiperazine-N-2-Ethane Sulfonic Acid
ICE	Interleukin-1Beta-Converting Enzyme
IL	Interleukin
IL-1β	Interleukin-1Beta
IL-1R	Interleukin-1 Receptor
IL-1RI	Interleukin-1 Receptor Type I
IL-1RII	Interleukin-1 Receptor Type II
IL-1Ra	Interleukin-1 Receptor Antagonist
LDH	Lactate Dehydrogenase
Mca	7-Methoxycoumarin
MIACT	Matrix-Induced Autologous Chondrocyte Transplantation
MMP	Matrix Metalloproteinase
MMPI	Matrix Metalloproteinase Inhibitor
MRI	Magnetic Resonance Imaging
mRNA	Messenger Ribonucleic Acid,

MSC	Mesenchymal Stem Cell
NE	Nanoemulsion
NO	Nitric Oxide
NP	Nanoparticle
NSAID	Non-Steroidal Anti-Inflammatory Drug
OA	Osteoarthritis
PBS	Phosphate-Buffered Saline
PCL	Polycaprolactone
PFA	Paraformaldehyde
PGA	Polyglutamic Acid
PGE_2	Prostaglandin E2
PLA	Poly(Lactic Acid)
PLGA	Poly(Lactic-*Co*-Glycolic Acid)
P/S	Penicillin/Streptomycin
RFU	Relative Fluorescence Unit
RT	Room Temperature
RT-qPCR	Real-Time Quantitative Polymerase Chain Reaction
ROS	Reactive Oxygen Species
SEM	Standard Error of The Mean
sGAG	Sulfated Glycosaminoglycan
Sox9	SRY-Box Transcription Factor 9
TACE	Tumor Necrosis Factor-Alpha-Converting Enzyme
TE	Tris-EDTA
TGF-β	Transforming Growth Factor Beta
TIMP	Tissue Inhibitor of Metalloproteinases
TJA	Total Joint Arthroplasty
TNF-α	Tumor Necrosis Factor-Alpha
TNFR	Tumor Necrosis Factor Receptor
TNFRI	Tumor Necrosis Factor Receptor I
TNFRII	Tumor Necrosis Factor Receptor II

1. INTRODUCTION

1.1. DEVELOPMENT, FUNCTION AND COMPOSITION OF ARTICULAR CARTILAGE

1.1.1. ARTICULAR CARTILAGE FORMATION AND GROWTH

Cartilage formation is one of the earliest steps in the embryonic development whilst being the first involved in endochondral ossification [1], where hyaline cartilage is substituted by bone and gives rise to the majority of embryo's skeletal structures [2]. It becomes clear that in these early stages, cartilage function is mainly to provide stability to the growing embryo [3].

The process of cartilage formation is named chondrogenesis and occurs in multiple stages, beginning with recruitment, migration and proliferation of mesenchymal cells [4]. Afterward, it involves the subsequent condensation of those precartilagineous mesenchymal cells, their posterior commitment to the chondrogenic lineage, and their final differentiation into chondrocytes [2, 5, 6]. When differentiating, chondrocytes can either remain as resting cells, this is, as the persistent extracellular matrix (ECM)-producing chondrocytes that will form the hyaline cartilage or undergo proliferation, hypertrophic maturation and be further replaced by bone during the endochondral ossification [4-6].

Undifferentiated mesenchymal cells are already able to produce ECM components, namely collagen type I, hyaluronan, tenascin and fibronectin, but there is a marked change in this composition as they become chondrocytes, [1]. Chondrocytes produce cartilage-specific matrix proteins, as collagens II, IX and XI, and aggrecan, leading to a significant tissue growth [1, 3, 4].

The synthesis of some cartilaginous proteins, like collagen type II, requires the expression of an important nuclear transcription factor, SRY-Box Transcription Factor 9 (Sox9) [4], as it transcriptionally activates genes for these ECM constituents [7]. Sox9 is one of the features helping in the lineage commitment, being repressed on hypertrophic chondrocytes while permanently expressed in chondrocytes of healthy articular cartilage [4, 7]. Thus, it not only has a pivotal role on the early stages of chondrogenesis but also in adult cartilage [7].

Along the journey from cartilage formation until its maturation in adults (18-21 years old), chondrocytes experience substantial changes, namely related to their activity and phenotype, in response to the differently applied mechanical loads [5]. As a result, ECM production, composition and structure also vary along time, where the major observed modifications are associated with the organization and the content of collagen and proteoglycans [5]. Both the cartilaginous tissue and the skeleton reach the maturity at the same time and, at this point, the proliferation rate of chondrocytes

is almost null, leading these cells to stay in a quiet state for many decades, with low proliferative and metabolic activities [5].

1.1.2. Adult Articular Cartilage Function and Composition

Cartilage is found in numerous parts of the human body, such as the ears, trachea, ribs, joints and pubic symphysis, being responsible for a structural or morphological role [5, 8]. It can be divided into three different subtypes, distinguishable by their different features [5]: elastic cartilage, fibrocartilage and articular cartilage [9]. Elastic cartilage is flexible due to the presence of elastin fibers [5] and maintains the shape of outer ear and trachea [9]. Fibrocartilage is abundant in type I collagen [5] and can be found in the meniscus [3] and in the intervertebral disks [5]. In its turn, hyaline cartilage is present in adult joints, being usually referred to as articular cartilage [5].

Articular cartilage is a key component of diarthrodial joints [10] - also known as synovial joints -, forming a white-coloured thin layer on the surface of subchondral bones in joints as the shoulder, elbow, hip and knee [9]. The principal function of this specialized connective tissue is the mechanical capability of these movable joints to bear and transfer weight loads [5, 9, 11]. It is also responsible for providing a smooth articulating surface and a higher contact area between the adjoining bones, allowing for low-friction rotational and translational movements [5, 9].

A fibrous capsule surrounds the entire diarthrodial joint and the synovial membrane secretes the synovial fluid, which contacts with the cartilaginous articulating surfaces [9] (Figure 1) and is very important for the nourishment and biomechanical properties of the cartilaginous tissue [5, 15].

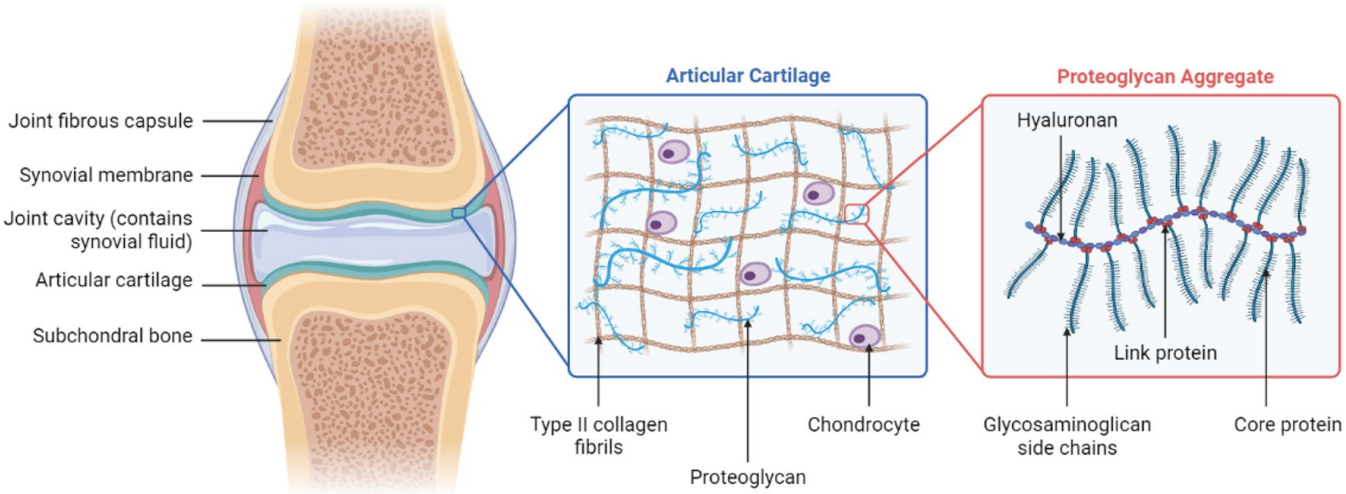

Figure 1 - Synovial joint structure and articular cartilage composition. Schematic illustration produced using image resources from BioRender (biorender.com). Illustration content adapted from [12-14].

Articular cartilage, whose thickness ranges from 2 to 4 mm [16], has a fluid and a solid phase [15] and the tissue biomechanical behaviour depends on their interaction

[16]. The fluid phase is mostly composed by water, which contributes to around 70-80% of the whole tissue wet weight and leads it to be highly hydrated [15, 16].

The solid phase is made of ECM, a highly organised network that is largely composed by collagen type II (90-95% of all collagen subtypes) [14, 17] and large proteoglycans (aggrecans) [18, 19], making these the two main phenotypic markers of articular cartilage [20]. ECM also contains less abundant molecular components as minor collagens, non-collagenous proteins and glycoproteins [11, 14].

Collagen is a fibrous protein [9] that holds the responsibility for the tensile strength of the tissue [5].

Proteoglycans are negatively charged molecules [14] that are constituted by glycosaminoglycan (GAG) chains covalently attached to a core protein [15, 17]. Moreover, given their hydrophilic behaviour, proteoglycans play an important role in water retention [5, 14] and allow cartilage to withstand compressive forces with minor deformation [14, 21].

Aggrecan is the most predominant of the proteoglycans, having the unique ability to bind (via link proteins) to hyaluronan, the largest GAG produced by chondrocytes [5], thereby forming large proteoglycan aggregates (Figure 1) [14].

ECM-embedded chondrocytes [22, 23] are the unique tissue-resident cellular component of adult articular cartilage [24, 25], characterised by maintaining a stable phenotype and resisting cell proliferation [8].

In order to preserve the matrix composition and organisation that were determined during the embryonic and postnatal periods, the tissue homeostasis and turnover are a responsibility of chondrocytes [26, 27]. Thus, these cells are responsible for maintaining the balance between the degradation and the secretion of ECM proteins [22, 23]. They are able to secrete both ECM components and proteinases, namely metalloproteases and cathepsins, which are matrix-degrading enzymes [14, 16], as well as growth factors and inflammatory mediators [15].

The cartilage ECM constitutes a “signalling scaffold” [10], being a reservoir of diverse growth factors and cytokines, therefore regulating the cell behaviour and sustaining the normal equilibrium of the tissue [22, 28]. Under normal conditions, chondrocytes are also sensitive and responsive to external factors and stressful stimuli such as of mechanical or biochemical origin [16, 26, 29].

1.2. MATURE ARTICULAR CARTILAGE STRUCTURE

There are four distinct zones between the articular surface and the subchondral bone, in which the cell phenotype, shape and number, the ECM structure and composition (namely collagen organization and proteoglycan content), and the functional and mechanical properties differ [8, 9, 14, 15]. As schematized in Figure 2, these layers are the superficial or tangential zone, the middle or transitional zone, the deep or radial zone, and the calcified zone [14, 15].

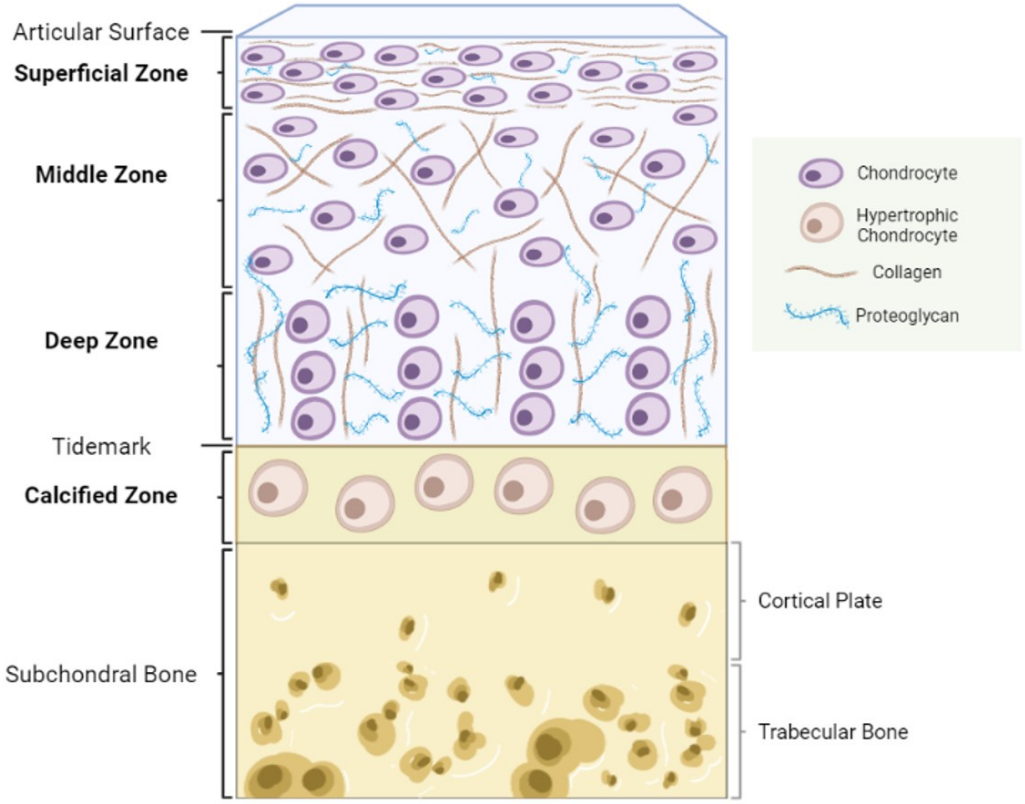

Figure 2 - Articular cartilage structure. Schematic illustration produced using image resources from BioRender (biorender.com) and Servier Medical Art (smart.servier.com). Illustration content adapted from [14, 30, 31].

In the superficial zone, chondrocytes are flattened and elongated, and are oriented in parallel to the articular surface, similarly to the collagen fibrils [14, 16]. This layer has the lowest proteoglycan and the highest collagen concentrations [8]. It is responsible for the protection of the deeper layers, resisting to shear stresses, and interacts with the synovial fluid due to its increased permeability [8, 14, 16].

The middle zone occupies most volume of the total cartilage (40-60%), where chondrocytes are round and collagen fibrils are organised obliquely [5, 14, 16].

The deep zone is highly constituted by proteoglycans, while chondrocytes have a more spherical shape and are in a columnar spatial distribution [14, 16]. The collagen fibrils are thicker than in the above layers and arranged in an orientation perpendicular to the surface [14, 27]. Due to its raised proteoglycan content, this layer provides the greatest resistance to compressive forces [16].

The tidemark, hydroxyapatite-constituted [5], makes a clear distinction between the deep zone and the calcified zone surface and does not allow vascular penetration in the overlying regions [16, 32].

Lastly, in the calcified zone, chondrocytes are most voluminous and in a very low density [14]. These cells have a low metabolic activity and exhibit a hypertrophic phenotype, synthesising collagen type X, which is a very important component for providing structural integrity [33]. This layer allows cartilage attachment to the bone

surface, by anchoring the collagen fibrils of the deep zone to the underlying subchondral bone [14, 16].

Throughout cartilage depth, proteoglycan content, the thickness of collagen fibrils and cell volume progressively increase whereas, generally, the density of water, collagen and chondrocytes decrease [9, 14, 15, 27].

Subchondral bone also has a layered structure, being composed of a cortical plate (compact bone) and trabecular bone (cancellous or spongy bone), which is underneath and much more porous than the first [31].

Articular cartilage and the subchondral bone together form the osteochondral unit and their dynamic interaction is of major importance for the maintenance of joint health and integrity [32, 34]. Additionally, the bone marrow of subchondral trabecular bone encloses mesenchymal stem cells (MSCs) that possess a chondrogenic-like potential [32].

1.3. AETIOLOGY OF COMMON ARTICULAR CARTILAGE INJURIES AND INTRINSIC MECHANISM OF REPAIR

Each year, injuries to the articular cartilage disturb more than one million people worldwide [35]. The most common causes of cartilage failure are focal chondral lesions, mainly due to traumatic injuries, aging and early osteoarthritis (OA) [36-38]. The lack of joint activity can also lead to cartilage degradation, as regular motion and dynamic load are important for maintaining a healthy cartilage structure and function [16, 39]. There are two types of focal articular cartilage lesions, the chondral (partial thickness defects) that only affect cartilage, and the osteochondral (full thickness defects), where the underlying subchondral bone is also targeted (Figure 3) [40, 41].

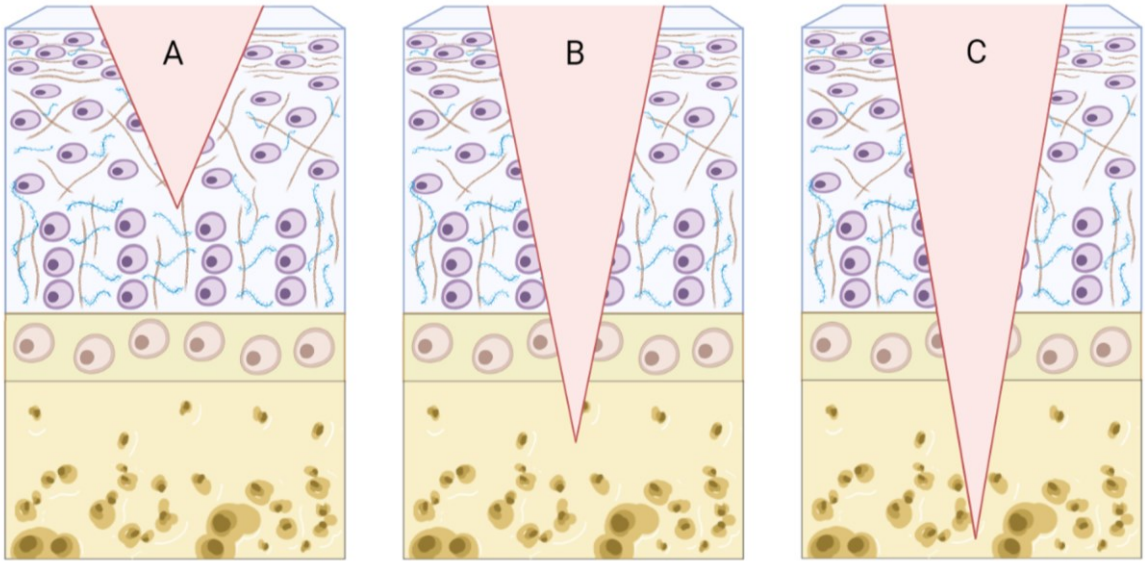

Figure 3 – Schematic representation of: A - chondral lesion; B - cortical osteochondral lesion; C - osteochondral lesion with trabecular bone penetration, reaching the bone marrow. Schematic illustration produced using image resources from BioRender (biorender.com). Illustration content adapted from [42].

In case the defect penetrates the subchondral bone, it can be limited to the cortical plate or go deeper into the bone marrow [42]. Lesion self-repair is only possible if it reaches the vascular bone marrow, where MSCs are present and able to produce a fibrocartilaginous tissue [42-44]. However, fibrocartilage has a lower content of collagen type II and of proteoglycans than articular cartilage, exhibiting poorer biomechanical properties and being a more susceptible target to gradual erosion and degeneration [38]. Moreover, as the joint continues to function with the repaired cartilage, degeneration may occur in the tissue surrounding the previous defect, as well as in the cartilage covering the opposing bone [38]. This progression can eventually result in diffuse cartilage degeneration and OA [38, 45].

Therefore, defects that do not extend to the bone marrow tend to increase in size and in depth and generally do not repair on their own [33]. This occurs because when cartilage suffers any kind of chondral lesion, its homeostasis is compromised and ECM destruction occurs [29]. Once chondrocytes are very sensitive to stressful stimuli, namely of mechanical and biochemical nature [26], they also start synthetizing new proteins, other than matrix degrading enzymes as a response to this damage [29].

Hence, if the defect in their surroundings is minor and there is a minimal loss of ECM, these cells are presumably able to restore the matrix [14, 46]. However, if the loss rate of collagen and proteoglycans outweighs their deposition rate, the newly-produced ECM has a changed structure and composition and is not sufficient to fill the gap caused by the lesion [4, 14, 29, 47].

Another concern relates to the cell loss or dysfunction caused by the injuries, which potentiates the inability of chondrocytes to mend the generated defect and to remodel the matrix, as the remaining chondrocytes are very sparse and cannot divide to compensate for the lost or malfunctioning cells [21, 26].

This way, cartilage lesions tend to increase in size if left untreated, leading to a progressive deterioration of ECM, along with the tissue irreversible loss of lubrication, integrity and biomechanical properties [36, 48]. The subsequently verified redistribution of loads results in new mechanical stress affecting the cells adjacent to the defect and possible cell death [3, 44]. Taking this into account, the appearance of chronic and progressive joint diseases seems unpreventable [14].

Symptoms associated with cartilage injuries include pain, swelling and joint dysfunction, and the clinical diagnosis is mostly performed with magnetic resonance imaging (MRI) [36, 49]. Currently, steps are being taken towards the development of innovative and advanced diagnosis tools, like in the MIRACLE project, where the employed imaging technology enables to evaluate the quality of the cartilage lesion, by measuring the biocomposition of the cartilaginous tissue in real-time [50].

1.3.1. Traumatic Injuries

Acute and repetitive trauma can damage articular cartilage and generate isolated defects [3]. In addition to ECM disruption that, in turn, leads to increased hydration and cartilage fissuring, the injury also triggers cellular degeneration and cell death [33].

Acute injuries are usually caused by a single traumatic event, such as abrupt heavy impact to the joint surface [33], while repetitive trauma can derive from joint overuse, as it happens in active athletes [39]. An excessive mechanical stress has been proved to damage ECM and to shift the cartilage homeostatic metabolism towards a catabolic activity [39].

Furthermore, a post-traumatic inflammatory response usually follows cartilage impaction, where chondrocytes and synoviocytes are activated and start producing inflammatory mediators and matrix-degrading enzymes that induce cartilage self-destruction, even though chondrocytes temporarily attempt to compensate this phenomenon by secreting anti-inflammatory cytokines [26]. In brief, if not timely treated, larger and isolated lesions can evolve towards OA [3, 44].

1.3.2. Aging

During the course of natural aging, chondrocytes dissipate from superficial towards deeper layers, leading to a different zonal organization of these cells [16, 29]. Adding to this redistribution, there are also alterations in the phenotype of chondrocytes, such as senescence-related decreased anabolism [21, 51] and cell depletion [21].

As cartilage cellularity changes, also does ECM, due to their mutual dependence. In fact, aging is associated with progressive ECM loss and reduced ability of the articular cartilage to recover from deformation [52], which leads the underlying bone to sustain increased mechanical forces [16].

Another aging consequence is the decrease in the number and size of proteoglycan aggregates [16, 29], whereas collagen molecules experience an increased crosslinking [51]. Overall, these changes contribute to a decrease in articular cartilage thickness and biomechanical properties, and to an increase in tissue stiffness [21, 52]. Additionally, aging might accelerate the degeneration of articular cartilage, and OA development [21, 51].

1.3.3. Osteoarthritis

Osteoarthritis is a musculoskeletal condition that affects joints subjected to long chronic use or injury and has a high impact in society, greatly contributing to disability worldwide [17, 53, 54].

The basis of OA symptomatology is intermittent pain in the affected joint during physical activity [55]. However, with increasing disease severity, pain becomes chronical, as it occurs even when patients are at rest [55], deeply decreasing their

quality of life [32], while limiting their mobility [14, 56] and leading to expensive treatments [52]. The occurrence of this pathology rises with age [55] and it can affect not only weight-bearing joints, such as knee, hip and spine, but also peripheral and axial articulations that are subjected to stress, like the small joints in the hands or the temporomandibular joint [53, 57]. Between these, the ones with the higher prevalence of this disease are firstly the knee and secondly the hip [58], usually requiring surgical intervention [59].

This disorder can be divided in two categories: primary OA, which arises from aging-associated wear and tear, and secondary OA, which involves predisposing factors for degeneration. Among these factors are trauma or abnormal mechanical stress, congenital joint abnormalities, obesity, genetic predisposition and previous systemic inflammatory joint disease, as rheumatoid arthritis [57, 60, 61].

Osteoarthritis involves joint degeneration, due to articular cartilage loss, as well as alterations in the subchondral bone, like an increase of its thickness [31, 55, 57]. Other features include synovial inflammation, joint swelling, and osteophyte (prominent osteochondral nodule [62]) formation [61].

Although affecting all joint components, the changes observed in the articular cartilage are the most significant [63], with particular degradation of collagen type II and aggrecan [17]. Along with articular cartilage thinning, fissures and flanks are also observed, thus increasing the exposure of the subchondral bones existent in each side of the articulation [31], causing the these opposing bones to rub together [64].

1.4. INFLAMMATION AND CARTILAGE DESTRUCTION IN OSTEOARTHRITIS

As a response to inductive stimuli, such as mechanical forces, oxidative stress, and changes in cell-matrix interactions and in growth factors that occur during OA, the tissue homeostatic balance is disrupted and chondrocytes start synthesising pro-inflammatory cytokines, particularly interleukin-1 beta (IL-1β) and tumor necrosis factor-alpha (TNF-α) [27, 39], and chemokines [26]. These cytokines induce the production of multiple catabolic mediators, namely matrix metalloproteinases (MMPs) and aggrecanases (ADAMTSs), enzymes that essentially degrade collagen and aggrecan [39] (Figure 4), while supressing ECM synthesis [26] by inhibiting chondrocytes' anabolic events [65].

With the progression of the disorder, cartilage breakdown products deriving from matrix degradation may further activate synovial cells [17] (fibroblasts and infiltrating macrophages [27]), provoking them to also release IL-1β and TNF-α (Figure 4), which are likewise distributed in the joint by the synovial fluid [26]. The cytokine release correspondingly potentiates the synthesis of more proteolytic enzymes that trigger ECM destruction and the subsequent release of additional inflammatory cytokines [17,

39, 66]. This synovitis manifestation initiates the recruitment of new mononuclear inflammatory cells into the joint lining that will similarly upregulate the production of proteinases [66]. Therefore, a positive feedforward cycle is propagated, with succeeding inflammatory cascades, largely contributing to a faster and perpetuated progression of the disease [17, 39, 66].

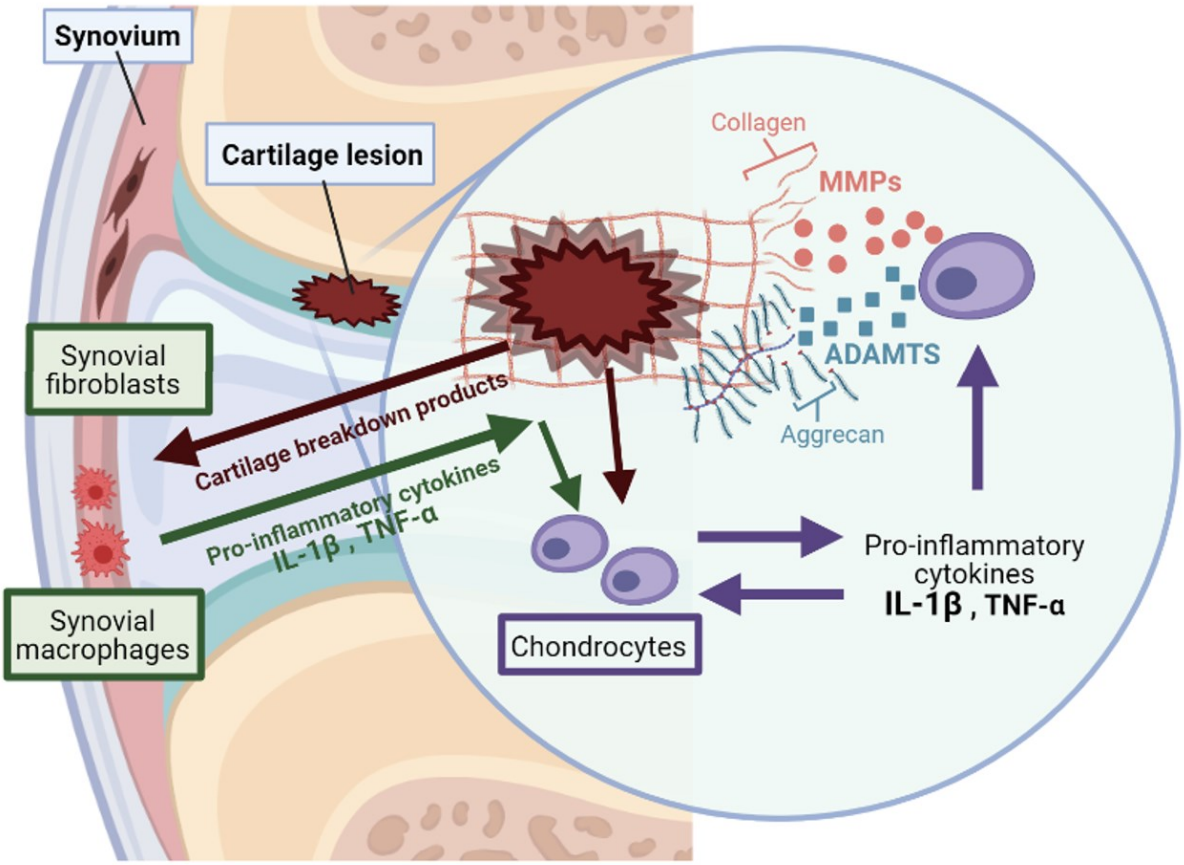

Figure 4 – Major cellular and molecular interactions in osteoarthritic cartilage destruction. Schematic illustration produced using image resources from BioRender (biorender.com). Illustration content adapted from [26, 27, 65].

In addition to influencing chondrocytes' metabolism, these cytokines induce other pro-catabolic responses, such as the production of nitric oxide (NO) [26, 27] and prostaglandins [27], the downregulation of tissue inhibitors of metalloproteinases (TIMPs) and the upregulation of non-specific ECM components [26].

After chronic exposure to these and other pro-inflammatory cytokines and chemokines, chondrocytes usually undergo cellular apoptosis, cluster formation (due to increased cell proliferation [25]), dedifferentiation or hypertrophy, losing their ability to form new ECM [14, 27].

1.4.1. Pro-Inflammatory Cytokines

Pro-inflammatory cytokines IL-1β and TNF-α are considered two secreted molecules with a critical role in OA, being usually detected in elevated levels in the

synovial fluid, synovial membrane, articular cartilage and even subchondral bone of osteoarthritic patients [65]. Although articular cartilage is avascular and aneural, it is well-known that these cytokines act in both in an autocrine and paracrine way to promote a catabolic microenvironment [67].

In addition to stimulating the metabolic activity of chondrocytes to produce MMPs and ADAMTs [68, 69], they can act synergistically or independently in suppressing the expression of important cartilage-specific genes as the ones of aggrecan (*ACAN*) and type II collagen (*COL2A1*) [25], and concomitantly enhancing the production of minor collagens, such as collagen types I and III, that are not normally ECM components [68].

Furthermore, IL-1β and TNF-α, along with stimulating their own production, may induce the production of a several other pro-inflammatory cytokines, like IL-6, IL-17, and IL-18 and chemokines, including IL-8, and prostaglandin E_2 (PGE_2) [25, 62, 65, 67]. Particularly, IL-1β and TNF-α stimulate the expression or activity of cyclooxygenase-2 (COX-2), leading to this verified increased synthesis of PGE_2, a pro-apoptotic molecule that also enhances the production and activation of MMPs, and inhibits the production of both ECM and IL-1 receptor antagonist (IL-1Ra) [25, 65].

Many of these inflammatory and catabolic factors can act together in increasing the synthesis of proteinases and decreasing TIMPs, thus propagating the inflammation [62, 65].

Other impacts of this inflammatory cascade include the synthesis of reactive oxygen species (ROS) and NO, which are major players in causing oxidative stress and the programmed cell death of chondrocytes [25], while reciprocally mediating the catabolic activity of the already upregulated catabolic cytokines [68]. IL-1β and TNF-α contribute to the exacerbation of these oxidative effects by downregulating the expression of antioxidant enzymes that have a protective role against ROS, including superoxide dismutase and glutathione peroxidase that scavenge free radicals [25, 65].

1.4.1.1. Signalling pathways driven by IL-1β

IL-1β is synthesised intracellularly as a precursor, pro-IL-1β, and released in the extracellular compartment in a mature form [67]. In the plasmatic membrane, caspase-1, originally named as IL-1β-converting enzyme (ICE), cleaves the prodomain from inactive pro-IL-1β, thereby generating its bioactive form [67, 70] that is the one found in OA tissue [71].

The biological activation of chondrocytes and synovial cells by IL-1β is mediated through an association with specific cell-surface IL-1 receptors (IL-1R) [65, 67]. Two types of IL-1R have been identified, type I (IL-1RI) and type II IL-1R (IL-1RII) [65, 67]. IL-1RI acts as a signal transducer and is upregulated in osteoarthritic chondrocytes and synovial cells, leading to an increased binding of IL-1β and thus making these cells more susceptible to the stimulation by this cytokine [65, 67, 72].

After IL-1β binds to IL-1RI, the signal is further transferred by this type of receptors to the nucleus and, after various signalling transduction pathway, it results in messenger RNA (mRNA) upregulation and further MMP increased synthesis [73].

On the contrary, IL-1RII can bind to IL-1β but is not able of signal transmission [65, 67, 70]. Therefore, IL-1RII is a natural inhibitor of IL-1β activity, as well as the IL-1Ra, which binds to both IL-1 receptors without transducing a signal, being a competitive antagonist of IL-1β [65, 70], and thus exhibiting anti-inflammatory properties [65]. In OA pathophysiology, there is a decrease in the expression of IL-1Ra [72] mainly because NO in concert with PGE_2 inhibits chondrocytes from producing this antagonist [65, 67].

As previously mentioned, the verified increase in IL-1β secretion induces the production of other inflammatory downstream mediators and the production of degrading enzymes [68]. In particular, IL-1β stimulates the synthesis of MMP-1, MMP-3, MMP-9 and MMP-13 both by chondrocytes, macrophages and fibroblasts, and of ADAMTS-4 only by the chondrogenic cells [72, 74-76]. This pro-inflammatory molecule also supresses the anabolic activity in cartilage tissue by inhibiting the expression of type II collagen and aggrecan [65, 72].

1.4.1.1. Signalling pathways driven by TNF-α

TNF-α is also firstly secreted in an inactive proform that needs a proteolytic cleavage at the cell surface by a TNF-α-converting enzyme (TACE) and an upregulation of the gene associated with this enzyme and mRNA expression are verified in OA cartilage [67, 72], along with an overexpression of TNF-α itself [72].

Similarly to what occurs for IL-1β, TNF-α induces chondrocytes, macrophages and synovial fibroblasts to synthesise the same set of MMPs (MMP-1, MMP-3, MMP-9 and MMP-13) [74, 75], and the production of ADAMTS-4 [17, 65, 76].

Moreover, TNF-α supresses the synthesis of proteoglycan, link proteins and type II collagen in chondrocytes [65, 72]. Both TNF-α and IL-1β can have a synergic effect during OA inflammatory process [72].

Once released in the extracellular milieu, the cytokine binds to two specific membrane receptors named TNF receptors (TNFR) [65, 67]. One of those is the TNF receptor I (TNFRI), the one with the most predominant role in mediating the activity of TNF-α in chondrocytes and synoviocytes [65, 67], and the other is TNF receptor II (TNFRII), which is also actively implicated in signal transduction but linked to different intracellular protein cascades [65]. Even in early studies, an enhanced expression of TNFRI in these cells in OA conditions has been reported [77, 78].

1.4.2. Matrix Degradative Enzymes

The metzincin is the name given to a super family of zinc endopeptidases that comprises three different families: MMPs, adamalysins (or a disintegrin and metalloproteinases (ADAMs)), and ADAMTSs [79, 80].

Although these proteinases have a zinc catalytic domain in common [80], most of them have other domains that confer the specificity either for the substrate cleavage or for the cellular or ECM localisation [79].

Both MMPs and ADAMTSs are responsible for orchestrating the degradation of ECM by degrading the two dominant structural components of cartilage ECM, collagen type II and the proteoglycan aggrecan [79]. These proteins can be secreted either in a soluble or membrane-associated form [79].

1.4.2.1. Matrix Metalloproteinases

Damage to the articular cartilage in OA is predominantly mediated by MMPs [81], which cleave collagen fibrils and other ECM components, therefore causing anatomic and functional alterations in the tissue [68].

The biologic activity of the MMPs is tightly regulated, namely by physiologic proteolytic activators that convert prometalloproteases into active enzymes and by the specific tissue inhibitors, TIMPs [68, 80]. In physiologic conditions, TIMPs try to counterbalance the activity of MMPs by specifically binding to their active site, however, in OA cartilage the synthesis of the proteinases far surpasses the synthesis of these inhibitors, amplifying the ECM destruction [68].

Among the soluble MMPs that degrade distinct substrates are the collagenases, which are responsible for the degradation of native mature collagen, the gelatinases for the degradation of denatured collagen (gelatin), and the stromelysins for the degradation of proteoglycans [68]. On the other hand, membrane-type MMPs include MMP-14 and are involved both in aggrecan and collagen degradation [82]. The degradation of collagen in cartilage is an irreversible step and the tissue cannot be repaired after this component is destroyed [80].

In the family of collagenases, the ones that have been identified in human cartilage are MMP-1 (collagenase 1), MMP-8 (collagenase 2) and MMP-13 (collagenase 3) [68]. Only collagenases and, in a much lesser extent, MMP-14 can degrade mature type II collagen fibrils [80]. Once denatured into gelatins, these collagen fragments are susceptible to be digested by gelatinases, which are MMP-2 and MMP-9, being the last the only of the two that is enhanced in OA [68, 80], thus inducing further MMPs and cytokines [83].

As for the stromelysins, the enzymes identified in humans are MMP-3 (stromelysin-1), MMP-10 (stromelysin-2) and MMP-11 (stromelysin-3) [68].

The MMPs known to have the most important role in OA are MMP-1, MMP-3, and MMP-13 [65, 66, 84]. While MMP-1 is only able to act on collagens (I, II and III), MMP-

13 has a dual role in ECM destruction, as it also degrades aggrecan [17, 82], and MMP-3 is likewise able to destroy both various proteoglycans and collagens [82].

1.4.2.2. A Disintegrin And Metalloproteinase With Thrombospondin Motifs

Concomitantly with stromelysins, ADAMTSs also degrade proteoglycans but at rather higher levels, having the extra ability to cleave collagen pro-peptides [17]. The largest proteoglycan, aggrecan, is sensitive to degradation at various sites of its length and its degradation is an early event in the development of OA [69, 80].

Belonging to the ADAMTS family, aggrecanases are extracellular proteins are considered the major aggrecan-degrading enzymes involved in cartilage degradation in the pathophysiology of OA [25]. These proteases are secreted as multidomain zymogens that need an intracellular activation by pro-protein convertases to become mature enzymes [76, 80].

Several ADAMTSs are expressed in cartilage as ADAMTS-1, which also cleaves aggrecan, and ADAMTS-2, ADAMTS-3 and ADAMTS-14 that process procollagens [85], but the two aggrecanases that have been widely documented to intervene in cartilage degradation in OA are ADAMTS-4 (aggrecanase-1) and predominantly ADAMTS-5 (aggrecanase-2) [65, 66, 80]. However, while ADAMTS-4 is dependently up-regulated during OA in an IL-1β and TNF-α dependent manner, the levels of ADAMTS-5 are not altered, being this just constitutively expressed in both healthy and OA cartilage [65, 76, 80, 81].

The regulation of these aggrecanases activity involves a specific inhibitor of ADAMTs, TIMP-3, that effectively acts on ADAMTS-4 and ADAMTS-5 and can likewise inhibit MMPs, being a central inhibitor of ECM turnover and whose deletion is significantly increased during cartilage degradation [69, 76, 80].

1.4.4. Anti-Inflammatory Cytokines

Typical immune cells can produce anti-inflammatory cytokines, but so do non-immune cells present in connective tissue, like chondrocytes and fibroblasts [26], in order to counteract the activity of IL-1β, TNF-α and the other above-mentioned pro-inflammatory cytokines [68].

The main cytokines with an anti-inflammatory capacity involved in OA are IL-4, IL-10, and IL-13 [67, 68, 86]. These cytokines act through numerous mechanisms, which results in a down-regulation of IL-1β, TNF-α and MMPs production, along with the up-regulation of TIMPs and of IL-1Ra [67], being the latter mainly induced by IL-10 [68].

Notwithstanding, their responsibilities are not limited to an antagonist effect of IL-1β and TNF-α, as they also exert functions in the growth and differentiation of articular cartilage [68], and IL-10 appears to possess a chondroprotective capacity [26].

1.5. CURRENT THERAPEUTIC APPROACHES FOR TRAUMATIC AND DEGENERATIVE ARTICULAR CARTILAGE

As previously explained, cartilage damages most commonly occur due to trauma and aging, causing chondral or osteochondral lesions or even a more diffused loss of cartilage tissue, like in OA.

Since the hip and the knee are the weight-bearing joints where these defects are highly prevalent and studied [87], the following described approaches (summarized in Figure 5) are directed to those locations. It should be noted that the volume of available information on the restoration of articular cartilage in the knee far exceeds the one for the hip [88]. However, most of the methods currently used for cartilage repair of the hip are based on the ones initially developed for the knee, being essentially built over the same principles [88].

The primary goal of the treatment of chondral and osteochondral lesions is to relieve pain and improve the joint function, ultimately allowing patients to return to their normal lifestyle [45, 89]. Treatment decision-making criteria must include some important aspects, such as the patients' level of activity and age, defects' cause, size, shape, location and depth and the extent of degeneration of the surrounding articular cartilage [42, 45]. The success of the chosen option depends both on these factors and on the quality of further rehabilitation [42].

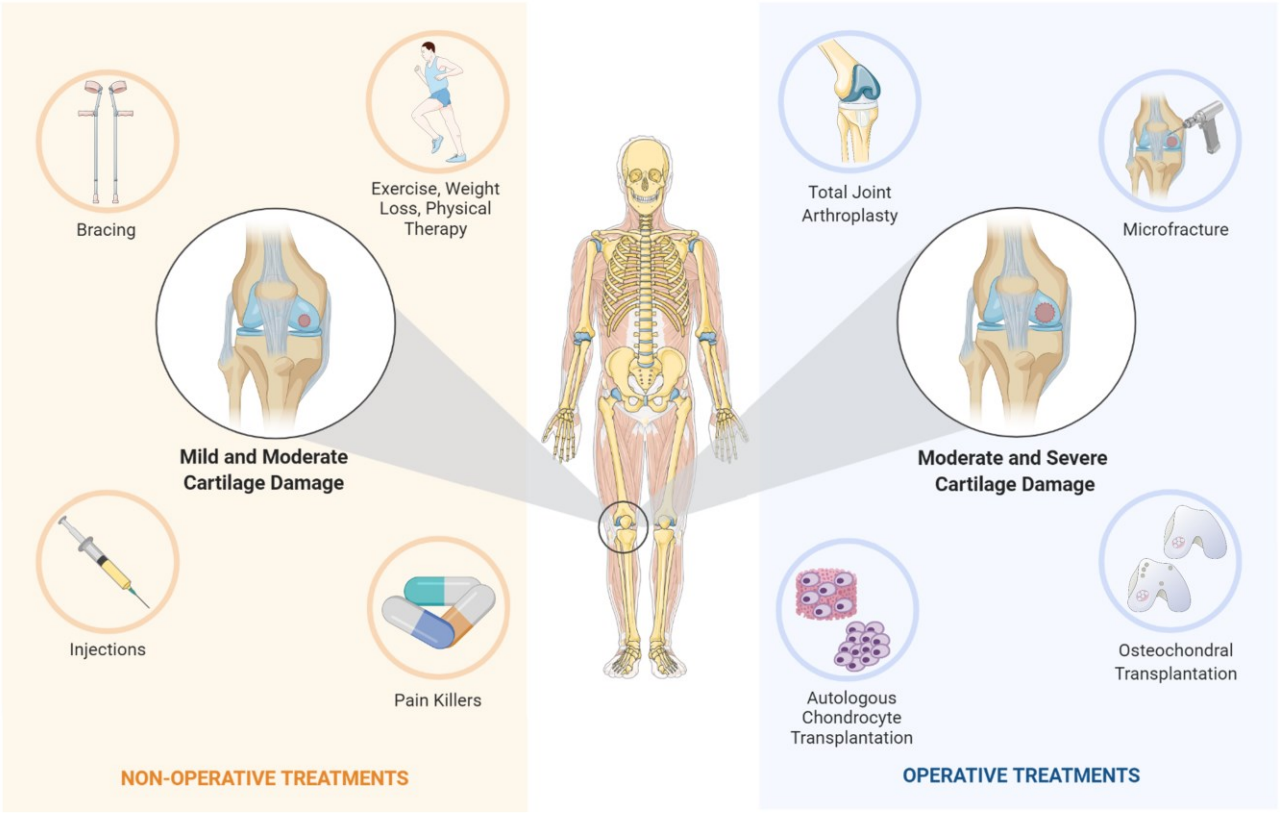

Figure 5 – Current non-operative and operative treatments in clinical practice for mild, moderate and severe cartilage damage in knee and hip joints. Schematic illustration produced using image resources from BioRender (biorender.com) and Servier Medical Art (smart.servier.com). Illustration content adapted from [14, 41, 60].

1.5.1. Non-Operative Options

Non-operative options of treatment are usually primarily intended to patients with mild and moderate joint damage [14, 90]. These treatments are able to provide a definitive option in these particular conditions, whereby they commonly alleviate pain and some of them can prevent further joint degeneration [14, 91].

1.5.1.1. Non-Pharmacological Treatments

The most common non-pharmacological treatments rely on exercise, weight loss, physical therapy and bracing, which, although not promoting the healing of damages or slowing OA progression, generally result in pain reduction and improved joint function [36, 90, 91].

1.5.1.2. Pharmacological Treatments

1.5.1.2.1. Pain Killers

When non-pharmacological treatments cease to relieve pain in the affected joint, analgesics are normally recommended as an adjunctive therapy [91].

Paracetamol is a frequent choice for OA, yet it produces only minimal improvement in pain and joint function in osteoarthritic knee or hip [92, 93]. Other widely prescribed oral medications are non-selective non-steroidal anti-inflammatory drugs (NSAIDs), however they have been associated with gastrointestinal toxicity, increased cardiovascular harm and other side-effects [94, 95]. For instance, NSAID diclofenac was previously associated with increased OA progression in hip and knee over an average duration of 6.6 years of follow-up [96].

1.5.1.2.2. Intra-Articular Injections

Intra-articular injections constitute a minimally invasive procedure that consists in delivering compounds directly to the damaged joint [60]. However, they are not easy to perform in the hip, requiring imaging support [95]. Local injections of compounds like corticosteroids, hyaluronic acid and bone marrow aspirate concentrate are approved by the Food and Drug Administration (FDA) [97, 98]. Also, although not FDA-approved, injections of platelet rich plasma can be legally performed and are increasingly being used [60, 99]. There are some disadvantages associated with intra-articular administration of biologic agents, namely the need for positioning the needle strictly within the joint cavity, patient discomfort, risks related with successive injections and drug clearance from the articular joint via the lymphatic network [71].

1.5.1.2.2.1. Corticosteroids

Corticosteroids are anti-inflammatory agents [60] whose beneficial effects are observed at low doses and in short-term, whereas with high doses and prolonged

exposure chondrocyte toxicity and cartilage damage are observed [60, 100]. In fact, it has been reported great cartilage loss and no relevant difference in patients with OA-induced knee pain after 2 years of intra-articular corticosteroids injections [101].

1.5.1.2.2.2. Hyaluronic Acid

Hyaluronic acid is naturally present in the synovial fluid, but there is a shift in this component towards its lower molecular weight form with the progression of OA, which is associated with decreased viscoelastic properties and with higher intensity of pain [102]. These injections aim to restore the concentration and molecular weight of this component [60, 102] but although not harmful, they are currently not recommended either in the hip or in the knee, because of their lack of efficacy, exhibiting a performance no better than placebo for pain, stiffness and improvement of function in patients with symptomatic OA [103-105].

1.5.1.2.2.3. Bone Marrow Aspirate Concentrate

Bone marrow aspirate concentrate (BMAC) is obtained from density gradient centrifugation of the bone marrow aspirate that is usually removed from the iliac crest [100]. This concentrate contains both MSCs and high levels of growth factors and cytokines, which are molecules that normally promote the increase of blood supply to the subchondral bone, allow the chondrogenic differentiation of MSCs and have anti-inflammatory effects [102]. The synergy between MSCs and these molecules promotes decreased pain, functional improvement of the joint and articular cartilage repair [100, 102], leading to improved and long-term outcomes in patients with OA [97, 100]. However, further studies to determine the safety of injected MSCs with BMAC, its optimal dose and frequency of treatment are required [97, 100].

1.5.1.2.2.4. Autologous Platelet-Rich Plasma

Lastly, the platelet-rich plasma is prepared through blood differential centrifugation, being highly concentrated in platelets and showing varying volumes of signalling proteins like growth factors, cytokines, chemokines, and proteases [60, 99]. It is a costly treatment and even though it is thought to promote tissue repair, there is a lack of reliable evidence on its effectiveness [60, 99, 103].

1.5.2. Surgical Treatment Options

Conservative non-operative approaches constitute the first line of cartilage damage treatment but in case of failure to relieve patients' pain and/or damage progression, which often occurs for larger and full-thickness cartilage injuries, they must be replaced by surgical-based techniques [49, 106, 107].

1.5.2.1. Total Joint Replacement

Total joint arthroplasty (TJA) is a commonly employed therapy for aged patients with severe either hip or knee OA [45]. Although cost-effective [108], it is an irreversible procedure and prosthetic components have a limited average lifespan of around 15 years [109-111]. Implant survival relies on many factors and the causes of TJA failure include aseptic loosening, metal allergy and infections, as many patients have to be subjected to costly and challenging revision surgeries [111]. Therefore, it is not recommended for patients younger than 60 years, unless other approaches have failed or are contraindicated [109, 110]. Because this procedure replaces the joint instead of stimulating tissue repair, several other surgical therapeutic techniques relying on cartilage restoration are widely used in clinical practice [60, 111].

1.5.2.2. Surgical Treatment Options for Articular Cartilage Repair

The range of techniques currently used in clinical practice for cartilage restoration include microfracture, osteochondral transplantation and autologous chondrocyte transplantation [5, 49, 60] (Figure 6). As repair approaches, they attempt to generate a neo-cartilage tissue that resembles to the native cartilage, but that does not necessarily have the same features [33]. However, the produced tissue in these treatments is fibrocartilaginous, having inferior biomechanical properties and durability than hyaline cartilage, and eventually allowing the progression of articular degeneration and OA occurrence [45, 112]. Of these, microfracture appears to be the least long-lasting approach, which is in agreement with a 2019 review study that compared the effectiveness between these five techniques [113]. As previously mentioned, the outcomes of each are expected to vary according to distinct parameters, but generally increasing ages are associated with poorer outcomes, namely in microfracture [41].

1.5.2.2.1. Microfracture

Microfracture is a marrow-stimulating technique that involves perforating the subchondral bone, after cleaning and debridement of the articular defect, to allow the recruitment of bone marrow-derived MSCs [5, 60, 114]. The generated holes promote bleeding from the bone and the subsequent formation of a fibrin clot, allowing the formation of a fibrocartilaginous repair tissue at the defect site [5, 36, 44] (Figure 6).

This tissue formation usually takes 12 to 16 months, leading to a demanding recovery [5]. In order for this to be an adequate strategy, some studies indicate that the chondral defects must be smaller than 4 cm^2 [41, 45, 115, 116]. This is a widely used technique that is simple and relatively inexpensive, and involves a minimally invasive surgery, [36, 60, 117]. Still, due to the deterioration of the originated repair tissue, microfracture shows optimal outcomes only in the short-term, usually not lasting more than 5 years [118-120]. In case of failure, more invasive repair methods

are then performed [44]. In most of the cases, this technique provides pain relief and improved functionality of the joint [44, 117], but the outcome is often unpredictable [117], and it has been progressively replaced by the following procedures [119].

1.5.2.2.2. Osteochondral Transplantation

The transplantation of osteochondral grafts aims to reconstruct either the cartilaginous or the osteocartilaginous defects in a single procedure, as an osteochondral biopsy of 12 to 15 mm depth is performed, and the donor tissue can be of autologous (autograft) or allogenic (allograft) origin [5, 110].

When compared to the other cell-based cartilage repair surgical techniques, the osteochondral grafts are the ones allowing the fastest rehabilitation, mostly because they are able to bear loads shortly after the surgery [41].

1.5.2.2.2.1. Osteochondral Autograft Transplantation

Osteochondral autograft transplantation, also commonly referred to as mosaicplasty, involves removing intact osteochondral cylindrical plugs from less-demanding load bearing areas of the affected hip or knee [36, 43].

These plugs are then transplanted to the previously full depth drilled and debrided defect area, consequently forming a mosaic pattern [36, 43] (Figure 6), where the remaining space between the round plugs is ultimately filled with newly-formed fibrocartilage [36]. Potential donor sites include the inferior portion of the femoral head and the peripheral portion of the femoral trochlea of the knee [88].

The advantages of this technique are mainly related to the transfer of mature hyaline cartilage into the defect, in addition to being a single-stage procedure [88]. Reduced pain and improved joint function have been reported for small and medium sized osteochondral lesions [43, 121]. At the same time, to obtain optimal results, it is not indicated for chondral or osteochondral lesions larger than 2 cm^2, otherwise significant donor-site complications and morbidity tend to occur [5, 41, 49]. Other disadvantages include graft availability [41], technical difficulties in the restoration of curved surfaces [121], and potential dead space between the grafts [88].

At a mean long-term follow-up of 12 years after the performance of the procedure in the knee, a study reported poor outcomes or failure in 40% of the treated patients [122]. Other results showed progressive degeneration of the knee after the same period of time, even though not significantly affecting the satisfactory follow-up of the evaluated patients [123].

1.5.2.2.2.2. Osteochondral Allograft Transplantation

In osteochondral allograft transplantation, osteochondral plugs containing cartilage with the same thickness as the patients' own are removed from a cadaveric donor [36]. Hence, opposing to mosaicplasty, no donor site morbidity is observed, and the

grafts can be chosen with the purpose of matching the lesion as much as possible, since there is no restriction in terms of size or number of the plugs [5, 36, 42].

Nevertheless, different graft storage conditions distinctively affect the viability of chondrocytes and longer storage times are associated with decreased cartilage biomechanical properties and cell viability, which strongly affects the clinical outcomes [5, 121, 124]. In order to use a fresh graft, difficult and well-organised logistics are required between the date of surgery and obtaining the tissue in a timely manner [45, 125]. On the other hand, the fresher the transplants, the greater is the probability of the occurrence of an immune rejection response or disease transmission, due to the difficulty in fully removing the donors' blood from the grafts [45]. Additionally, this is an expensive procedure [45].

This technique is considered an option when microfracture, mosaicplasty or autologous chondrocyte transplantation fail in promoting articular cartilage repair, and it is increasingly being used as the primary method for the treatment of lesions larger than 3 cm^2, either of chondral or osteochondral origin [5, 49, 121]. Several published results reveal that good outcomes remain for around 20 years after surgery [126-128].

1.5.2.2.3. Autologous Chondrocyte Transplantation

Unlike the above explained techniques, autologous chondrocyte transplantation (ACT) is a procedure with two steps, where firstly cartilage tissue is extracted from a non-weight bearing area to prepare chondrocyte cultures and secondly, expanded cells are transplanted into the defect site [36, 38, 45] (Figure 6).

After excising the cartilage biopsy in the first surgery, ECM is enzymatically digested and chondrocytes are released and isolated to be further expanded in culture [3, 42, 43]. In the second surgery, the expanded chondrocytes are injected under a periosteal patch made of autologous periosteum, which is sutured over the injury [43].

Expansion is important because the volume of harvested cartilage and its cellular content is very small when compared to the volume and cell density needed at the target defect site [38].

Advantages over other treatments are the less damage in subchondral bone [45] and the formation of hyaline-like tissue [121]. On the other hand, disadvantages of ACT include being costly, two-staged, logistically demanding and requiring a long and challenging rehabilitation [3, 45, 121, 127]. Another limitation is associated with fibrocartilage formation, often occurring due to chondrocytes' expansion-driven dedifferentiation [60], which is a process where the cells lose their chondrogenic potential [38]. Like in mosaicplasty, in ACT donor-site complications may also occur and not every patients have a healthy region from where the biopsy can be removed [38]. Furthermore, symptomatic hypertrophy of the periosteum can also occur [107].

Although distinct success rates have been reported, several studies demonstrate good and functional long-term outcomes for 20 years after the transplantation [129-131] and chondral lesions should be larger than 2 cm^2 [115, 130, 132].

1.5.2.2.4. Matrix-Induced Autologous Chondrocyte Transplantation

Matrix-induced autologous chondrocyte transplantation (MIACT) consists in transplanting a collagen scaffold with autologous expanded chondrocytes into the defect site [60, 107].

As shown in Figure 6, MIACT is performed similarly to ACT until the step involving the expansion of chondrocytes, but instead of injecting, the cells are after seeded on a three-dimensional biodegradable matrix to be further transplanted on top of the lesion and secured to it with a fibrin glue [26, 107]. The scaffold is biodegradable in order to temporarily support chondrocytes only until they produce their own supportive matrix [133].

The many drawbacks associated with cell expansion are the same as in ACT, but this procedure has the advantage of keeping chondrocytes within a scaffold that provides them support for distribution, proliferation and release of ECM-like components [5, 134]. The fact that a periosteal patch is not used may decrease surgical time and morbidity [112].

In most studies, MIACT is currently preferred for cartilage defects larger than 2 cm^2 [107, 135-137], that can either have a chondral or osteochondral extent [135, 136].

Although the major follow-ups found in literature with effective clinical outcomes do not go further than 5 years [137-140], a study from 2016 claims good and durable treatment of the injuries after 16 years [141].

The results of MIACT-based treatment can be enhanced by combining growth factors to stimulate the growth of chondrocytes, and anti-inflammatory mediators to prevent post-traumatic cartilage inflammation and further development of secondary OA [26, 133].

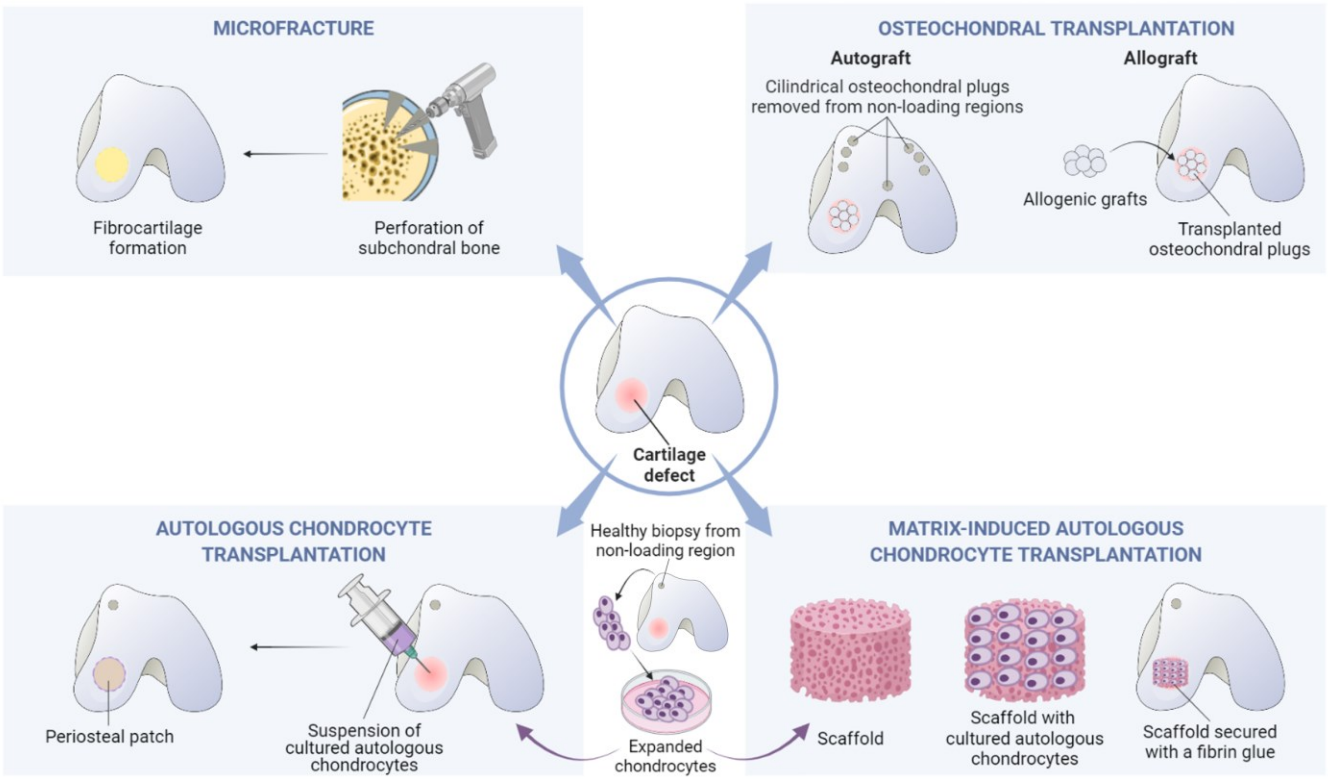

Figure 6 - Main steps involved in the most commonly used surgical techniques for cartilage repair. Schematic illustration produced using image resources from BioRender (biorender.com) and Servier Medical Art (smart.servier.com). Illustration content adapted from [43, 60].

1.6. POTENTIAL THERAPEUTIC TARGETS FOR THE HALTING THE PROGRESSION OF OA

As previously described, the effects of pro-inflammatory cytokines are exerted in chondrocytes through the intermediation of cell surface receptors, where the signal is further transduced in the nucleus, leading to the synthesis of more inactivated MMPs [73]. Cells are also able to produce TIMPs that naturally inhibit MMPs activity, but their action is not sufficient to control OA matrix degradation driven by locally exceeding MMPs [73].

As such, three main regulatory steps that lead to matrix degradation are identified: cell stimulation through cytokines and receptors, intracellular signalling, and MMPs activation and inhibition. Each of them can be potential targets for therapeutic intervention [73]. The main goals for the management of OA are symptom reduction, functional disability minimization and limited progression of the occurring structural changes [67]. Cartilage loss is an important therapeutic target, essentially because even though not directly associated with pain, the level of cartilage loss is a strong predictor for the risk of undergoing TJA [142]. In fact, the factors that drive pain occurrence and magnification are the same that induce cartilage destruction, which

means that targeting the molecular mechanisms of cartilage breakdown might also reduce pain levels on patients [71].

Herein the two principal of these targeted therapeutic strategies, which are the inhibition or the modulation of the effects of either major pro-inflammatory cytokines [71] or of MMPs, will be discussed, as their understanding has evolved significantly and made possible their identification as potential targets for altering the course of the disease [67].

1.6.1. Targeting Pro-Inflammatory Cytokines Activity

Due to the preponderant role of IL-1β and TNF-α in the degeneration of articular cartilage, they are prime targets of research for therapeutic strategies aiming to slow down the structural progression of OA [65, 71].

Anti-cytokine therapies tested in clinical trials or animal studies most normally include the administration of monoclonal antibodies against IL-1β (ex: Gevokizumab, Canakinumab) or TNF-α (ex: Adalimumab, Infliximab), of recombinant human IL-1Ra (ex: Anakinra) [65, 143], and, less frequently, of inhibitors of ICE or TACE [67].

The cytokines antagonists possess a low oral bioavailability, meaning that when systemic administration is required, their entrance into body must be parenteral, that is, by intravenous, intramuscular or subcutaneous route [71], making the treatment expensive and inconvenient [144]. Actually, in most of the studies, the administration of anti-IL-1β and anti-TNF-α is usually subcutaneous or intravenous [71, 143] and of IL-Ra is by intra-articular injections either of the protein itself or of the associated gene using retroviral or adenoviral vectors [65, 67, 71].

However, IL-1Ra and monoclonal antibodies are not associated with encouraging results [142, 145], as they leave the joint too fast to exert successful results, particularly when administered intra-articularly [71]. Another disappointing observation is that they need to be injected repeatedly in order to effectively reduce pain [71]. Also, systemic toxicity and allergic reactions can occur due to systemic therapy and therefore alternative routes of administration should be an option whenever possible [71]. Subcutaneous and intravenous administration of monoclonal antibody to IL-1RI has also been reported, although with minimal clinical benefits [146]. In addition, a problem associated with the prolonged use of therapeutic antibodies is the possible production of neutralising antibodies as a consequence in some host patients [144].

It is important to notice that anti-inflammatory approaches for OA should be wide-ranging enough to be effective, but still sufficiently selective not to cause deleterious off-target effects [84].

1.6.1.1. Ibuprofen

Ibuprofen, a commonly prescribed NSAID, is one of the most commonly used anti-inflammatory, antipyretic and analgesic drugs [147]. In addition, it is widely used for the clinical management of rheumatic disorders like OA [147, 148], as it has relatively low risk for adverse effects, such as upper gastrointestinal toxicity, when compared with other NSAIDs [147]. It has poor aqueous solubility and slow dissolution rate [149].

This compound works by blocking the COX-mediated production of prostaglandins, which is the primary anti-inflammatory mechanism of NSAIDs, and thus the preventing the further upregulated synthesis of matrix-degrading enzymes (Figure 7) [147].

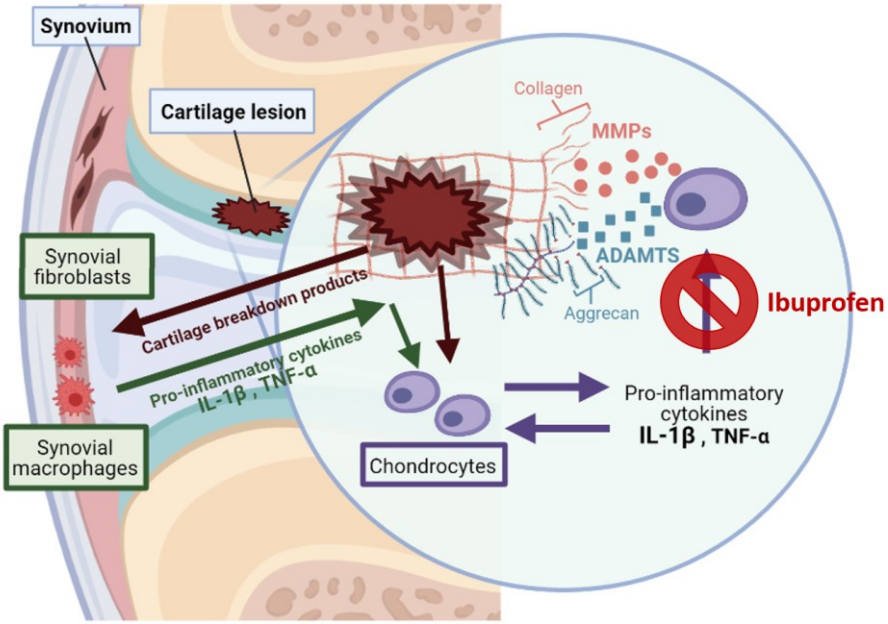

Figure 7 – Ibuprofen action in blocking MMPs and ADAMTs synthesis, induced by prostaglandins, in the osteoarthritis pro-inflammatory vicious cycle. Schematic illustration produced using image resources from BioRender (biorender.com).

In a recent study, ibuprofen was found to supress IL-1β-induced inflammation, by inhibiting the expression of IL-1β-induced synthesis of PGE_2 and NO in rabbit chondrocytes [148]. In another one, it alleviated pain and knee function in patients with symptomatic OA, by supressing pro-inflammatory cytokines such as IL-6 and TNF-α [150]. Furthermore, Sun et al. conducted a study in a human chondrocyte cell line treated with TNF-α and observed that ibuprofen-treated cells significantly had the expression levels of collagen I, MMP-1 and MMP-13 reduced [151].

1.6.2. Targeting Metalloproteinase Activity

Apart from inhibiting IL-1β and TNF-α, other strategy is to impede the activity of MMPs and ADAMTSs that these cytokines increase [65].

Research on blocking of cartilage ECM degradation has been focused essentially on the breakdown of its two major components, collagen type II and aggrecan [152]. Thus, dysregulated MMPs and ADAMTSs are strong potential targets for the development of drugs with the capacity of modifying the course of disease progression [80, 85]. This is of greater importance because by significantly reducing joint destruction, the function of joints at long term can be preserved, severe disability could be avoided and osteoarthritic patients could experience an improved quality of life [79].

Mainly two groups of compounds are able to inhibit MMPs, including TIMPs and small molecule MMP inhibitors (MMPIs) [144].

As previously referred, TIMPs are the endogenous inhibitors with specific affinities to either MMPs, ADAMs, and ADAMTSs [153], but there are some limitations with regard to their production and administration, and *in vitro* results were reported ineffective [67, 144].

Synthetic inhibitors of zinc metalloproteinases rely on a peptide sequence that is recognised by the targeted protease and interacts with the catalytic zinc ion at the active site, therefore binding to it and blocking its catalytic activity [17, 67, 73, 79]. This peptide sequence has a backbone that mimics the one at the substrate cleavage site [17, 73].

Taking into account the chemical structure of the zinc-binding group, four different categories of zinc metalloproteinases inhibitors have been described: the ones having a hydroxamate, a carboxylate, a thiolate, or a phosphinyl group [17, 73, 79].

Generally, several studies and clinical trials with MMPIs have had little success or unclear benefit and revealed poor bioavailability and efficacy, mainly because of their broad-spectrum inhibitory effects [65, 144]. Another reported difficulty relies on the estimation of dosage to prevent drug toxicity [154], which varies in an exposure-dependent and dose-dependent manner and frequently manifests as reversible musculoskeletal side effects, like joint pain and stiffness, inflammation and reduced mobility [142, 144, 154, 155]. However, in osteoarthritic animal models of rat and guinea pig, cartilage structural damage was demonstrated to be abrogated by these compounds [156].

Although not yet in clinical translation for OA purpose, the class of MMPIs receiving most attention are hydroxymates, which have been proved to be very potent inhibitors of metalloproteinases, but poor selectivity has been reported [79]. Among these hydroxamate-containing moieties, are batimastat (BB-94) and its orally bioavailable form, matimastat (BB-2516) [17, 73, 144]. They have been involved in many studies for cancer treatment and together are able to inhibit several MMPs, like MMP-1, -2, -3, - 7, -9, and -12 [73, 144].

1.7.3.2. Batimastat

BB-94 has long been known to be a low molecular weight, synthetic and broad-spectrum inhibitor of many MMPs [73, 157]. It was the first of the MMPIs to be studied in humans and to initiate clinical trials for cancer treatment [144, 157, 158].

Its collagen-mimicking hydroxamate structure chelates the zinc ion and leads it to inhibit the proteases in a potent and specific manner [157, 159]. It essentially inhibits the activity of MMP-1, MMP-2, MMP-7, and MMP-9 [158, 159], blocking further ECM degradation (Figure 8), and shows extremely low water solubility, and so a poor oral availability [73, 157, 159].

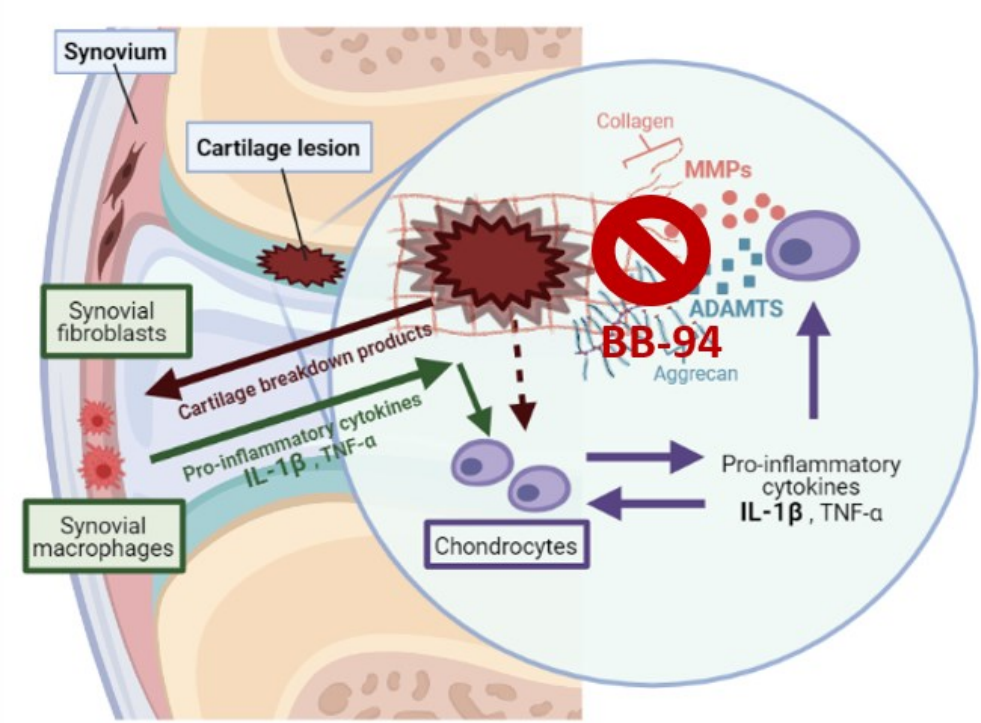

Figure 8 - BB-94 action in blocking MMPs activity in the osteoarthritis pro-inflammatory vicious cycle. Schematic illustration produced using image resources from BioRender (biorender.com).

1.7. DRUG NANODELIVERY SYSTEMS FOR OA THERAPY

Drug delivery into the affected joint is very challenging, due to poor bioavailability for therapeutics administered systemically and to the rapid clearance of drugs after intra-articular injection [66]. To overcome these limitations and maximize drug supply, innovation is needed in delivery systems, such as applications of nanotechnology [66, 160], to selectively and safely target OA joints in a more durable way [160]. This is very important, once to enable a potential disease-modifying effect an optimal therapeutic level of the compound in the joint should be maintained [65].

Nano-scale materials can be engineered in size to clear the drug more slowly than its free form, thus improving drug time of residence and its biodistribution in the joint

[66]. Also, nanomaterials can penetrate ECM and cell barriers, being able to release drugs either within cartilaginous ECM or intracellularly [66].

In fact, nanomaterials have reliably shown improved features when comparing to the administration of the free drug, such as improved retention profiles within the joint space [66, 161].

Nanomaterials exist in many forms and designs, providing opportunities for the delivering of several classes of drugs [66]. For instance, lipid-based carriers and nanoemulsions are suitable for loading lipophilic and poorly soluble compounds while polymeric nanoparticles with adjustable degradation rates can encapsulate either hydrophobic and hydrophilic drugs [66, 162]. Therefore, nanomaterials can accommodate a wide range of therapeutics classes that can be disease-modifying, including cytokine and enzyme inhibitors [66].

1.7.1. Nanoparticles

Currently, the most innovative nanomaterials for management of OA are nanoparticles (NPs) [163]. NPs aim to release drugs in a prolonged fashion, ensuring an improved bioavailability by sustained release and delivery [163], while showing increased pharmacodynamics actions and targeting effects [164]. Additionally, these nanodelivery systems can also promote increased drug solubility [162] and decreased toxicity [165]. Overall, these are very attractive features for OA therapy [163].

A variety of materials can be used for the production of NPs, namely natural polymers like chitosan, BSA, HA and chondroitin sulfate [163], and synthetic ones as poly(lactic-co-glycolic acid) (PLGA), polylactic acid (PLA) and and polycaprolactone (PCL) [165, 166]. In addition, several compounds with different water solubility can be encapsulated in NPs, namely NSAIDs as ibuprofen. An enhanced solubility and dissolution rate in water solvent has been reported for ibuprofen NPs in comparison to the free drug [149].

1.7.1.1. Poly(Lactic-Co-Glycolic Acid)

PLGA is one of the most frequently used polymers for preparing NPs [166], essentially because its excellent biocompatibility, biodegradability, and mechanical strength features [166, 167]. This polyester copolymer is approved by the FDA and the European Medicine Agency (EMA) for many medical and pharmaceutical applications, including drug delivery [167]. This inert polymer has been successfully employed to for the sustained release of NSAIDs, anti-TNF-α and IL-Ra therapies in arthritis models [168].

Different nanoencapsulation techniques can be used for loading either hydrophobic or hydrophilic drugs into PLGA NPs [169]. Studies involving the delivery of ibuprofen by PLGA NPs have been conducted, showing promising results as an anti-proliferative approach for cancer cells [170, 171].

1.7.1.2. Chitosan/ Polyglutamic Acid

Chitosan, a natural polysaccharide that derives from chitin, is a biocompatible, biodegradable, non-toxic, low-immunogenic and highly stable material [162, 164, 172, 173]. Its structure is similar to the GAGs found in articular cartilage [174], providing a microenvironment adequate for ECM synthesis and chondrocyte proliferation [173]. Besides, additional properties of chitosan useful for damaged cartilage applications are related with its ability to reduce inflammatory profile of chondrocytes and induce chondrogenic differentiation [173].

Previously reported results showed that carboxymethyl-chitosan, a soluble derivative of chitosan, could inhibit IL-1β-induced apoptosis of rabbit chondrocytes [175].

Like PLGA NPs, the chitosan ones also support a controlled drug release, but their profile is characterised by an initial fast phase followed by a delayed phase [176]. Zhou et al. reported good stability and this expected two-staged releasing profile of chitosan NPs *in vitro* [164].

As for polyglutamic acid (PGA), it is natural biopolymer that also possesses biocompatibility, biodegradability and non-immunogenicity properties, which have attracted much interest for its use in biomedical applications [177].

There are two forms of PGA, poly-α-glutamic acid (α-PGA) and poly-γ-glutamic acid (γ-PGA), and both are water-soluble [177]. In fact, γ-PGA was proved to improve the MSCs chondrogenic differentiation and increase ECM production in a 3D pellet culture [178].

In the case of PGA-based NPs, they are frequently used to improve the stability of water-soluble and insoluble drugs [177].

Chitosan/γ-PGA NPs have been tested in several studies, for instance in a degenerative intervertebral disc *ex vivo* model, where NPs loaded with the NSAID diclofenac had a role in inflammation control and ECM remodelling [179]. As chitosan and γ-PGA present opposite charges, they spontaneously self-assemble in an environment with controlled pH [179]. They are stable at pH 5.0 and have been studied as delivery systems for a variety of molecules [179].

1.7.2. Nanoemulsions

Nanoemulsions (NEs) are basically emulsions with nano-sized droplets [180], whose mean diameters are typically below 200 nm [180, 181].

These delivery systems usually consist of a mixture of two immiscible liquids, normally oil and water, which can form spherical droplets of on phase in the other phase [180, 181]. NEs can exist either in an oil-in-water (o/w) or water-in-oil (w/o) form, where the droplets are made of oil or water, respectively [181].

NEs are produced to improve the delivery of active pharmaceutical compounds [180] and are effective drug delivery systems [181]. Their main advantages include

improved drug bioavailability, enhanced physical stability, and greater dissolution and loading of poorly water-soluble drugs while protecting them from enzymatic degradation [180, 181].

As such, can be used for the encapsulation and further administration of a wide variety of more lipophilic/poorly soluble anti-inflammatory agents, including BB-94.

1.7.3. Scaffold-Embedded Nanodelivery Systems

Scaffolds are of utmost importance for cartilage tissue engineering, as they provide an appropriate three-dimensional (3D) environment for chondrocytes [182]. They should be porous, biocompatible, biodegradable and mechanically stable, in order to withstand the high loads to which the native cartilage was subjected to [5, 174, 183]. Another advantage is that they can be molded in an unlimited diversity of shapes to fit the cartilage defect [184].

After implantation, scaffolds components will constitute a physical support for chondrocytes attachment, migration and eventual production of new cartilaginous tissue [174, 183].

These supporting structures can be synthesised with natural or synthetic biomaterials and numerous compounds have been investigated for such purpose [182]. Even though the best material for an ideal scaffold production is not consensual [182], the most studied are made of alginate, PLGA, chitosan, collagen and PLA [174, 183-187].

A common cartilage tissue engineering strategy is to combine scaffolds and therapeutic delivery systems to act locally at the defect site [188, 189]. This way, bioactive molecules with a controlled release are incorporated within the scaffolds, being a promising approach for OA treatment [189].

1.7.3.1. COPLA® Scaffold

In order to sustain the mechanical loads, specialized scaffolds can be produced by combining two or more materials [185]. As the native cartilage structure is formed by a collagen network with proteoglycans, a structural protein as collagen is a potential scaffold material [174].

However, collagen cannot bear all the mechanical forces involved in the damaged microenvironment alone [174]. As an adjuvant, other polymer with good mechanical properties can be added to the structure, like PLA or PLGA, forming a hybrid scaffold to combine their strengths [174]. This way, it is possible to retain the advantages of the two materials.

PLA is a biocompatible, low-immunogenic and biodegradable synthetic material that is produced by polymerization of lactic acid [187, 190]. It also demonstrates good thermal/mechanical properties and has been broadly used in drug delivery systems [191].

Haaparanta et al. showed that among collagen/PLA, chitosan/PLA, and collagen/chitosan/PLA hybrid scaffolds, the ones with most potential for cartilage tissue engineering are collagen/PLA hybrids [174].

COPLA® Scaffold is a 3D biodegradable, highly porous polymer scaffold for application in the cartilage repair of affected weight-bearing joints [192].

Although COPLA® Scaffold was designed to be applied in humans, it is currently only used in veterinary medicine, like in dogs and horses suffering from cartilaginous damage [193, 194]. It is surgically implanted onto the previously debrided defect site and secured to it with a fibrin glue [192, 193]. It works both for chondral and osteochondral defects, once it is easily tailored for any size or depth of the target location, promoting a microenvironment favourable for new synthesis of tissue [192].

2. MOTIVATION

Each year, injuries to articular cartilage disturb more than one million people worldwide [35]. If left untreated, these damages can progress towards OA [3, 195], a chronic and progressive joint disease [14] that is currently one of the main global causes of disability [196, 197].

World Health Organization estimates that approximately 9.6% of men and 18.0% of women aged over 60 years have symptomatic OA [198] and predictions point out that 237 million of people worldwide are affected by OA [199]. Of those, 80% are likely to have limitations in movement and 25% are expected not to be able to perform their daily life activities [198], leading to expensive treatments [52] and having a tremendous negative impact in their health and quality of life [95].

Although it is very challenging to compare the OA socioeconomic weight among different countries, the annual average of direct medical costs (e.g., including treatments and hospital stays) in United States of America per osteoarthritic patient in 2015 ranged from US$1.442 to US$21.335 [200], whereas it ranged from €534 to €1.788 per patient across Europe, between 2004 and 2012 [201].

In addition to leading to a high socioeconomic burden both for patients and society, musculoskeletal disorders like OA are highly prevalent and, even so, the number of affected patients is projected to increase in future years [95].

The first line of cartilage damage treatment consists of conservative approaches, such as physical therapy, bracing, analgesics, and intra-articular injections. If these fail to decrease patients' pain and/or damage progression, then surgical-based techniques have to take place [49, 106].

TJA, a common and helpful surgery for aged and end-stage osteoarthritic patients, is a definitive procedure and is not advised for younger patients [45, 106, 202]. This last contraindication is essentially based in orthopaedic prosthesis generally not fully restoring joint function and usually failing during the patient's lifetime [127], mostly due to wear, components loosening and periprosthetic joint infection [203, 204].

However, symptomatic OA is the reason why more than 95% of all knee [108] and more than 90% of all hip replacements are preformed [205].

According to the statistical data provided by the Portuguese Arthroplasty Register of the Portuguese Society of Orthopaedics and Traumatology, between January 2019 and May 2021, around 4640 knee and 4030 hip arthroplasties were performed in Portugal. Of those, around 240 of the knee and 350 of the hip TJA surgeries were of revision. These data relate only to public hospitals on the mainland [206].

Still, global statistical projections point out that the performance of total hip arthroplasties will grow up to 174% by 2030, towards 572000 procedures, and by 673% in the case of the knee, towards 3,48 million procedures, followed by an also expected increase in revision surgeries [207].

Despite these data, it is gradually more recognised that OA does not affect only the elderly, but also many young individuals and athletes, mainly as a consequence of repetitive trauma, as in doing sports [63, 208].

Therapies more suitable for younger ages and able to fully restore joint function are increasingly needed, therefore cartilage repair approaches arise as a clinical alternative. These techniques are often grouped into 3 categories: marrow stimulation-based (as microfracture), osteochondral transfer (osteochondral auto- and allografts transplantation) and cell-based cartilage repair (including autologous chondrocyte transplantation) [133].

However, each of these clinical treatments has limitations of usage and diversified long-term outcomes [209]. Overall, in all of the surgical techniques that aim to promote cartilage repair, a transversal problem is the quality of the newly formed cartilage as a fibrocartilaginous tissue is formed, being less durable and less able to bear loads than native articular cartilage. As such, so far no method as resulted in repair tissue of desirable quality [186].

As such, current clinical therapies typically try to control pain and improve joint function [65] with slight effectiveness and particularly do not halt the pro-inflammatory environment that the joint experiences in cartilage damage, meaning they have to be reconsidered [71]. Moreover, being the progressive destruction of cartilage an important hallmark in OA, this highlights the need of developing treatments that can effectively slow down or halt this structural progression of the disease, namely by the exploration of drugs that have this ability rather than simply alleviate symptoms [71, 143]. This is especially important once there is currently no approved drug available in clinical practice capable of modifying or treating the disease, which makes this area of research of major significance [210].

Furthermore, the determination of the optimal route for biologic agents administration in OA remains a challenge [71] and so the improvement of drug delivery strategies is an urgent clinical need [66].

Considering all this, this work arises from the pressing need to find new approaches to halt the progression of articular cartilage lesions and eventually treat the damaged area. Furthermore, this work is, therefore, motivated by the urgency to provide a better quality of life to patients affected with cartilage lesions and to prevent them from evolving towards OA, along with the goal to achieve a more tailored therapy for each patient. A reasonable approach is to therapeutically target the originated inflammatory cascade [84].

3. AIMS

To meet the demand for the development of an appropriate and effective therapy for handling cartilage lesions, *in vitro* experiments were conducted with human articular chondrocytes (hACs) to mimic the microenvironment and the behaviour that cells experience *in vivo*.

Herein, the local delivery of anti-inflammatory and anti-proteolytic compounds through the implantation of a biodegradable, biocompatible and nanoenabled COPLA® Scaffold in the defect site is proposed as a treatment for cartilage lesions, as an attempt to slow or halt their progression and restore joint function.

For that to be accomplished in the future, this work aimed to assess the chondroprotective effects of nanosystem-delivered ibuprofen and BB-94 on the pro-inflammatory microenvironment of cartilage lesions.

To meet this main goal, several tasks were carried out as follows:

1. Establishment and characterization of primary hACs 3D pellet cultures;
2. Establishment of pro-inflammatory conditions in 3D pellet cultures;
3. Evaluation of the chondroprotective effects of ibuprofen-loaded PLGA nanoparticles, ibuprofen-loaded chitosan/PGA nanoparticles, BB-94-loaded nanoemulsions, tri-combinatory nanoemulsions (ibuprofen, BB-94 and nisin), and mupirocin-loaded nanoemulsions in the 3D pellets cultured under pro-inflammatory conditions;
    a. Assessment of ibuprofen-loaded PLGA and Ch/PGA nanoparticles, and BB-94-loaded, tricombinatory nanoemulsions and mupirocin-loaded concentrations with reproducible chondroprotective effects.
4. Evaluation of the capacity of COPLA® Scaffolds to support human chondrocytes' adhesion, differentiation and ECM production;
5. Establishment of a pro-inflammatory microenvironment in COPLA® Scaffolds.

4. MATERIALS AND METHODS

4.1. MATERIALS

Isolation Medium

Isolation medium was composed of Dulbecco's modified Eagle's medium high glucose (DMEM; 4.5% glucose, Gibco®) containing 5% penicillin/streptomycin (P/S; Gibco®) and 10% fungizone (Sigma-Aldrich).

Digestion Medium

For the digestion of articular cartilage, 0.15% collagenase B (Roche) was dissolved in DMEM-high glucose (4.5% glucose, Gibco®) and 5% fetal bovine serum (FBS; Gibco®) [211].

Because of the enzyme, the use of gloves while preparing and using this medium is of major importance [18]. The collagenase B should only be added to the medium immediately before the isolation procedure is carried out, and after this enzyme addition the medium should be filtered through a 100 µm pore-sized strainer to remove any contamination.

Expansion Medium

The expansion medium used throughout the study was composed of DMEM (4.5% glucose, Gibco®) supplemented with 10% FBS (Gibco®), 1% N-2-hydroxyethylpiperazine-N-2-ethane sulfonic acid (HEPES buffer, 1 M, Gibco®), 1% sodium pyruvate (Gibco®) and 1% P/S (Gibco®). In addition, 1 ng/mL transforming growth factor beta 1 (TGF-β1; R&D) and 5 ng/mL basic fibroblast growth factor (bFGF; Sigma-Aldrich) were freshly added to the medium [211].

Basal Medium

This medium was formulated from DMEM-high glucose (4.5% glucose, Gibco®), 10% FBS (Gibco®) and 1% P/S (Gibco®) [211].

Chondrogenic Medium

The chondrogenic medium supporting the 3D cultures was prepared with DMEM-high glucose (4.5% glucose, Gibco®) supplemented with 5 µg/mL insulin (Sigma-Aldrich), 5 µg/mL Transferrin (Sigma-Aldrich), 1 mM sodium pyruvate (Gibco®), 5 ng/mL selenous acid (Sigma-Aldrich), 0.1 µM dexamethasone (Sigma-Aldrich), 0.17 mM ascorbic 2-phosphate acid (Sigma-Aldrich), 0.35 mM proline (Sigma-Aldrich), 1.25 mg/mL bovine serum albumin (BSA; Sigma-Aldrich). Lastly, 10 ng/mL TGF-β3 (R&D) were freshly added to the medium [211].

4.2. METHODS

4.2.1. Collection of Human Articular Cartilage Samples

Human articular cartilage samples were collected from osteochondral leftovers from the hip or knee joints of patients undergoing total joint replacement at Centro Hospitalar Universitário de São João, after the Hospital ethics committee approved the study (ethical approval ref. 196/19) and an informed consent was given by all patients.

After surgery, osteochondral specimens were immersed in a sterilized 250 mL bottle containing an adequate amount of isolation medium and then transported to the laboratory for further processing. During transportation, the osteochondral tissue was kept in cold with ice to prevent the tissue from cell death [212]. The cartilage samples were then taken from regions of the joint with no macroscopic signs of articular degeneration and mechanically dissected with a nº11 scalpel blade in a petri dish with isolation medium, originating approximately 2x2 mm pieces of cartilage tissue (Figure 9).

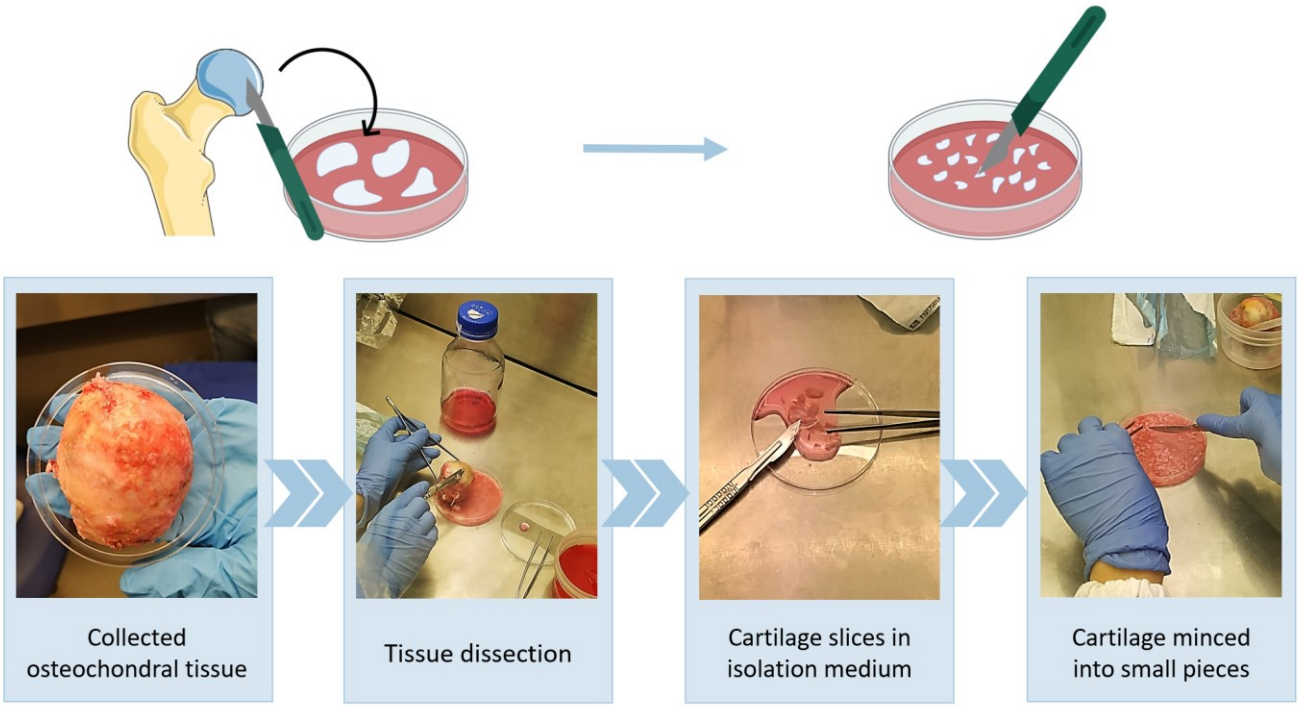

Figure 9 - A step-by-step scheme of cartilage isolation from osteochondral tissue. Schematic illustration produced using image resources from BioRender (biorender.com) and pictures taken at the i3S facility.

4.2.2. Cartilage Digestion and Cellular Expansion of Isolated Primary Human Articular Chondrocytes in Monolayer Culture

The minced cartilage was left in an incubator shaker overnight at 37°C, 100rpm, in a shot flask with digestion medium containing 0,15% of collagenase B. Upon digestion,

hACs effectively extracted from ECM were filtered through a 100µm pore-sized cell strainer (as previously described [213]) to a 50 mL conical tube and centrifuged twice at 1200 rpm for 12 min. Cells were gently resuspended in expansion medium after each centrifugation. To determine cell density and viability, 10µL of the suspension were transferred into an Eppendorf tube and mixed with 10µL of trypan blue solution (Sigma-Aldrich) and placed in the hemocytometer for cell counting.

Afterwards, cells were subcultured into 75 cm^2 culture flasks. Following the extraction of chondrocytes from cartilage, the first culture performed is known as passage 0 (P0) [214]. Chondrocytes were reseeded under the same conditions for a maximum of 4 passages (P4) or until reaching the necessary cell quantity for the succeeding experiments, and kept in an a humidified 37°C/5% CO_2 incubator in expansion medium. The cells were observed regularly with an inverted microscope and expansion medium was changed twice a week until reaching 70-90% cell confluency. These steps are schematically summarized in Figure 10.

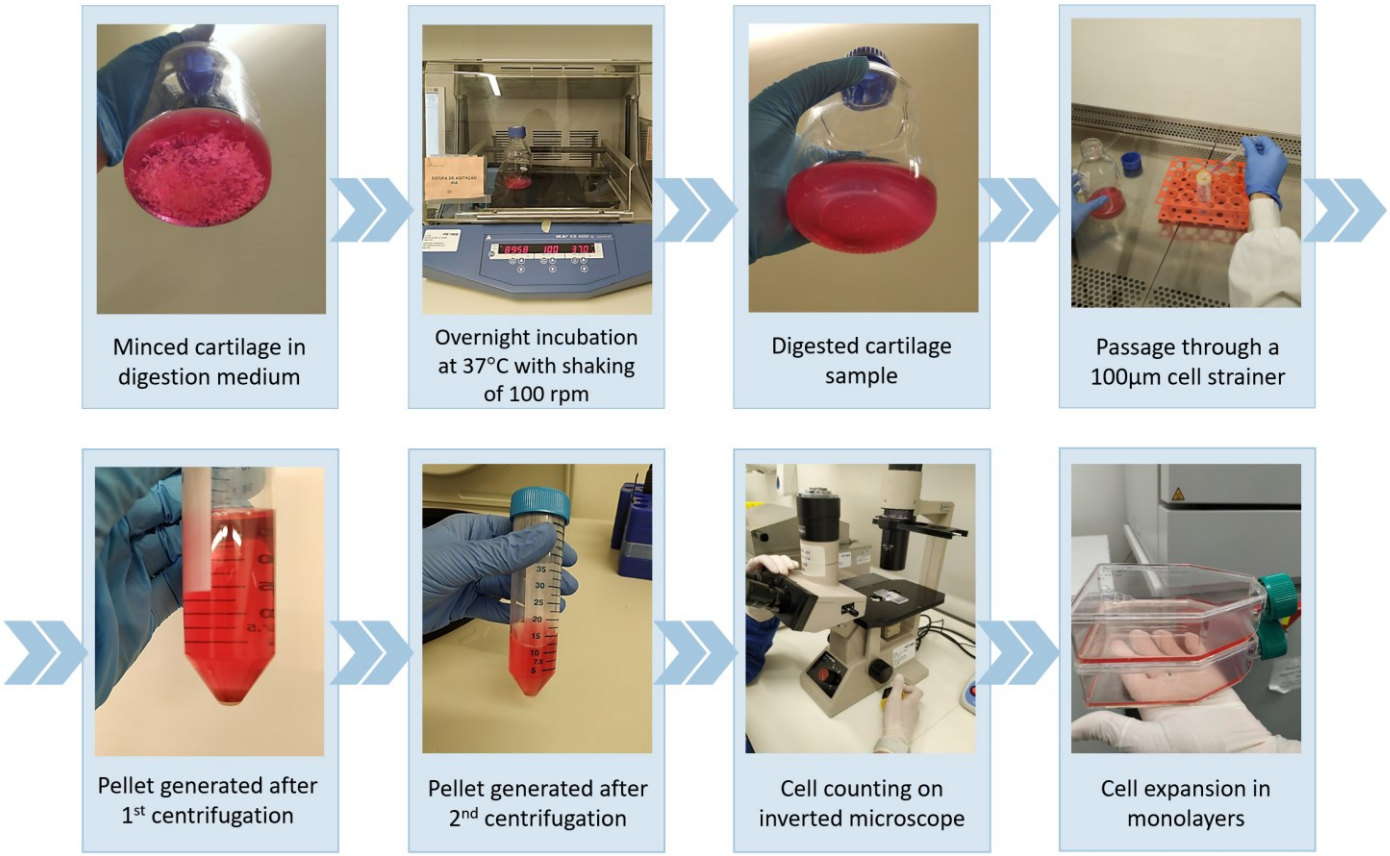

Figure 10 - Steps involved in the process of cartilage digestion and cellular expansion in monolayers. Pictures taken at the i3S facility.

4.2.3. 3D Pellet Culture of Human Articular Chondrocytes

When confluence and the needed amount of cells was reached, passaged cells were washed with phosphate-buffered saline (PBS) and detached with 0,25% trypsin. FBS in basal medium inactivates the activity of trypsin [212] and the cell detachment was observed with an inverted microscope. Cells were then seeded in 15 mL polypropylene conical tubes with a filter on the lid (to facilitate gas exchange) at a density of 1×10^6 cells/tube/1mL with basal medium [211].

A centrifugation of 5 minutes at 390 *g* was conducted and the resultant chondrocyte pellets were then cultured in basal medium and placed into a 5% CO_2 incubator at 37°C [211]. When 24 hours have passed, 3D pellets were cultured under different conditions according to each further explained experiment: 1) characterization of primary hACs in 3D pellet cultures (28 days differentiation experiment); 2) establishment of the pro-inflammatory conditions; 3) evaluation of the effects of ibuprofen-loaded PLGA NPs, ibuprofen-loaded chitosan/PGA NPs, BB-94-loaded NEs, tri-combinatory NEs (Ibuprofen, BB-94 and Nisin), and mupirocin-loaded NEs in the 3D pellets cultured under pro-inflammatory conditions. Every experiment was performed in triplicates.

In each experiment, chondrocytes were induced to redifferentiate in conical tubes with the above mentioned cell density each, giving rise to pellets that were further analysed at different timepoints, that is, either fixed for histological and immunohistochemical analysis or processed for RNA extraction and whose supernatant was collected for cytotoxicity assay and cytokine profiling.

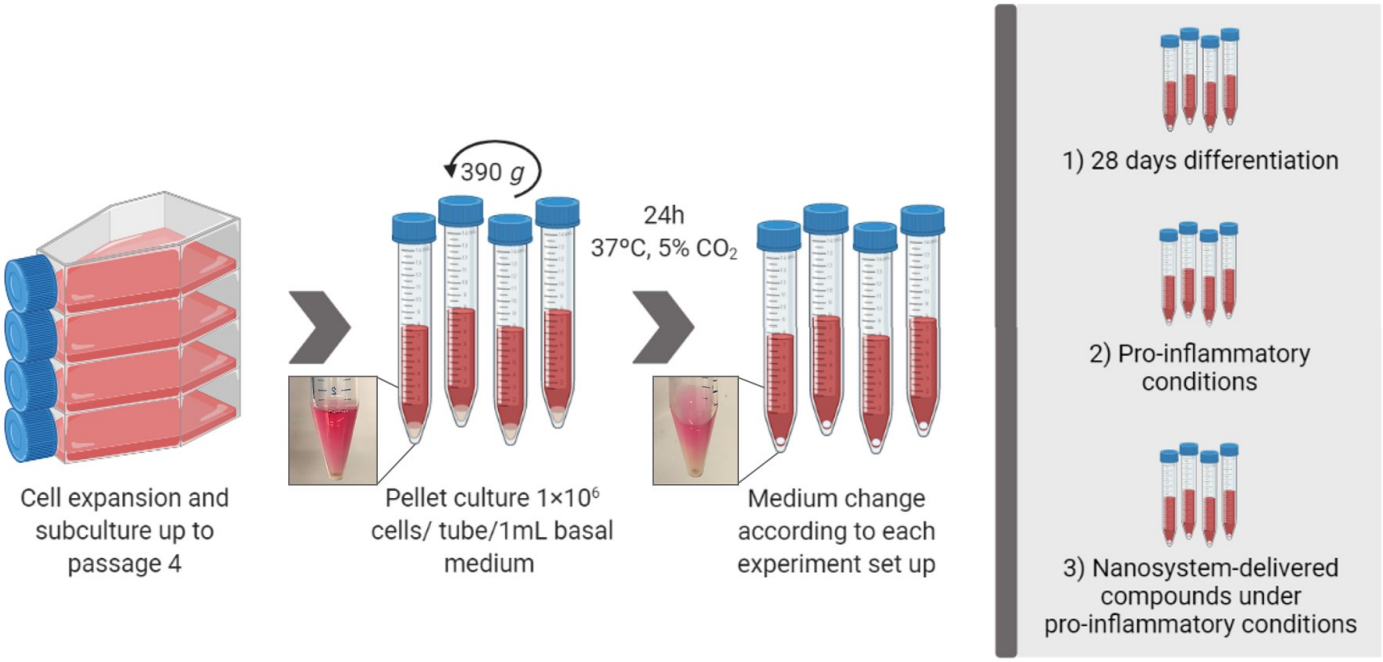

Figure 11 - Schematic representation of the experimental design to culture human articular chondrocytes in 3D pellet culture and their subsequent utilization in different experiments. Schematic illustration produced using image resources from BioRender (biorender.com). Pictures taken at the i3S facility.

4.2.4. 28 days of Chondrogenic Differentiation Experiment

A day after the pellets were formed, the volume of basal medium was fully replaced by 1 mL of either chondrogenic or fresh basal medium (for the control condition). In this experiment, the day of medium replacement is established as the day 0 of culture and further collection timepoints are counted following that day. Medium was further changed twice a week during the 28 days of culture. Both pellets and conditioned mediums were collected at days 3, 7, 14, 21 and 28 of culture (Figure 12).

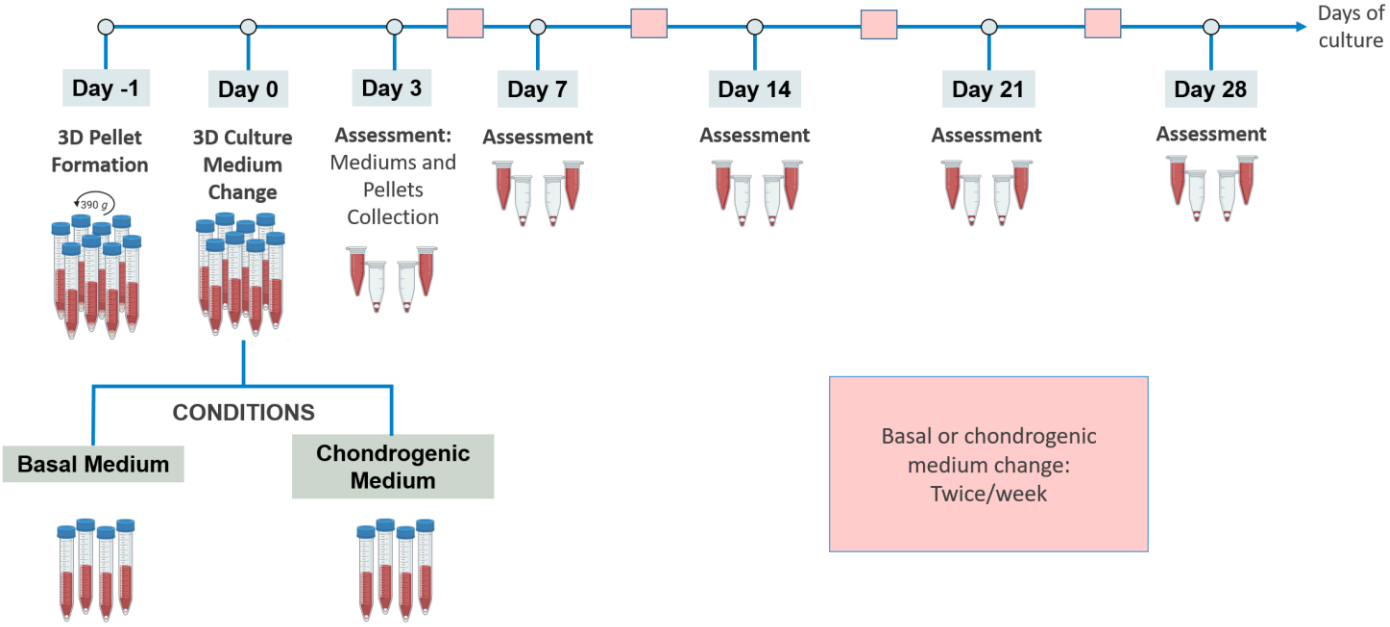

Figure 12 - Experimental set up of the 28 days of 3D chondrogenic differentiation experiment. Schematic illustration produced using image resources from BioRender (biorender.com)

4.2.5. Establishment of Pro-Inflammatory Conditions In Primary Human Chondrocytes 3D Pellet Cultures

A day after the pellets were formed, basal medium was fully replaced by 1 mL of chondrogenic medium. Pellets were then left to redifferentiate for 7 days and, during that time of culture, the total volume of chondrogenic medium was once changed.

After the 7 days of differentiation, freshly chondrogenic medium was added to the pellets along with pro-inflammatory conditions, IL-1β (Prepotech®) and/or TNF-α (ImmunoTools).

For this purpose, pellets were divided into 7 groups: 1) chondrogenic control; 2) IL-1β 10 ng/mL; 3) IL-1β 100 ng/mL; 4) TNF-α 10 ng/mL; 5) TNF-α 100 ng/mL; 6) IL-1β and TNF-α at 10 ng/mL each; 7) IL-1β and TNF-α at 100 ng/mL each (Figure 13).

In this experiment, the day 0 of treatment is considered the day where the pro-inflammatory cytokines are added to the 3D pellets and further timepoints of mediums and pellets collection were counted following this day. The assessment was made at

day 3 (equivalent to the day 10 of differentiation) to further study the effect of these cytokines on cell viability, expression of chondrogenic markers, pro and anti-inflammatory cytokines release, MMPs and ADAMTSs expression.

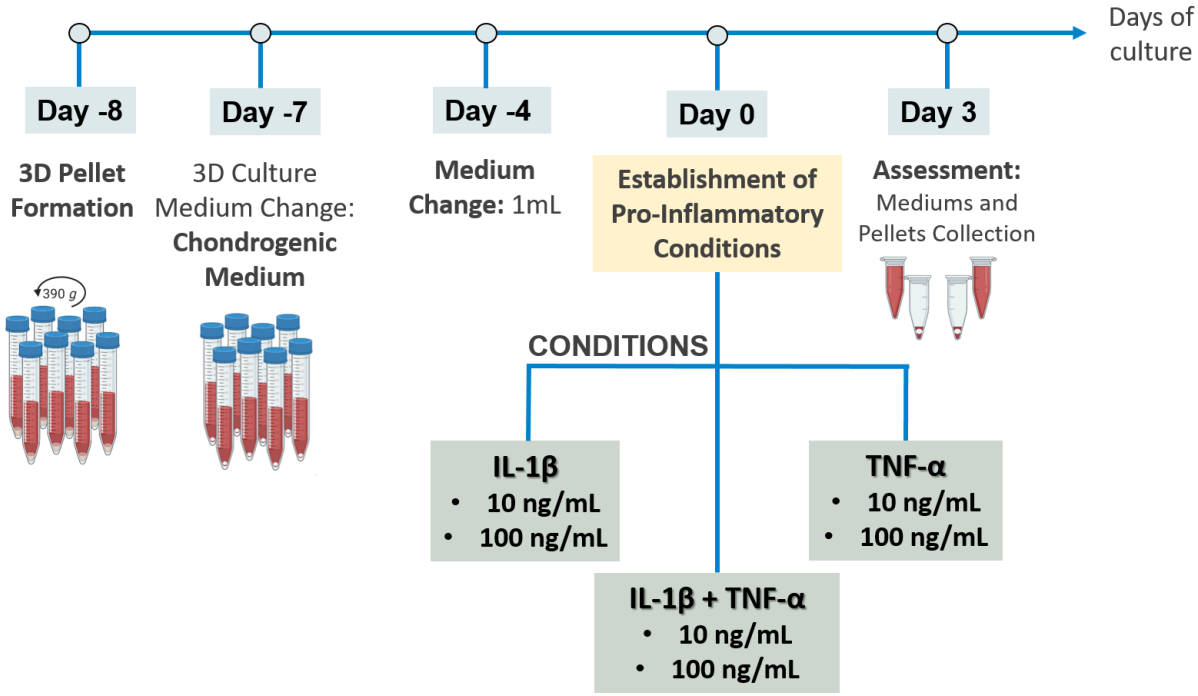

Figure 13 - Experimental set up of the experiment regarding the establishment of pro-inflammatory conditions in 3D pellets. Schematic illustration produced using image resources from BioRender (biorender.com). IL-1β – Interleukin-1Beta; TNF-α – Tumor Necrosis Factor-Alpha.

4.2.6. Addition of Nanosystem-Delivered Anti-Inflammatory and Anti-Proteolytic Compounds to 3D Pellets Under Pro-Inflammatory Conditions

A day after the pellets were formed, basal medium was fully replaced by 1 mL of chondrogenic medium. Pellets were then left to differentiate for 7 days and, during that time of culture, the total volume of chondrogenic medium was once changed.

After the 7 days of differentiation, chondrogenic medium was replaced by a fresh one supplemented with pro-inflammatory cytokine IL-1β at 100 ng/mL, and 3h later the different nanocarriers were added to the pellets (Figure 14). This is considered the day 0 of treatment.

The effects on cell viability, GAGs deposition, synthesised levels of collagen type II and aggrecan, cytokine secretion and MMPs expression or activity were analysed 3 days after the exposure to these treatments. Every experiment was performed in triplicates.

In each experiment for the addition of the distinct nanocarriers, two controls were performed: a chondrogenic control, where pellets stayed in culture just in

chondrogenic medium, and an inflammatory control, where pellets where only exposed to the 100 ng/ml of IL-1β.

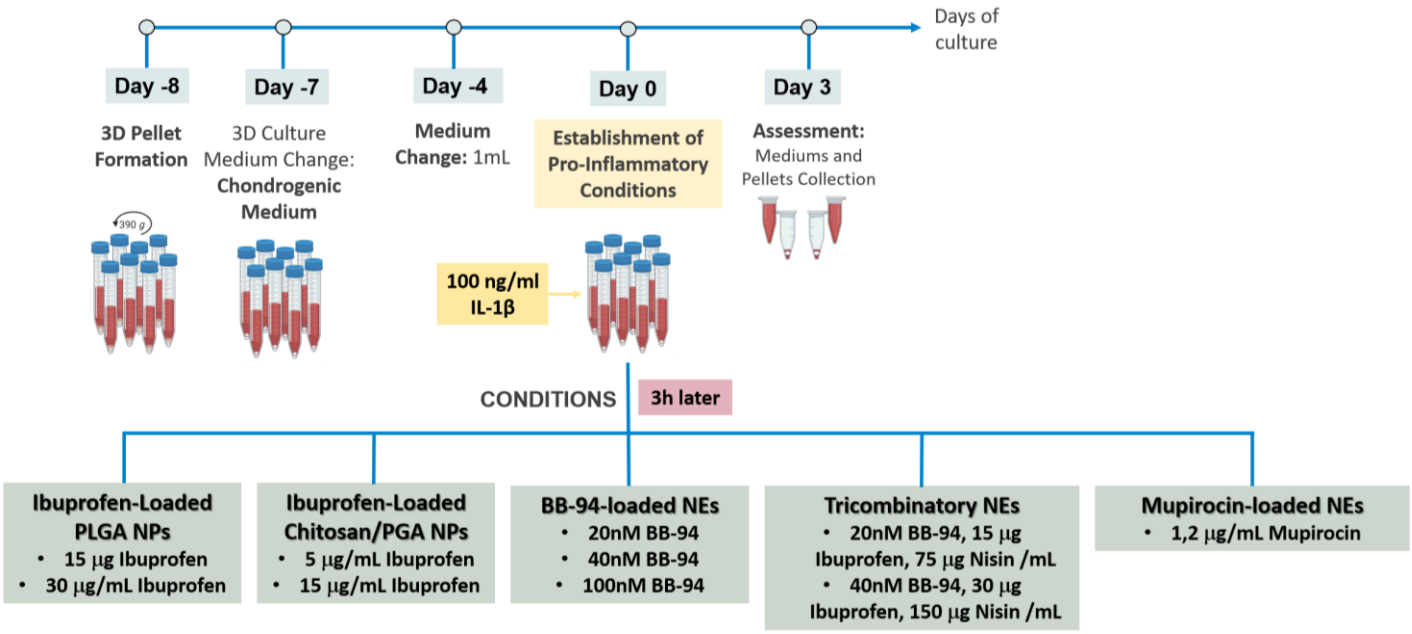

Figure 14 - Experimental set up of the experiment regarding the addition of nanosystem-delivered anti-inflammatory and anti-proteolytic compounds to the 3D pellets exposed to pro-inflammatory conditions (100 ng/mL IL-1β). Schematic illustration produced using image resources from BioRender (biorender.com). IL-1β – Interleukin-1Beta; NPs – Nanoparticles; NEs – Nanoemulsions; PLGA – Poly(Lactic-Co-Glycolic Acid); PGA – Polyglutamic Acid; BB-94 – Batimastat.

The exact conditions tested in each nanodelivery-system experiment are summarized in Table 1.

Information regarding the formulations of the employed NPs and NEs is summarized in Annex 1.

Table 1 - Experimental conditions tested in each experiment to evaluate the effects of Ibuprofen-loaded PLGA NPs, Ibuprofen-loaded Ch/PGA NPs, BB-94 loaded-NEs, Tricombinatory NEs, and Mupirocin-loaded NEs in the 3D pellets established pro-inflammatory microenvironment. NPs – Nanoparticles; NEs – Nanoemulsions; PLGA – Poly(Lactic-Co-Glycolic Acid); Ch – Chitosan; PGA – Polyglutamic Acid; BB-94 – Batimastat.

NANOCARRIER	EXPERIMENTAL CONDITIONS
IBUPROFEN LOADED-PLGA NANOPARTICLES	**Chondrogenic control**: Chondrogenic medium
	Inflammatory control: Chondrogenic medium + 100 ng/mL IL-1β
	Chondrogenic medium + 100 ng/mL IL-1β + **15 µg/mL** of **Ibuprofen** (free form)
	Chondrogenic medium + 100 ng/mL IL-1β + 100 µg/mL of **unloaded** PLGA NPs (concentration of NPs used to encapsulate **15 µg/mL** of ibuprofen in their loaded form)
	Chondrogenic medium + 100 ng/mL IL-1β + 100 µg/mL of **Ibuprofen-loaded** PLGA NPs

	(concentration of NPs that allows an encapsulation of **15 µg/mL** of ibuprofen)
	Chondrogenic medium + 100ng/mL IL-1β + 200 µg/mL of I**buprofen-loaded** PLGA NPs (concentration of NPs that allows an encapsulation of **30 µg/mL** of ibuprofen)
IBUPROFEN-LOADED CH/PGA NANOPARTICLES	**Chondrogenic control**: Chondrogenic medium
	Inflammatory control: Chondrogenic medium + 100 ng/mL IL-1β
	Chondrogenic medium + 100 ng/mL IL-1β + **5 µg/mL** of **Salt Ibuprofen** (free form)
	Chondrogenic medium + 100 ng/mL IL-1β + **15 µg/mL** of **Salt Ibuprofen** (free form)
	Chondrogenic medium + 100 ng/mL IL-1β + 3 µg/mL of **unloaded** Ch/PGA NPs (concentration of NPs used to encapsulate **5 µg/mL** of Salt Ibuprofen in their loaded form)
	Chondrogenic medium + 100 ng/mL IL-1β + 9 µg/mL of **unloaded** Ch/PGA (concentration of NPs used to encapsulate **15 µg/mL** of Salt Ibuprofen in their loaded form)
	Chondrogenic medium + 100 ng/mL IL-1β + 3 µg/mL **Salt Ibuprofen-loaded** Ch/PGA NPs (concentration of NPs that allows an encapsulation of **5 µg/ml** of Salt Ibuprofen)
	Chondrogenic medium + 100 ng/mL IL-1β + 9 µg/mL Ibuprofen-loaded Ch/PGA NPs (concentration of NPs that allows an encapsulation of **15 µg/ml** of Salt Ibuprofen)
BB-94 LOADED-NANOEMULSIONS (FORMULATION 1)	**Chondrogenic control**: Chondrogenic medium
	Inflammatory control: Chondrogenic medium + 100 ng/mL IL-1β
	Chondrogenic medium + 100 ng/mL IL-1β + **20 nM** BB-94 (free form)
	Chondrogenic medium + 100 ng/mL IL-1β + **40 nM** BB-94 (free form)
	Chondrogenic medium + 100 ng/mL IL-1β + **100 nM** BB-94 (free form)
	Chondrogenic medium + 100 ng/mL IL-1β + 1.25 mg/mL of **unloaded** NEs (concentration of NEs used to encapsulate **20 nM** of BB-94 in their loaded form)
	Chondrogenic medium + 100 ng/mL IL-1β + 2.5 mg/mL of **unloaded** NEs (concentration of NEs used to encapsulate **40 nM** of BB-94 in their loaded form)
	Chondrogenic medium + 100 ng/mL IL-1β + 6.25 mg/mL of **unloaded** NEs (concentration of NEs used to encapsulate **100 nM** of BB-94 in their loaded form)
	Chondrogenic medium + 100 ng/mL IL-1β + 1.25 mg/mL **BB94-loaded** NEs (concentration of NEs that allows an encapsulation of **20 nM** of BB-94)
	Chondrogenic medium + 100 ng/mL IL-1β + 2.5 mg/mL **BB94-loaded** NEs (concentration of NEs that allows an encapsulation of **40 nM** of BB-94)
	Chondrogenic medium + 100 ng/mL IL-1β + 6.25 mg/mL BB94-loaded NEs (concentration of NEs that allows an encapsulation of **100 nM** of BB-94)

BB-94 LOADED-NANOEMULSIONS (FORMULATION 2)	**Chondrogenic control**: Chondrogenic medium
	Inflammatory control: Chondrogenic medium + 100 ng/mL IL-1β
	Chondrogenic medium + 100 ng/mL IL-1β + **20 nM** BB-94 (free form)
	Chondrogenic medium + 100 ng/mL IL-1β + **40 nM** BB-94 (free form)
	Chondrogenic medium + 100 ng/mL IL-1β + **100 nM** BB-94 (free form)
	Chondrogenic medium + 100 ng/mL IL-1β + 25 μg/mL of **unloaded** NEs (concentration of NEs used to encapsulate **20 nM** of BB-94 in their loaded form)
	Chondrogenic medium + 100 ng/mL IL-1β + 50 μg/mL of **unloaded** NEs (concentration of NEs used to encapsulate **40 nM** of BB-94 in their loaded form)
	Chondrogenic medium + 100 ng/mL IL-1β + 125 μg/mL of **unloaded** NEs (concentration of NEs used to encapsulate **100 nM** of BB-94 in their loaded form)
	Chondrogenic medium + 100 ng/mL IL-1β + 25 μg/mL **BB94-loaded** NEs (concentration of NEs that allows an encapsulation of **20 nM** of BB-94)
	Chondrogenic medium + 100 ng/mL IL-1β + 50 μg/mL **BB94-loaded** NEs (concentration of NEs that allows an encapsulation of **40 nM** of BB-94)
	Chondrogenic medium + 100 ng/mL IL-1β + 125 μg/mL BB94-loaded NEs (concentration of NEs that allows an encapsulation of **100 nM** of BB-94)
TRICOMBINATORY NANOEMULSIONS	**Chondrogenic control**: Chondrogenic medium
	Inflammatory control: Chondrogenic medium + 100 ng/mL IL-1β
	Chondrogenic medium + 100 ng/mL IL-1β + **1.25 mg/mL** of **unloaded** NEs (concentration of NEs used to encapsulate **20 nM** de BB-94, **15 μg/mL** of Ibuprofen and **75 μg/mL** of Nisin in their loaded form)
	Chondrogenic medium + 100 ng/mL IL-1β + **2.5 mg/mL** of **unloaded** NEs (concentration of NEs used to encapsulate **40 nM** de BB-94, **30 μg/mL** of Ibuprofen and **150 μg/mL** of Nisin in their loaded form)
	Chondrogenic medium + 100 ng/mL IL-1β + **1.25 mg/mL Tricombinatory NEs** (concentration of NEs that allows the encapsulation of **20 nM** de BB-94, **15 μg/mL** of Ibuprofen and **75 μg/mL** of Nisin)
	Chondrogenic medium + 100 ng/mL IL-1β + **2.5mg/mL Tricombinatory NEs** (concentration of NEs that allows the encapsulation of **40 nM** de BB-94, **30 μg/mL** of Ibuprofen and **150 μg/mL** of Nisin in their loaded form)
MUPIROCIN LOADED-NANOEMULSIONS	**Chondrogenic control**: Chondrogenic medium
	Inflammatory control: Chondrogenic medium + 100 ng/mL IL-1β
	Chondrogenic medium + 100 ng/mL IL-1β + **1.2 μg/mL** Mupirocin (free form)

	Chondrogenic medium + 100 ng/mL IL-1β + 10 μg/mL of **unloaded** NEs (concentration of NEs used to encapsulate **1.2 μg/mL** of Mupirocin their loaded form)
	Chondrogenic medium + 100 ng/mL IL-1β + 10 μg/mL **Mupirocin-loaded** NEs (concentration of NEs that allows an encapsulation of **1.2 μg/mL** of Mupirocin)

4.2.7. Seeding of Primary Human Chondrocytes on COPLA® Scaffold

The first step was to cut COPLA® Scaffolds, with an original size of 20 x 20 mm, into round-shaped scaffolds with a 5 mm diameter, by using a punch biopsy tool.

Subsequently, cell seeding on top of COPLA® Scaffolds was performed in two different ways: 1) with human chondrocytes previously expanded in 2D culture monolayers; 2) with human chondrocytes directly seeded after their isolation from cartilage samples.

In the first case, similarly to the procedure that precedes 3D pellets formation, cells were detached from the culture flasks after confluence was reached, as described in 4.2.3. A second approach was to seed the cells on the scaffold right after the isolation procedure from the cartilage samples was completed.

For either experimental set ups, a cell suspension in chondrogenic medium, containing $300x10^6$ cells, was firstly added on top of each COPLA® Scaffold in a 48 well plate and incubated for 5 minutes at 37°C/5% CO_2 (Figure 15). Afterwards, the volume of each well was filled until reaching a total volume of 300 μL/well.

These cell-cultured scaffolds kept in an a humidified 37°C/5% CO_2 incubator in chondrogenic medium and further destined either for a 28-day/14-day experiment or exposed to an IL-1β-induced pro-inflammatory microenvironment.

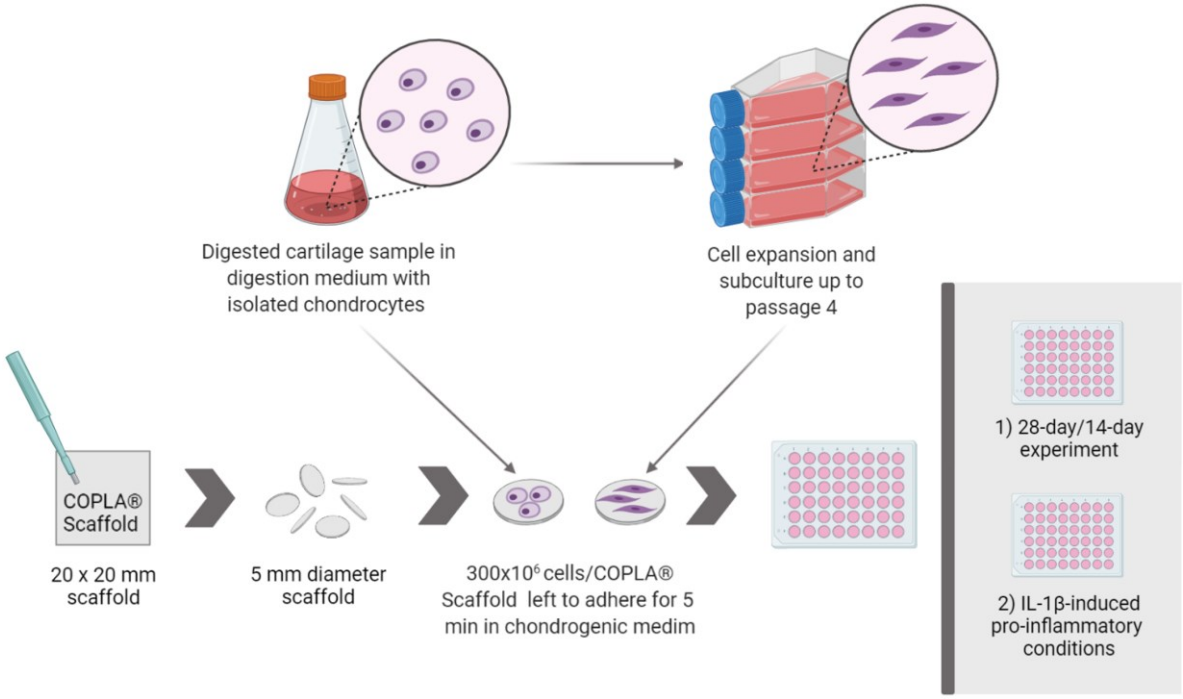

Figure 15 - Experimental set up of the experiments of seeding primary human chondrocytes onto COPLA® Scaffolds and their subsequent utilization in 28-day/14-day of culture and pro-inflammatory experiments.

4.2.8. Culture of Chondrocytes On COPLA® Scaffolds

In order to further evaluate cell adhesion, redifferentiation (when cells were previously expanded) and ECM production, COPLA® Scaffolds seeded with expanded chondrocytes were culture for 28 days and the ones with readily isolated chondrocytes stayed in culture for 14 days. The respective scaffolds and conditioned medium were collected at different timepoints: days 3, 7 and every 7 days after that. Chondrogenic medium was changed twice a week during culture period.

4.2.9. Establishment of a Pro-Inflammatory Microenvironment on Chondrocyte-Cultured COPLA® Scaffolds

The procedure of exposing chondrocyte-cultured COPLA® Scaffolds to IL-1β-induced pro-inflammatory conditions differed between scaffolds with previously expanded chondrocytes and with chondrocytes directly seeded after isolation. In both, experimental conditions were tested in duplicates.

For expanded chondrocytes, cells were first left to redifferentiate in the scaffolds for 7 days (similarly to the pro-inflammatory experiments in pellets, see 4.2.5.) and the total volume of chondrogenic medium was once changed until then. As seen in Figure 16, freshly chondrogenic medium supplemented with 100 ng/mL of IL-1β was added to the scaffolds at day 7. In this experiment, the assessments were made at day 3 (equivalent to the day 10 of differentiation) and day 7 (equivalent to the day 14 of differentiation) to further study the effect of this pro-inflammatory microenvironment on cell viability, expression of chondrogenic markers and pro and anti-inflammatory cytokines release.

Four days after establishing the pro-inflammatory conditions, the 300 µL of medium were replaced by chondrogenic medium without pro-inflammatory cytokines, in order to provide fresh nutrients to the cells.

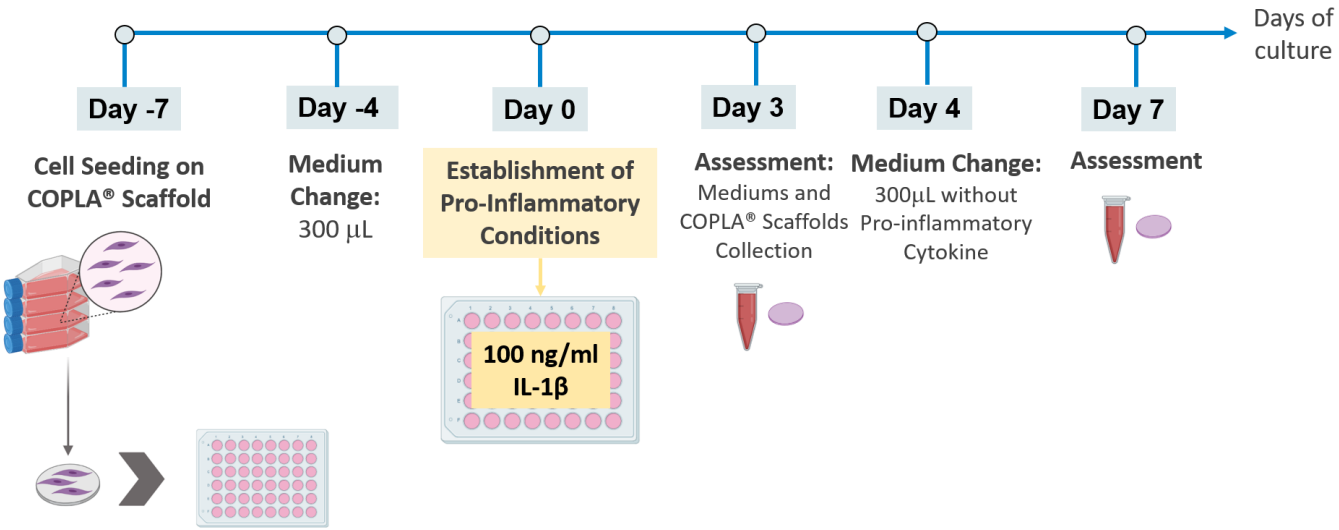

Figure 16 - Experimental set up of the pro-inflammatory experiment in COPLA® Scaffolds seeded with cells that were firstly expanded in monolayer culture. Schematic illustration produced using image resources from BioRender (biorender.com). IL-1ß – Interleukin-1Beta.

As for the chondrocytes directly seeded after isolation from the cartilage sample, two different conditions were tested: one where the IL-1β was immediately added to the medium after cells adhered to the scaffold for 5 minutes (0h); and another where the IL-1β was added to the wells 3 hours after the cell seeding on the scaffold. In this case, timepoints for the collection of conditioned mediums and COPLA® Scaffolds were set as days 3, 7 and 14 (Figure 17). After day 3, the total volume of chondrogenic medium per well was changed twice a week without adding more pro-inflammatory cytokine to it.

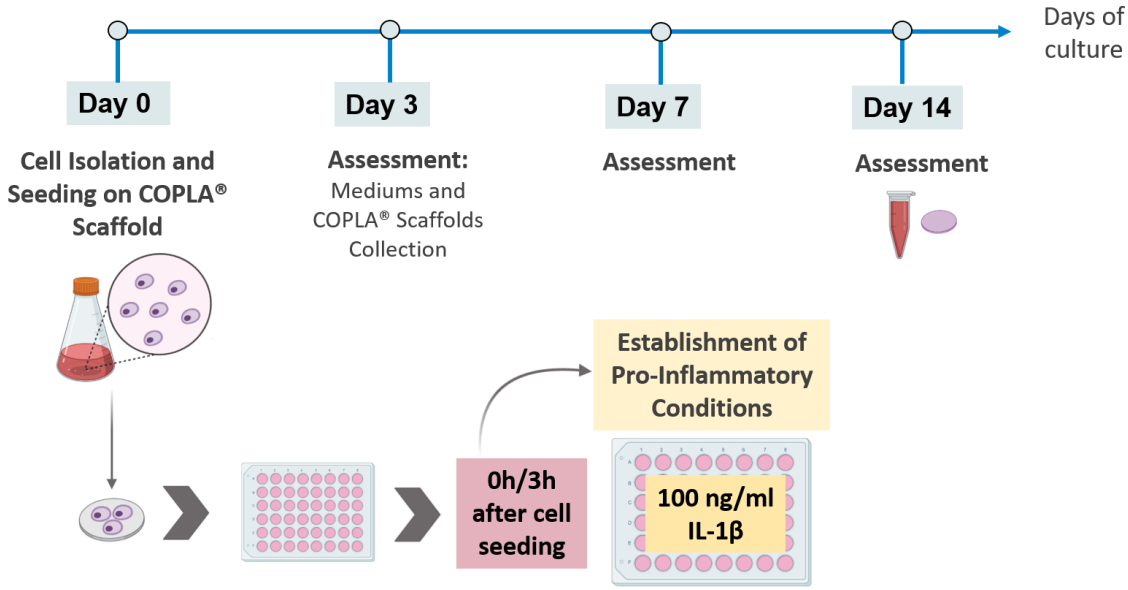

Figure 17 - Experimental set up of the pro-inflammatory experiment in COPLA® Scaffolds directly seeded with freshly isolated cells. Schematic illustration produced using image resources from BioRender (biorender.com). IL-1β – Interleukin-1Beta.

4.2.7. Cytotoxicity Assay

Experiments were analysed for cytotoxicity through the quantification of lactate dehydrogenase (LDH) release in the medium by the pelleted chondrocytes or by chondrocytes seeded on COPLA® Scaffolds, using the CytoTox 96® Non-Radioactive Cytotoxicity Assay (Promega). This was possible because LDH is a stable cytosolic enzyme that is released upon cell lysis and the kit allows for an enzymatic reaction where a colorimetric indicator of LDH activity, tetrazolium salt, is converted into a red formazan product [215]. The amount of resultant colour is proportional to the number of lysed cells.

First, 50 µL of supernatant samples were transferred to a 96 well plate and an equal volume of CytoTox 96® Reagent (prepared through the mixture of substrate mix and assay buffer) was added to each well and incubated for 30 minutes. Stop solution was added afterwards and the absorbance signal was measured at 490nm in a Synergy™ Mx Microplate Reader (BioTek). A sample of the blank control (only with medium) and of the positive control of total cell dead (maximum LDH release control) were also included. To generate this maximum LDH release control, the pellet was first

mechanically fragmented with a needle and then 100 µl of 10X lysis solution were added to the 1 mL of medium containing the pellet and incubated for 45 minutes. Pellets destined for the positive controls were destroyed in order to make possible the lysis solution to penetrate the ECM and reach the embedded chondrocytes.

As for the chondrocytes seeded on COPLA® Scaffolds, 50 µl of 10X lysis solution were directly added to the well and incubated for 45 minutes.

The percentage of cytotoxicity was calculated by subtracting the blank value to each measurement, then dividing the experimental LDH release of each sample by the maximum LDH release, and further multiplying the result by 100. These obtained results were converted into percentage of cell viability, where the negative control is therefore the maximum LDH release.

4.2.10. Histology and Immunohistochemistry

Pellets and COPLA® Scaffolds of each timepoint assessment were washed in PBS, fixed 15 minutes in paraformaldehyde (PFA, 4%) and then left in PBS after being washed in this solution. The COPLA® Scaffolds are then subjected to the immunohistochemical staining protocol.

As for the pellets, after fixation, they were subsequently placed in histology cassettes and were further processed with spin tissue processor (Microm STP 120, Thermo Fisher Scientific), where a series of alcohols is used to remove water from tissues, being then replaced by a medium that allows further paraffin infiltration. Next, pellets were embedded in paraffin, cut into 5 µm cross-sections in the microtome (HistoCore MULTICUT, Leica Bio Systems) and placed onto glass slides. Before histological or immunohistochemical procedures, the fixed pellets underwent dewaxing and hydration in a series of decreasing ethanol concentrations and washing with distilled water (Figure 18).

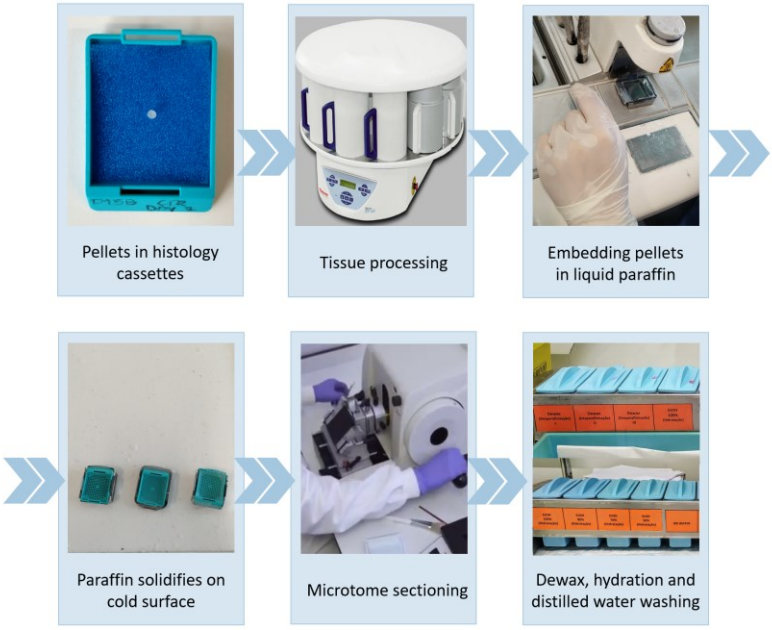

Figure 18 - Series of steps involved in the preparation of pellets for histological and immunohistochemical stainings.

4.2.10.1. Alcian Blue and Safranin-O Stainings

Only the pellets were stained with alcian blue and safranin-O for sulfated glycosaminoglycans (sGAG) and proteoglycans deposition.

For the alcian blue staining, pellet sections were incubated in alcian blue solution for 30 min and then washed with water. Chondrocytes' nuclei were counterstained either by immersion in nuclear fast red for 10 min, or in picrosirius red for 60 minutes followed by acidified water for 30 seconds, and rinsed in water once again [211]. For the safranin-O staining, pellet cuts were immersed in gill hematoxylin for 2 min, subsequently washed with water, incubated in fast green and in acetic acid afterwards; next, the glass slides were immersed in safranin-O for 30 min and then washed with 96% ethanol.

Finally, for the two stains, following dehydration in a series of increasing ethanol concentrations and clearing in xylene, the slides were coverslipped with resinous mounting medium (DPX mounting medium, VWR^{TM}). Images were acquired using an Olympus CX31 light microscope (Olympus) equipped with a Moticam 3+ digital microscope camera 3.0 MP (Motic).

4.2.10.2. Immunohistochemical Staining of Type II Collagen, Aggrecan and Actin

The deposition of the two most important markers of chondrogenic differentiation, collagen type II and aggrecan, in pellets and in COPLA® Scaffolds was assessed by immunohistochemistry. The cellular morphology in COPLA® Scaffolds was also assessed through actin fibers detection with phalloidin.

The slides containing pellets sections and the COPLA® Scaffolds to be immunohistologically examined were blocked for endogenous fluorescence with sodium borohydride 0.1% in tris-EDTA (TE), blocked for free aldehydes with 100 mM NH_4Cl in TE and washed with water or PBS after each blockage, respectively.

To block unspecific antibody binding, sections were then incubated in a solution with 10% FBS and 1% BSA for 1h at room temperature (RT) and incubated overnight at 4°C afterwards, with the respective primary antibody diluted in 10% FBS and 1% BSA (1:100 for collagen type II (Abcam), 1:50 for aggrecan (Santa Cruz Biotechnology, Inc.) and 1:100 for phalloidin (BioLegend)).

After washing with PBS, slides and scaffolds were incubated, light protected, with the secondary antibody (Alexa Fluor 488, Life Technologies), diluted 1:1000 in the before mentioned solution, for 1h at RT and then with 4',6-diamidino-2-phenylindole (DAPI; Sigma-Aldrich) for 5 min to nuclei staining. After each incubation, the samples were carefully washed in PBS. The last step for the slides was the montage with Fluoroshield Mounting Medium (Sigma-Aldrich). Images were acquired using a Leica TCS SP5 confocal microscope (Leica Microsystems).

4.2.11. Cytokine Profiling by Enzyme-Linked Immunosorbent Assay

The measurement of cytokine levels released by chondrocytes in the medium, either in pellets or on COPLA® Scaffolds, was performed by enzyme-linked immunosorbent assay (ELISA). This analysis was carried out for pro-inflammatory cytokines IL-6, IL-1β and TNF-α and for anti-inflammatory IL-10 with kits specific for each cytokine (ELISA MAX™ Deluxe Set, BioLegend®) and following the manufacturer's instructions.

In summary, for all the cytokines, the plate was firstly coated overnight with each monoclonal antibody. In the next day, the diluted standards and samples were added to the wells and the specific cytokine bound to the immobilized capture antibody. Afterwards, a monoclonal detection antibody against each human cytokine was added, producing an antibody-antigen-antibody "sandwich". Subsequently, avidin horseradish peroxidase was added, and a substrate solution was added next, producing a blue colour in proportion to the cytokine in evaluation present in the sample. Lastly, the stop solution was added, changing the reaction colour from blue to yellow. The absorbance was read at 450 nm and at 570 nm in a Synergy™ Mx Microplate Reader (BioTek). Each sample was run in duplicate and the mean value was used for all further calculations. The absorbance at 570 nm was subtracted from the absorbance at 450 nm.

To calculate the respective cytokine concentrations, a standard curve was plotted with standards concentration on the x-axis and their respective absorbance on the y-axis. The concentration of the cytokines in each experimental condition was then calculated using the equation of the curve and taking into consideration each sample dilution (1:1000 for IL-6 and for IL-1β in pellets; 1:250 for IL-6 and for IL-1β in scaffolds, and no dilution for IL-10 and TNF-α both in pellets and scaffolds).

4.2.12. MMP and ADAMTS Expression by Real-Time Quantitative Polymerase Chain Reaction

To quantify the mRNA expression of Sox9, type II collagen, aggrecan, MMPs and ADAMTSs for each experimental condition, the RNA was firstly extracted from the respective pellets, followed by cDNA synthesis and by RT-qPCR performance afterwards. As, unlike ibuprofen, BB-94 does not have an influence in the expression of these proteinases but rather on their activity, this RT-qPCR evaluation was not performed for the experiments were pellets were exposed to the action of BB-94-loaded NEs. This evaluation was not carried out for COPLA® Scaffolds, due to the difficulty in extracting RNA in those conditions.

4.2.12.1. RNA Extraction

For total RNA extraction, pellets were homogenised in TRIzol reagent (Invitrogen) while being cut as small as possible and forced to pass through a syringe and 3 needles of different sizes (19G, 21G and 25G) to cause the lysis of cell membranes.

For RNA isolation, the Direct-zol™ RNA Miniprep kit from Zymo Research was used and following the manufacturer's specifications. All steps were performed at RT and the centrifugations took place at 10000 *g* for 30 seconds.

Briefly, after a first centrifugation, the supernatant was transferred into a new tube and mixed with ethanol. The mixture was poured into a column placed on top of a collection tube, another centrifugation took place and the flow-through was discarded. A pre-wash solution and a wash buffer were added into the column once at a time and a centrifugation was performed after each addition (the second one took 2 min) and the flow-through was rejected. The column was further placed into an RNase-free tube and RNase-free water was placed in the middle of the column filter and centrifuged to elute RNA. The resultant was stored at -80ºC and a 2 µL aliquote was used to measure RNA amount and purity in a NanoDrop spectrophotometer (NanoDrop™ 1000 Spectrophotometer, Thermo Fisher Scientific). To calculate the concentration (ng/µL), absorbance was measured at 260nm, as it is the wavelength at which nucleic acids absorb [216]. The purity is assessed from the ratios of absorbance at 260 nm and 280 nm (260/280) and at 260 nm and 230 nm (260/230) to verify the presence of contaminants that absorb either at 280 nm or at 230 nm, respectively [216].

4.2.12.2. cDNA Synthesis

The NZY First-Strand cDNA Synthesis Kit from NZYTech was used to synthesise single-stranded cDNA from the RNA template to use in real-time quantitative polymerase chain reaction (RT-qPCR) and the instructions of the manufacturer were followed. Briefly, a master mix (containing the primers, deoxyribonucleotide triphosphates (dNTPs), $MgCl_2$ and an optimized RT buffer) and an enzyme mix (containing reverse transcriptase and the ribonuclease inhibitor to avoid RNA degradation), along with diethyl pyrocarbonate-treated water (and, therefore, RNase free) and RNA were placed into a nuclease-free microcentrifuge tube, then mixed and incubated first at 25ºC for 10 min in a thermal cycler (T100™ Thermal Cycler, Bio-Rad) and at 50ºC for 30 min afterwards.

To inactivate the reaction, the content was heated at 85ºC for 5 min and then chilled at 4ºC. RNase H (from *E. coli*) was added to degrade the RNA template and the resultant was incubated for 37ºC for 20 min. The cDNA product was stored at -20ºC until required.

4.2.12.3. Real-Time Quantitative Polymerase Chain Reaction

Using the obtained cDNA, the levels of gene expression of Sox9, type II collagen, aggrecan, MMPs and ADAMTSs, were analysed by RT-qPCR. In this technique, suitable reference genes (also called housekeeping genes) are needed to normalize the expression of the genes of interest [217]. Herein, beta2-microglobulin (B2m) reference gene, which is among the most stable reference genes in chondrocytes [217], was used as internal standard for normalization. Reaction mixtures included cDNA, PCR buffer, dNTPs, iTaq DNA polymerase and each forward and reverse primers. Primer design was performed using the Primer-BLAST and primer sequences are listed in Table 2.

Table 2 – Primer sequences used for RT-qPCR. FW – forward; RV – reverse.

GENE	PRIMER SEQUENCE
SOX9	FW: 5' - GCTCTGGAGACTTCTGAACGA - 3' RV: 5' - CCGTTCTTCACCGACTTCCT - 3'
TYPE II COLLAGEN	FW: 5' - CTGGAAAAGCTGGTGAAAGG - 3' RV: 5' - GGCCTGGATAACCTCTGTGA - 3'
AGGRECAN	FW: 5' - TCCCCTGCTATTTCATCGAC - 3' RV: 5' - CCAGCAGCACTACCTCCTTC - 3'
MMP-1	FW: 5'- CTGTTCAGGGACAGAATGTGCT - 3' RV: 5'- TCGATATGCTTCACAGTTCTAGGG - 3'
MMP-2	FW: 5' - AGTACCGCTGCTCTCTAACC - 3' RV: 5' - CTGGGGCAGTCCAAAGAACT - 3'
MMP-3	FW: 5'- TTTTGGCCATCTCTTCCTTCA - 3' RV: 5'- TGTGGATGCCTCTTGGGTATC - 3'
MMP-8	FW: 5'- CTCCCTGAAGACGCTTCCAT - 3' RV: 5'- TCCAGGTAGTCCTGAACAGT - 3'
MMP-9	FW: 5'- CTTCCAGTACCGAGAGAAAGC - 3' RV: 5'- ATAGGTCACGTAGCCCACTT - 3'
MMP-13	FW: 5'- TCCTCTTCTTGAGCTGGACTCTT - 3' RV: 5'- CGCTCTGCAAACTGGAGGTC - 3'
MMP-14	FW: 5'- TGCCTGCGTCCATCAACACT - 3' RV: 5'- CATCAAACACCCAATGCTTGTC - 3'
ADAMTS-5	FW: 5'- CGCTGCCACCACACTCAA - 3' RV: 5'- CGTAGTGCTCCTCATGGTCATCT - 3'
B2M	FW: 5'- CCAGCGTACTCCAAAGATTCAG - 3' RV: 5'- AGTCAACTTCAATGTCGGATGG - 3'

The RT-qPCR reactions were performed on a CFX384 Touch Real-Time PCR Detection System (Bio-Rad) for 1 cycle of 95ºC for 15 minutes and subsequent 40 cycles of 95ºC for 30 seconds and of the primers annealing temperatures (58ºC) for 30 seconds as well. At the end of the elongation cycle, product fluorescence was detected and a further melting curve analysis was conducted to confirm that a single gene

product was amplified. Each sample was run in duplicate and the mean value was used for all further calculations.

The cycle at which fluorescence reaches the threshold value (threshold cycle, C_t) determines the amount of starting material and thus the degree at which the gene of interest is activated under the examined conditions.

By analysing the data with Bio-Rad CFX Maestro™ Software, the expression levels of target genes in each sample were calculated by normalizing their expression to the C_t levels for B2m. As such, a comparative threshold cycle quantification (ΔC_t method) was executed to quantify DNA, using B2m as the reference gene.

Standard curves for all pair of primers were calculated by plotting the logarithm value of the starting concentration versus C_t and the respective correlation coefficients and slopes were calculated using Bio-Rad CFX Maestro™ Software. The efficiencies of PCR amplification reactions were determined based on the slopes of generated standard curves by using the equation $E\% = [10^{(-1/slope)}-1]\%$. The closest efficiency is to 100%, the more reproducible is the assay. Ideally, efficiency should be between 90-105%. The relative expression of each gene was calculated by using the fold differences as follows: $2^{(C_{t\,reference\,gene}-C_{t\,target})}$ $2^{(C_{t\,reference\,gene}-C_{t\,target})}$. In this method ($\Delta C_t$ method), it is assumed that the efficiency of both target and reference gene amplification is near 100%.

4.2.13. Gelatin Zymography

Either to complement the data of MMPs expression or to evaluate the anti-enzymatic activity of the tested compounds, MMPs activity was measured using gelatin zymography, once some of them can degrade this protein (namely gelatinases, which are MMP-2 and MMP-9).

Firstly, in order to assure that the same weight of protein was loaded on the gel for each condition (10 μg), protein quantification in the conditioned medium of each sample was performed using a Bio-Rad DC Protein Assay (Bio-Rad quantification kit). For this purpose, the first step was to prepare BSA standards from succeeding dilutions of a 10 mg/mL BSA solution, in order to further plot a standard curve. After, in a 96-well plate, 5 μL of each sample, 25 μL of reagent A and 200 μL of reagent B were added to each well in this exact order (in duplicates) and carefully resuspended. After a 15 minutes incubation at RT in the dark, the absorbance was read at 655 nm in a Synergy™ Mx Microplate Reader (BioTek).

After calculating the volume of each sample that contained 10 μg of protein, that volume was mixed with 5 μL of a sample buffer and the respective volume was filled to a final of 10 μL with deionised water. Later, those 10 μL were loaded on the gel and 10 μL of protein ladder (SeeBlue™ Plus2 Pre-stained Protein Standard, Thermo Fisher Scientific) were added to each well of the gel next.

The tank was filled with a running buffer and the used voltage for running the samples was of 125 V during 90 minutes. After electrophoresis, the gels were incubated in a renaturing buffer for 30 minutes at RT with gentle agitation. Subsequently, the renaturing buffer was replaced by a developing buffer and the gel was equilibrated for 30 minutes at RT with gentle agitation and fresh developing buffer was added to the gel afterwards. Followed to an incubation at 37°C for 4 hours, the gel was stained with comassie blue for 5 minutes and then the bands were de-stained with a de-staining solution until they were clear. The last step was to wash the gels with deionised water and gels were later on imaged using a GS-800 Calibrated Densitometer (Bio-Rad).

Lastly, the absolute density of the bands of each experimental condition was quantified in the taken images using ImageJ software (version: 2.1.0).

4.2.14. Pellet Size Measurement and Area Calculation

When collected at the established timepoints, pellets were photographed with an Olympus a SZX10 zoom stereo microscope equipped with an EP50 WLAN-enabled digital camera (Olympus) and analysed using ImageJ software (version: 2.1.0) for each experimental condition. After measuring the horizontal (a) and the vertical length (b) of each pellet in the software (Figure 19), their area was calculated as follows: $\frac{a}{2} \times \frac{b}{2} \times \pi$

To mimic their observed position in the 15 mL conical tube (Figure 19), pellets were put on their lateral side on the microscope to further measure the needed lengths.

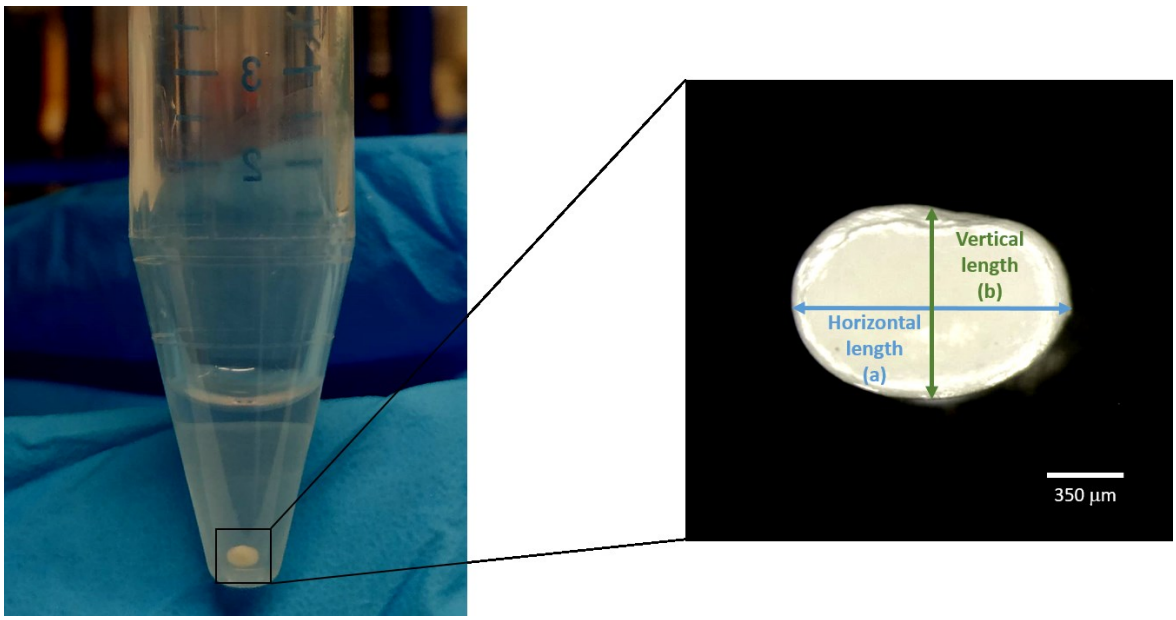

Figure 19 - Representation of the horizontal and vertical lengths measured in the pellets for size calculation. Scale bar = 350 µm.

4.2.15. Statistical Analysis

Statistical analysis was performed using the non-parametric tests, due to the low number of experiments, in GraphPad Prism version 9.1.2 (GraphPad Software, Inc.). All the data was analysed by non-parametric unpaired Kruskal-Wallis test followed by Dunn's multiple comparison test. Statistical significance was defined for values lower than 0.05 (* $p<0.05$; ** $p<0.01$) and the results contained in each graph are shown as mean ± standard error of the mean (SEM).

5. RESULTS AND DISCUSSION

5.1. ESTABLISHMENT AND CHARACTERIZATION OF PRIMARY HUMAN ARTICULAR CHONDROCYTES 3D PELLET CULTURES

5.1.1. Cellular Expansion in Monolayer Culture and Dedifferentiation

The most significant limitations on studies with hACs retrieved from small cartilage biopsies are their limited number, the difficulty in isolating and maintaining them in culture while preserving their chondrogenic potential [218, 219], and their low cell yield [220]. Many culture systems have been widely employed to support chondrocytes *in vitro* [219], namely traditional two-dimensional (2D) monolayer cultures and high cell density 3D cultures [219, 221]. In both methodologies, primary hACs are first mechanically and/or enzymatically released from their cartilage matrix and a following 2D culture-expansion is needed to obtain a workable and viable amount of cells [221]. Herein, after mincing the cartilage sample, the release was carried out by collagenase B, an enzyme that degrades ECM-containing collagen into small peptides [68] and that is known to preserve maximum cell viability [212].

Following this protocol, a good cell viability was always achieved even though the number of obtained cells was variable mostly because it was directly dependent on the quality and on the size of the collected osteochondral samples.

The employed monolayer culture is the most commonly used approach to propagate cells *in vitro*, essentially because it is economical and easy to perform [214]. It involves seeding the cells at a subconfluent density and detaching them from the generated monolayer surface once they achieve confluence [222]. This process of detachment and posterior reseeding of proliferating cells at a subconfluent density until achieving the needed amount of cells is called passaging [222].

When chondrocytes are growing in these 2D environments, a long-time of expansion and multiple passaging are needed, which induces cells to experiment a process called “dedifferentiation” [56, 221]. Dedifferentiated chondrocytes suffer morphological changes and phenotypic loss, since they are hindered to express cartilage-specific proteins [219], and become fibroblast-like cells [214, 219]. They lose their normal rounded shape and start synthesising type I collagen instead of the type II [15, 56, 214] and progressively lower quantities of aggrecan [19, 221, 223], which is the expression profile similar to the one of pre-chondrogenic mesenchymal cells [3, 224, 225]. This newly-formed ECM has poorer biomechanical properties [24, 38] and is more prone to degradation [15].

As seen in Figure 20, when observed a day after isolation (P0), chondrocytes displayed a typical round morphology but, after some days (still P0), they are more

polygonal and start exhibiting some filaments. As the number of passages increases, this dedifferentiation becomes more evident once chondrocytes shifted towards subsequently more elongated, flattened, fibroblast-like shape from P1 to P3 (Figure 20).

This corroborates what is described in the literature for the dedifferentiation phenomenon [15, 35], because chondrocytes' differentiated phenotype is unstable under a 2D microenvironment [226]. In fact, it is well know that chondrocytes are only able to execute a limited number of cell divisions [227], so this dedifferentiation process is critical to the cellular proliferation in the monolayer culture.

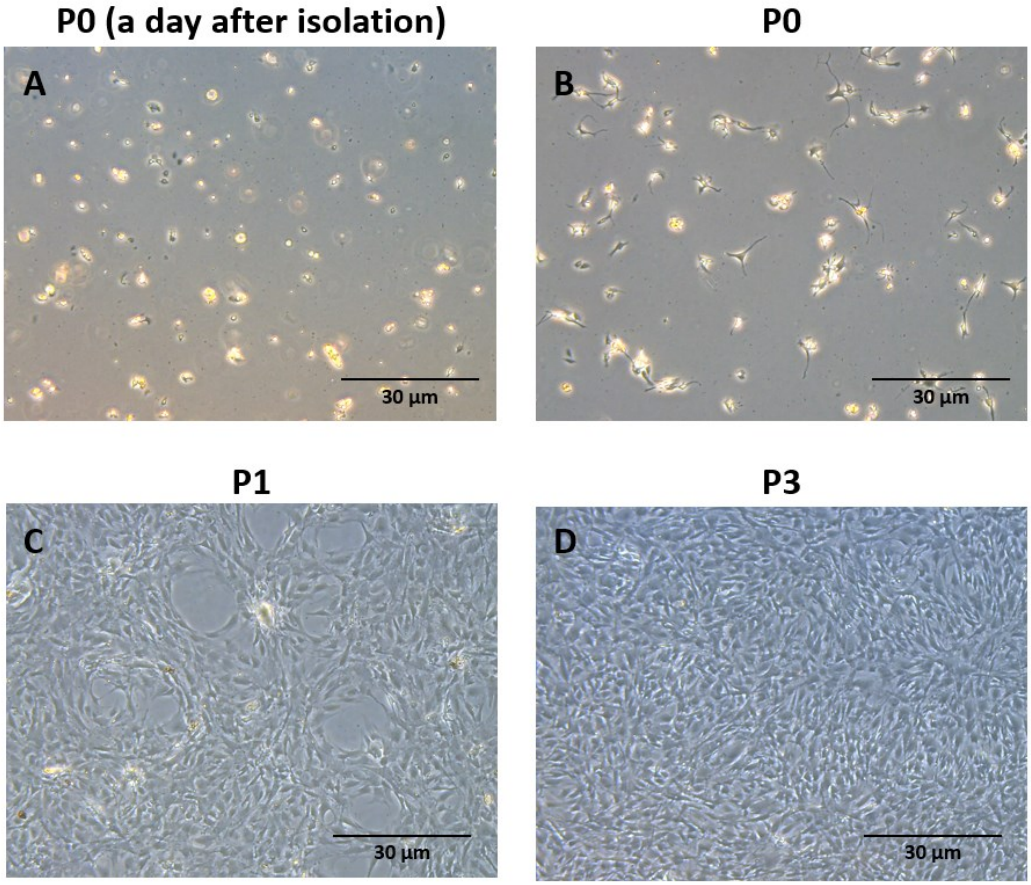

Figure 20 - Morphology of monolayer-cultured chondrocytes in A) Passage 0 (P0) one day after isolation; B) P0 four days after isolation; C) Passage 1 (P1); and D) Passage 3 (P3). Their shape changed from round/polygonal in P0 to fibroblastic in P1 and P3. Scale bar = 30µm.

During this expansion process, cells were exposed to two commonly employed growth factors (TGF-β1 and bFGF) [228] and serum, once this combination has been shown to maintain the redifferentiation capacity of culture-expanded cells [3]. Furthermore, it should be noted that cells were only reseeded up to passage 4 because it is described in the literature that high-passage chondrocytes (> P4) lose their ability to correctly redifferentiate into their native phenotype [26, 229, 230].

Additionally, 2D expansion allows the reprogramming of damaged chondrocytes, since cells that are actively dividing are able to resynthesize and replace mutated molecules [231].

5.1.2. 3D Pellet Culture of Human Articular Chondrocytes

Although many research groups are trying to find an alternative strategy to traditional 2D cell expansion, dedifferentiation still represents a major obstacle to overcome [15, 209, 232]. Therefore, after being expanded, cells need to be redifferentiated into their native chondrogenic phenotype [56], to correctly mimic what happens in the cartilaginous tissue *in vivo*.

This restoration of functional activity can be enhanced by the application of many different specific growth factors [56, 221, 222, 225] and by transferring chondrocytes to a 3D environment that supports their spherical morphology [214, 222, 232], such as in pellets [225], because a high cell density and extensive cell–cell and cell-matrix interactions have been described to be critical to the initiation of chondrogenic redifferentiation [26, 213, 232]. Actually, the pellet culture is the benchmark for studying the redifferentiation of chondrocytes *in vitro* [209, 232], where cells aggregate and deposit ECM, forming a macroscopic pellet (macropellet) [209].

In order for chondrocytes to regain their cartilaginous features in this 3D culture, the employment of a chondrogenic medium is of major importance, whereby it provides a phenotypic stability for the cells.

Insulin-Transferrin-Selenium (ITS) complex has the ability to prevent the dedifferentiation process [233] and to promote the formation of cartilage with higher matrix content [230]. Briefly, insulin essentially promotes the synthesis of proteins and nucleic acids, transferrin, along with being an iron carrier, can also help to decrease oxygen radicals and peroxide toxic levels, and selenium is employed as an anti-oxidant in the medium [234].

The combination of ITS and DMEM is linked to the enhancement the chondrogenic activity [212]. Similarly, TGF-β3 also stimulates the cell activity, which has been reported to result in a higher production of aggrecan in pellet cultures of human articular chondrocytes [235].

5.1.2.1 28-day Chondrogenic Differentiation Experiment

The characterization of primary hACs in 3D pellet cultures was carried out through the evaluation of their phenotype and mRNA expression in an experiment with the duration of 28 days of culture. The main objective was to evaluate the redifferentiation of chondrocytes after their expansion in order to assess at which timepoints they were already producing cartilage-specific ECM and expressing chondrogenic markers.

In order to verify the effectiveness of the chondrogenic medium components in stimulating the chondrogenic activity, a control where cells were only provided the basic environment and nutrients (glucose, amino acids, vitamins and growth factors

[236]) needed to maintain cell survival in culture was conducted (pellets in basal medium).

5.1.2.1.1. Cytotoxicity Assessment

The cytotoxicity throughout the 28 days of culture either in basal and in chondrogenic medium was analysed through the quantification of LDH release in the medium by the pelleted chondrocytes.

The cytotoxicity results obtained for one independent experiment were converted into cell viability and are displayed in Figure 21. Percentages of cell viability above 80% are considered as non-cytotoxicity, between 80% and 60% as weak cytotoxicity, in the range of 60%-40% as moderate cytotoxicity and below 40% as strong cytotoxicity [237].

Cell viability levels of pellets cultured in chondrogenic medium surpassed the 80% until day 14 and suffered a slight decrease for the longer periods of culture, that is, days 21 and 28, which means the culture conditions were not toxic in the first referred periods while represented a weak cytotoxicity on the last ones.

As for the pellets cultured in basal medium, cell viability values were below the 80% in every timepoint, demonstrating that this condition overall seems to have induced a moderate toxicity in chondrocytes during this single experiment.

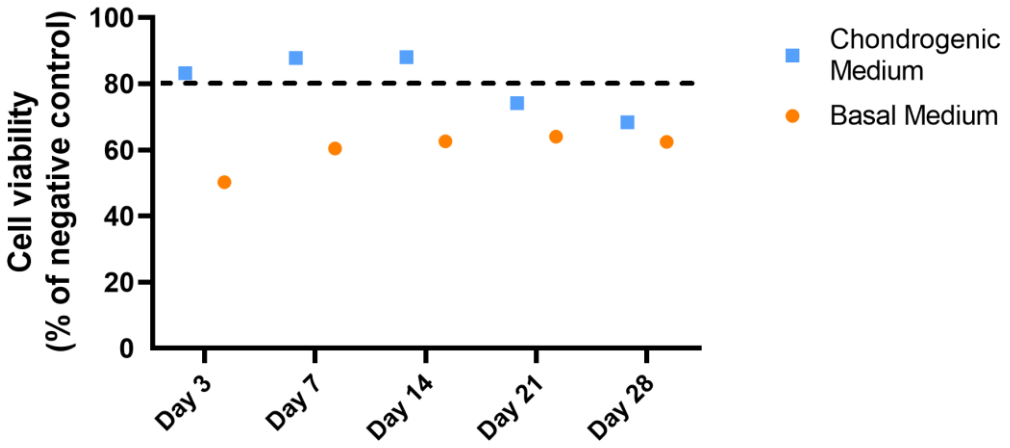

Figure 21 - Cell viability of 3D pellets cultured in chondrogenic and basal medium for 28 days. n = 1 replicate.

5.1.2.1.2. Alcian Blue and Safranin-O Stainings

Alcian blue is a cationic dye that strongly binds to sulfated GAGs [238] and safranin-O is also a cationic dye that binds to proteoglycans present in cartilage ECM [239].

As such, the ability of chondrocytes to produce sGAG and proteoglycans was confirmed by the alcian blue and safranin-O stainings, which showed blue and red staining in the ECM, respectively.

As illustrated in Figure 22, the sGAG deposition was not verified in basal medium culture. On the other hand, the blue staining observed from day 7 until day 28 in the sections of pellets cultured in chondrogenic medium demonstrates the deposition of

GAGs in these timepoints. It is also observed that some ECM-embedded cells started exhibiting a more round-shaped morphology as soon as day 7 (black arrows).

As for the production of proteoglycans as a whole (Figure 23), only a slight red staining is observed throughout the different timepoints for pellets cultured in basal medium, indicating a lower production of this component when compared to the culture in chondrogenic medium. In this medium containing chondrocytes-stimulating factors, proteoglycan deposition is detected as early as day 3 of culture and appears to be more prominent by day 14 of culture. Round-shaped cells surrounded by ECM were detected from the 7th day forward (black arrows).

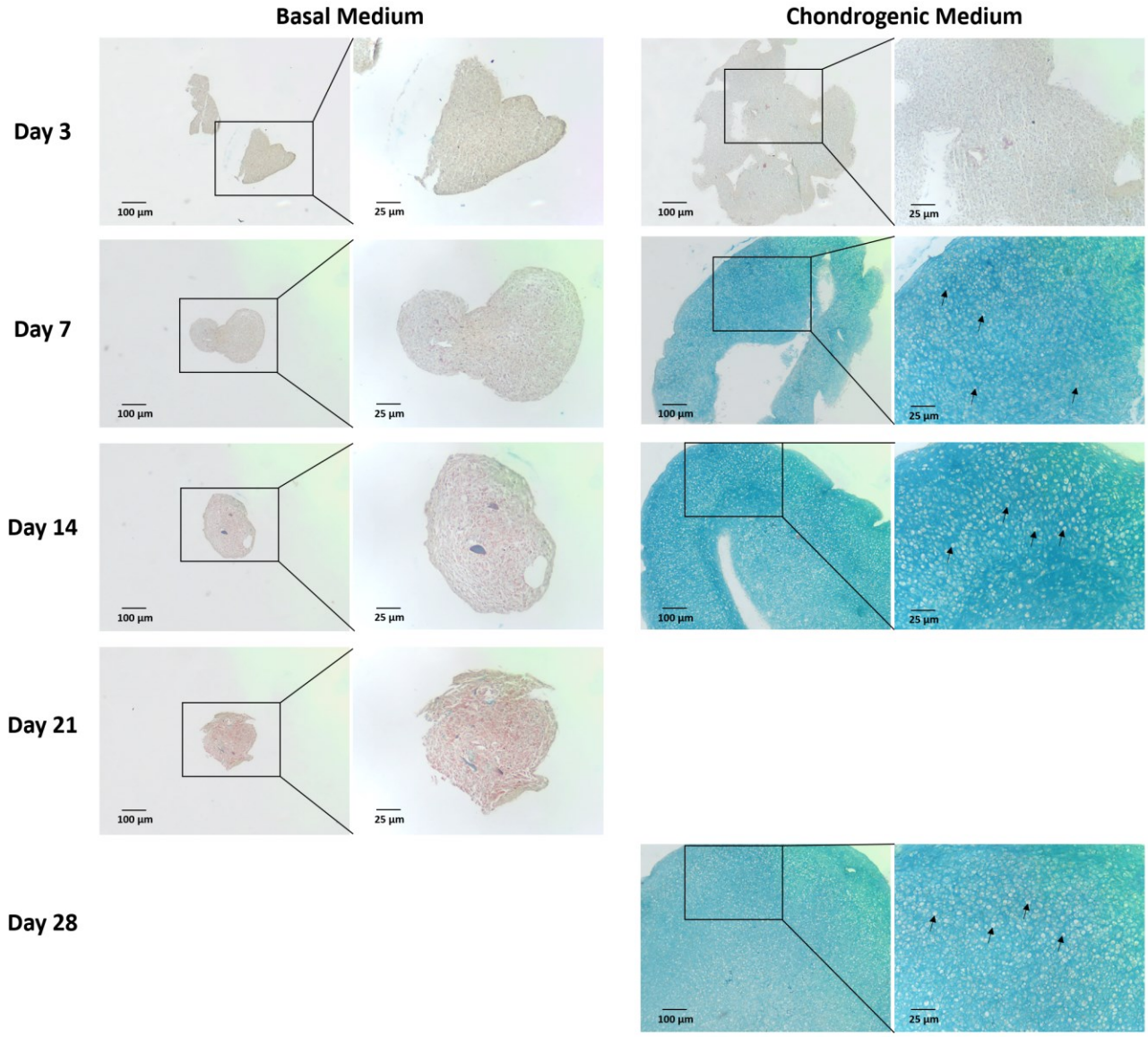

Figure 22 - Alcian blue histological stainings of 3D pellets cultured in basal and chondrogenic medium for 28 days. Black arrows point to the cells with a rounded shape. Scale bar of left images = 100 µm; Scale bar of right images = 25 µm.

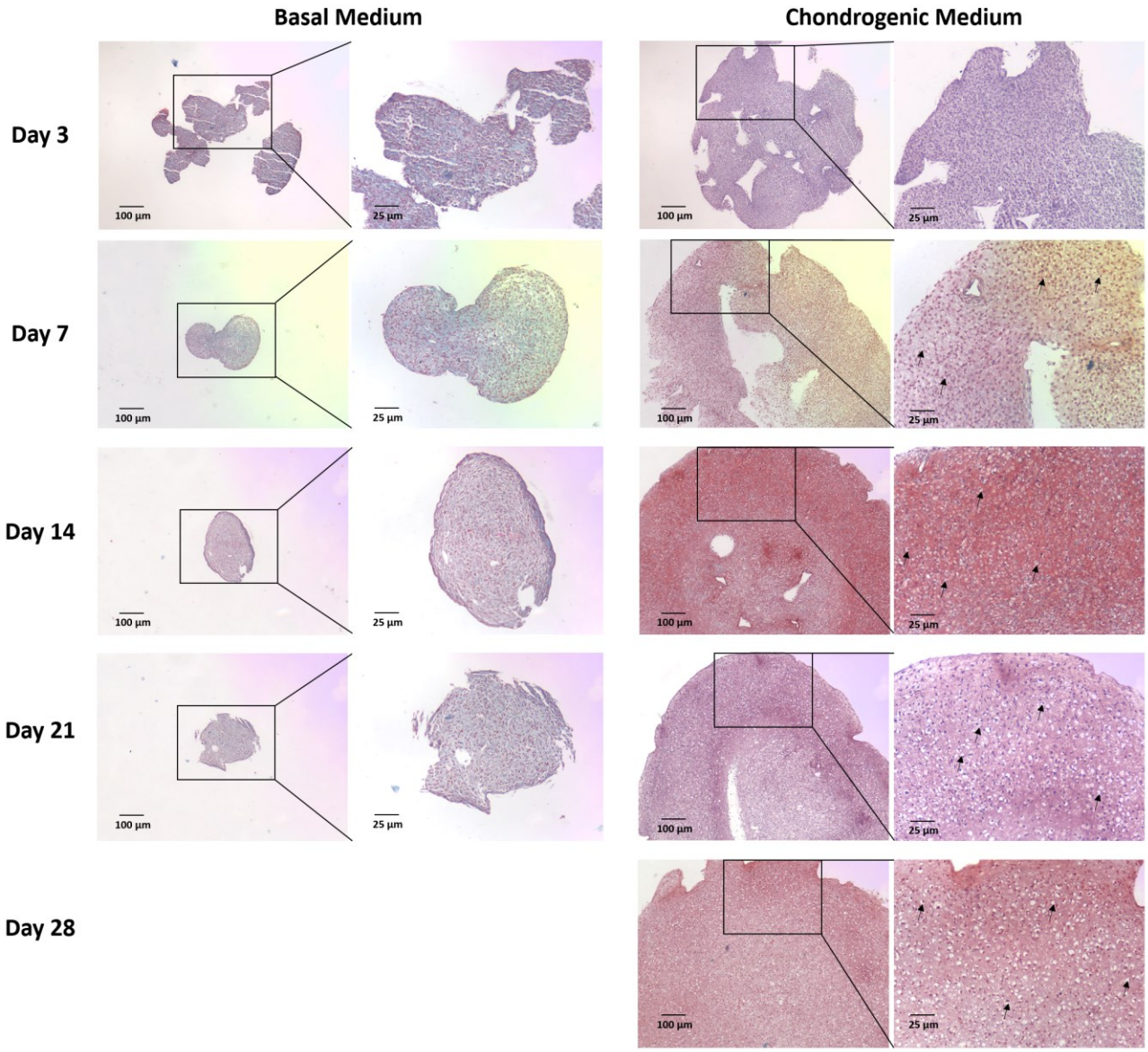

Figure 23 - Safranin-O histological stainings of 3D pellets cultured in basal and chondrogenic medium for 28 days. Black arrows point to the cells with a rounded shape. Scale bar of left images = 100 µm; Scale bar of right images = 25 µm.

5.1.2.1.5. Sox9, Type II Collagen and Aggrecan Expression

Redifferentiating articular chondrocytes should reexpress the chondrogenic markers [26]. Their phenotype is mainly characterized by the expression of genes encoding the synthesis of ECM components or their regulators, specially type II collagen, aggrecan and sox9, which are responsible for maintaining cartilage anabolism [8]. Therefore, their levels of mRNA expression were assessed.

Generally, sox9 mRNA expression levels in both basal and chondrogenic medium cultures decreased over time and the values on the first medium surpassed the ones on the second until day 7 (Figure 24 A). Moreover, after day 14 (days 14, 21 and 28) these levels of sox9 mRNA expression in both mediums show a trend to be diminished towards a much lesser extent than in the first two timepoints (days 3 and 7).

In terms of collagen type II mRNA expression, the levels are maintained throughout the experiment days of culture in pellets supplemented with chondrogenic medium and decreased along time in the ones cultured with basal medium (Figure 24 B).

Lastly, as observed in Figure 24 C, aggrecan only started to be expressed at day 7 and in subsequent days of culture. This expression was constant in days 7 and 14 in both mediums and presented higher levels at day 28 of culture in chondrogenic medium.

Overall, these results demonstrate that genes coding for cartilage-specific proteins were being transcribed. More experiments should be performed to validate these observations.

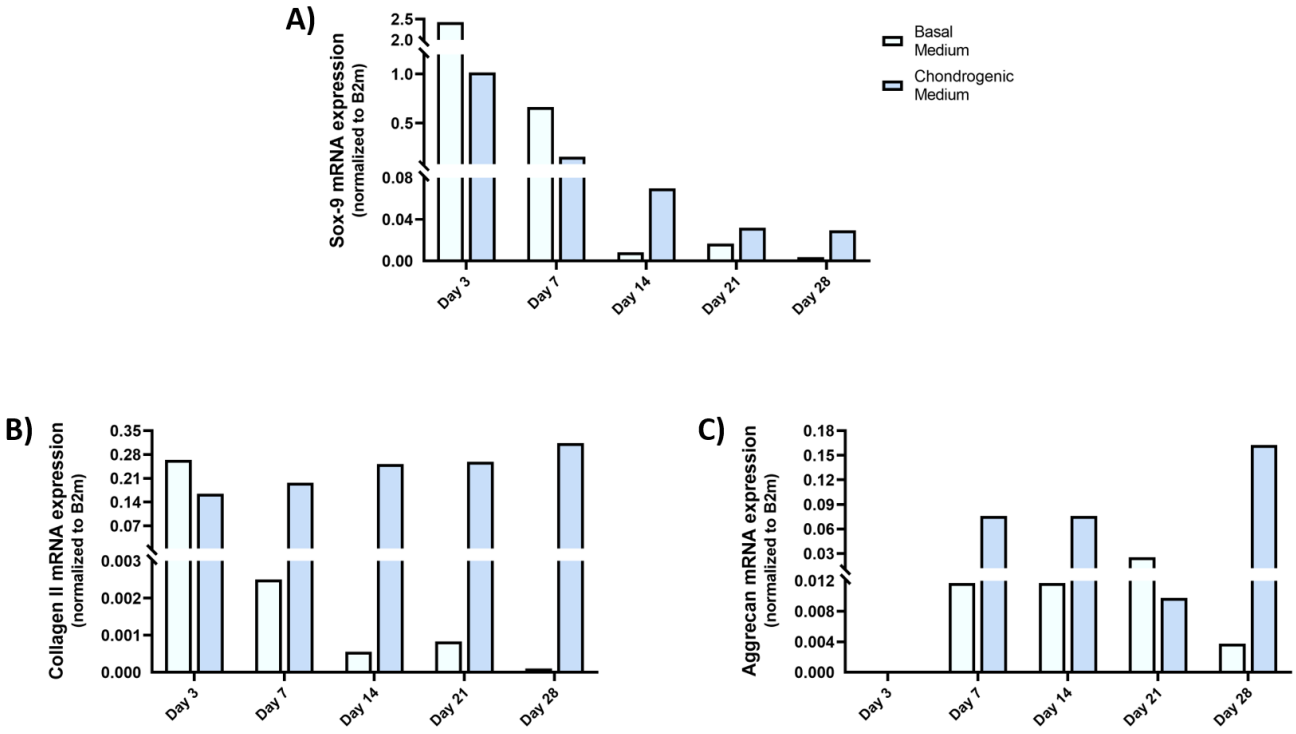

Figure 24 - mRNA expression levels of a) Sox9; B) Collagen Type II; and C) Aggrecan in 3D pellets cultured in basal and chondrogenic medium for 28 days. n=1 replicate.

5.1.2.1.6. Evaluation of Pellet Areas

Variations in pellets size (herein evaluated in terms of area) can be related to ECM production, cell proliferation or death and they are expected to increase in size during culture time in chondrogenic medium [178, 240]. In fact, in this experiment the area of pelleted chondrocytes in chondrogenic medium truly increased over time (Figure 25) which most probably is an indicator of the ECM production previously demonstrated in histological stainings.

In contrast, in control condition, the area values were fluctuant and always below the ones achieved in medium supplemented with chondrogenic factors (Figure 25), which is in agreement with the low ECM deposition overtime observed in alcian blue

and safranin-O stainings and with the moderate toxicity induced by this condition (Figure 22, Figure 23 and Figure 21, respectively).

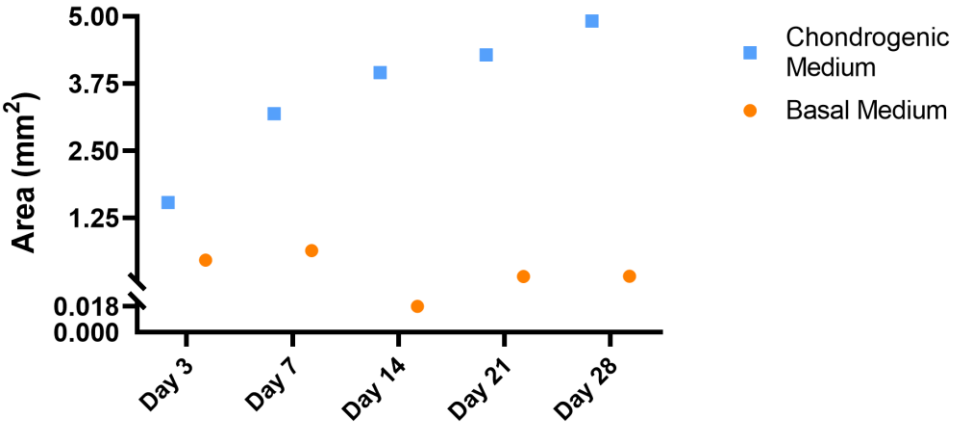

Figure 25 - Areas of 3D pellets cultured in basal and chondrogenic medium for 28 days. n=1 replicate.

5.1.2.1.7. Conclusion on the Minimum Time Period Allowing the Redifferentiation of Chondrocytes

By collecting all the results regarding cell viability, ECM deposition, chondrogenic markers expression and the evolution of pellets areas, a specific timepoint where chondrogenic redifferentiation was proved to be already on going had to be defined, in order to proceed with further experiments.

The performed experiment shows that day 7 of culture could proposed for such day. In fact, the data obtained in the performed experiment confirmed the results previously obtaining in the research group, showing that, by this day, culture conditions were not toxic, sGAG deposition was observed from that day on, proteoglycans were already being produced by that time, and mRNA of chondrogenic markers were also being expressed at that timepoint.

Therefore, at day 7 chondrocytes seem to be already showing their native phenotype restored, proven namely by the synthesis of cartilage-specific ECM and to the re-acquisition of a rounded shape.

5.2. ESTABLISHMENT OF A PRO-INFLAMMATORY MICROENVIRONMENT IN 3D PELLET CULTURES

In order to establish the more suitable, non-cytotoxic and reproducible pro-inflammatory microenvironment model in 3D pellet cultures and mimic the one at cartilage lesions sites, hACs were stimulated with the addition of IL-1β and TNF-α to the chondrogenic medium, once their key role in cartilage destruction is well-known [26].

Different concentrations of these two cytokines alone were tested, in accordance with established pro-inflammatory models of *in vitro* cartilage damage and OA in articular chondrocytes, reported by other authors (10 ng/mL of IL-1β [241-243], 10 ng/mL of TNF-α [244-246], 100 ng/mL of IL-1β [247, 248] and 100 ng/mL of TNFα [245, 246]). Two conditions of both cytokines in combination were also tested (IL-1β and TNF-α at 10 ng/mL each and IL-1β and TNF-α at 100 ng/mL each).

These pro-inflammatory stimuli were added to the 3D cultures after the 7 days of differentiation, to assure that cells with a chondrogenic phenotype were being exposed to these conditions.

5.2.1. Cytotoxicity Assessment

The cytotoxicity of the different pro-inflammatory stimuli in pelleted chondrocytes was analysed three days after the establishment of those conditions.

The cytotoxicity results obtained for one independent experiment were converted into cell viability and are displayed in Figure 26. The results show that no condition was toxic to the cells.

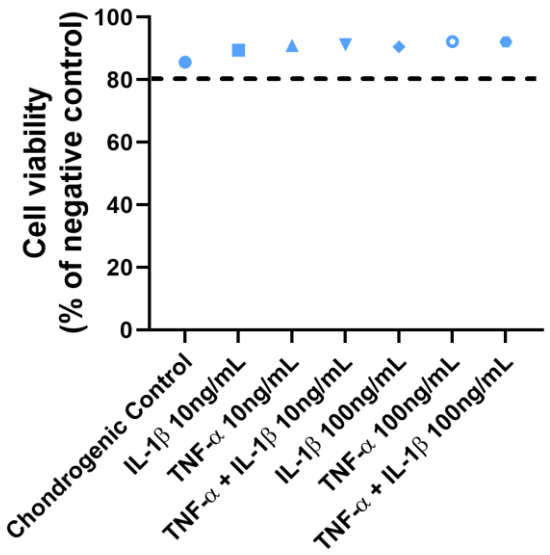

Figure 26 - Cell viability of 3D pellets three days after being stimulated under different pro-inflammatory stimuli. n = 1 replicate.

5.2.2. Cytokine Profiling

Usually, levels of IL-1β in normal cartilage samples are very little [249]. Herein, although statistical significance was not achieved between conditions in these experiments, the secretion levels of IL-1β in the chondrogenic control indeed seemed to be greatly bellow the ones detected for the pro-inflammatory-treated conditions (Figure 27 A). Moreover, the addition of 10 ng/mL of TNF-α and 100 ng/mL of IL-1β seemed to induce the lowest and the highest synthesis of this cytokine, respectively,

having the latter induced the production levels around 50 fold greater (around 5000 ng/mL) than the ones added to the medium.

The TNF-α concentrations quantified in conditioned mediums were notably lower than the ones observed for IL-1β (Figure 27 B). It is verified that TNF-α was not produced in pellets only held in chondrogenic medium and the highest levels seemed to be produced by cells where this cytokine was added either alone or in combination. The experimental conditions in which IL-1β was added alone either at 10 or 100 ng/mL seemed to stimulate cells for TNF-α production in a lower extent.

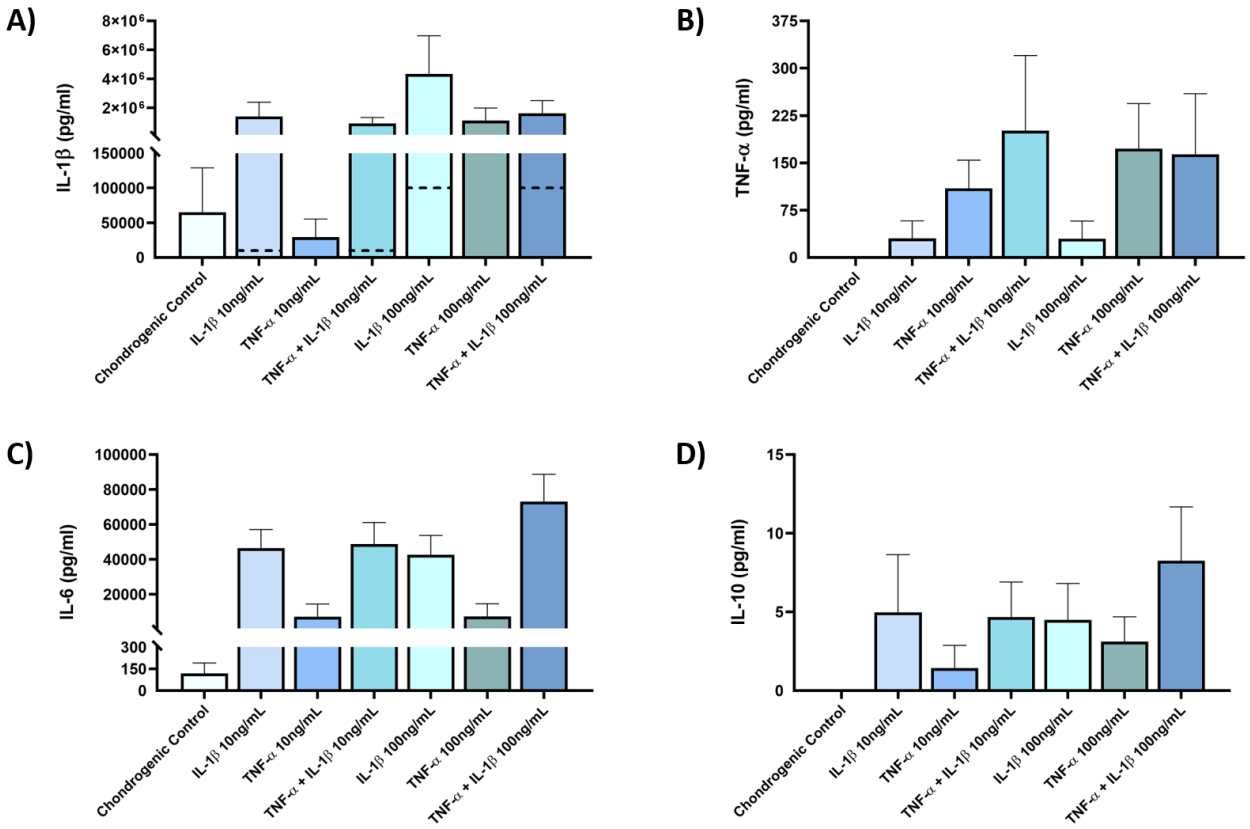

Figure 27 - Levels of A) IL-1β; B) TNF-α; C) IL-6; and D) IL-10 measured in the conditioned mediums of 3D pellets three days after being stimulated under different pro-inflammatory stimuli. The dashed line in the graph A) marks the amount of IL-1β added to the medium in the respective conditions (10 ng for the 10 ng/mL of IL-1β; 10 ng for the 10 ng/mL of IL-1β and TNF-α; 100 ng for the 100 ng/mL of IL-1β; and 100 ng for the 10 ng/mL of IL-1β and TNF-α). Results are presented as mean + SEM; n=4 replicates.

Under normal conditions, chondrocytes produce low levels of IL-6 [65], as shown in chondrogenic control (Figure 27 C). However, the synthesis of this pro-inflammatory cytokine is directly stimulated by IL-1β and TNF-α [65, 72], which was verified for the conditions where these two cytokines were added to the culture medium either alone or in combination. It seems that the condition potentiating a higher production of IL-6 was when the two cytokines were added to the pellets together at 100 ng/mL each

and the lowest was induced by the two conditions where TNF-α was added alone at 10 and 100 ng/mL.

IL-10 is an anti-inflammatory cytokine produced by chondrocytes as an attempt to counterbalance the pro-inflammatory microenvironment and protect their phenotype [26, 68]. Data displayed in Figure 27 D suggest that IL-10 was synthesised at low levels for all the conditions and inexistent in the chondrogenic control conditioned medium. Nevertheless, these levels seem to be increased in all of the pro-inflammatory conditions when compared to the control.

5.2.3. Sox9, Type II Collagen, Aggrecan, MMP and ADAMTS Expression

The mRNA expression of chondrogenic markers sox9, type II collagen and aggrecan was assessed for this pro-inflammatory establishment experiments.

Although no statistically significant differences between the tested conditions for these experiments was achieved, it seems that the all pro-inflammatory conditions decreased the mRNA levels of sox9 when compared to the ones in chondrogenic control (Figure 28 A). This decrease is more noticeable in IL-1β 100 ng/mL condition. These observations corroborate what has been previously described about decreased levels of sox9 mRNA expression being detected near the cartilage lesions [25].

As for collagen type II, mRNA levels seem to be overall lower in tested conditions than in the chondrogenic control and particularly almost untraceable in the 3D pellets cultured under IL-1β 100 ng/mL, TNF-α 100 ng/mL and IL-1β-TNF-α 100 ng/mL stimuli influence (Figure 28 B).

Accordingly, mRNA expression levels of aggrecan also seem to be downregulated in all pro-inflammatory conditions when compared to the chondrogenic control (Figure 28 C).

Generally, the lowest levels of sox9, collagen II and aggrecan transcripts seem to be induced by the higher concentration of IL-1β. This is accordance with a previous study, where chondrocytes were exposed to increasing concentrations of IL-1β and TNF-α (1, 10 and 100 ng/mL each) and, at the same concentrations, IL-1β produced lesser mRNA abundance of collagen II and aggrecan than TNF-α [247]. In the same study, overall the 100 ng/mL IL-1β treatment was the one producing the most pronounced decrease in these components' transcripts [247] (exactly as suggested in Figure 28).

In addition, IL-6 acts synergistically with IL-1β in reducing the expression of type II collagen [65]. This proves the cartilage-specific ECM synthesis might have been disturbed through these down-regulations in mRNA expressions.

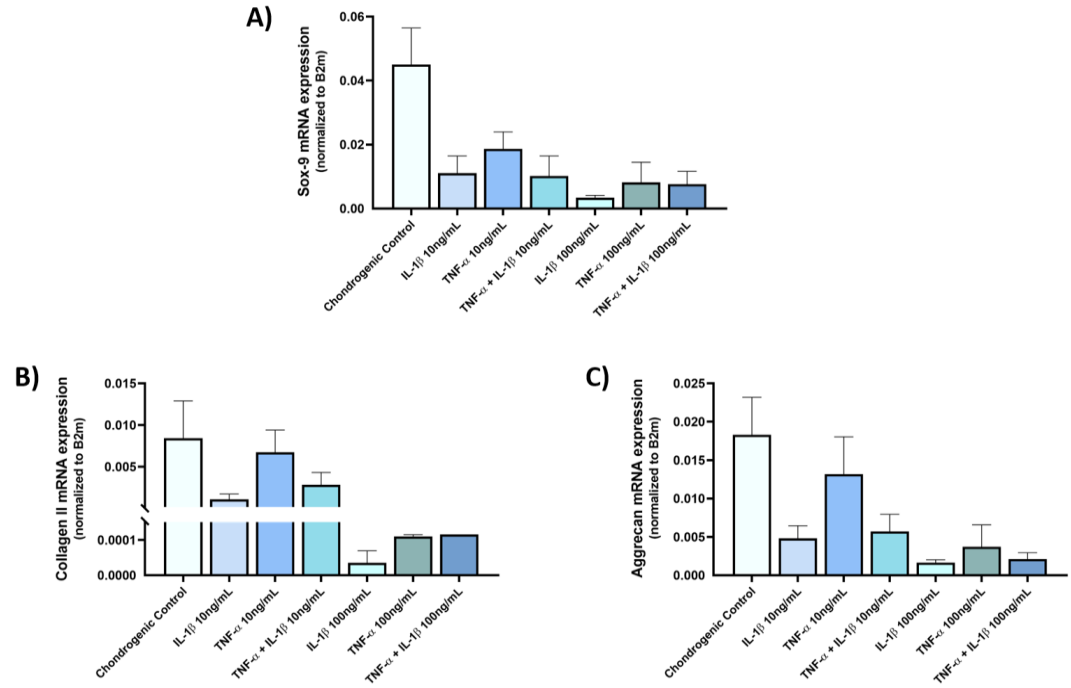

Figure 28 - mRNA expression levels of a) Sox9; B) Collagen Type II; and C) Aggrecan in 3D pellets three days after being stimulated under different pro-inflammatory stimuli. Results are presented as mean + SEM; n = 5 replicates.

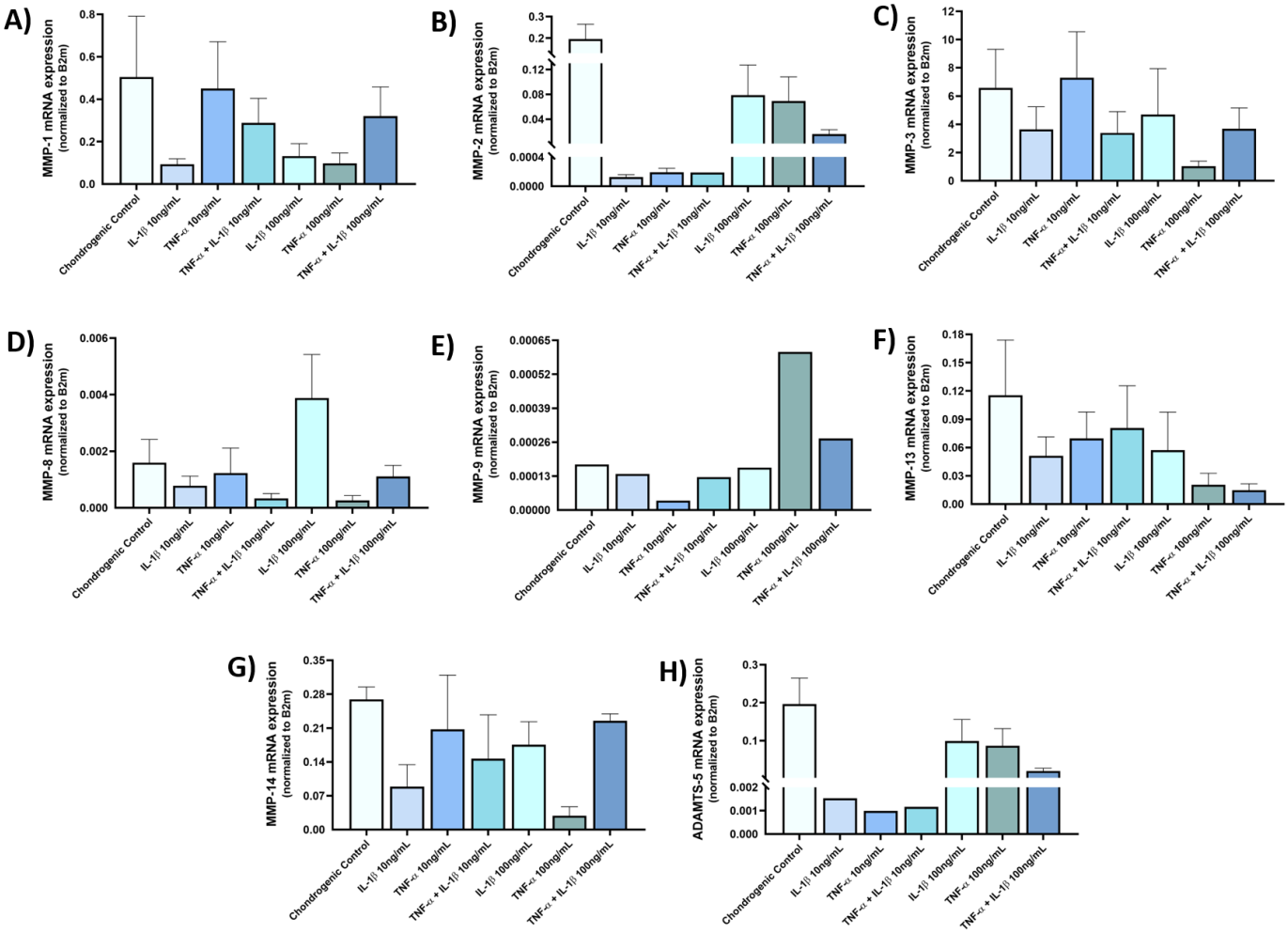

Figure 29 - mRNA expression levels of a) MMP-1; B) MMP-2; C) MMP-3; D) MMP-8; E) MMP-9; F) MMP-13; G) MMP-14; H) ADAMTS-5 in 3D pellets three days after being stimulated under different pro-inflammatory stimuli. Results are presented as mean + SEM; n = 5 replicates except for MMP-9, where n = 1 replicate.

The evidenced downregulation of the two main ECM components of cartilage is described to be resultant from an augmentation in the production and activation of proteolytic enzymes by chondrocytes once stimulated by IL-1β and TNF-α [39, 250]. To confirm the expected elevated levels, mRNA expression of MMP-1, -2, -3, -8, -9, -13 and -14 and of ADAMTS-5 were quantified (Figure 29).

Levels of transcribed MMPs genes particularly induced by IL-1β and TNF-α in chondrocytes (MMP-1, MMP-3, MMP-9, MMP-13) [74-76] and other also generally detected cartilage damage and degeneration as a result of subsequent downstream cascades (MMP-2, MMP-9, MMP8 ADAMTS-5 [68, 72, 80, 82]) were analysed. In particular, IL-6 upregulates MMP-1 and MMP-13 expression in combination with IL-1β and reduces the expression of type II collagen [65].

There were no significant changes between the tested conditions and when compared to the chondrogenic control. However, it is possible to observe that all analysed proteinases were being transcribed in all experimental conditions (Figure 29), including in the control as they are normally expressed in articular cartilage due to tissues' homeostasis [82].

Generally, MMP-3 appears to be the one with the highest mRNA expression, followed by MMP-1 and MMP-13 (Figure 29). In fact, MMP-3 is the MMP most strongly expressed in OA cartilage [69] and activates other enzymes like MMP-13 [80].

In summary, as MMP-1, -3, -9, and -13 are all directly induced by IL-1β and TNF-α and the major mediators of joint destruction [17, 66, 74, 79], and so these were the ones analysed in the experiments evaluated further in this study.

5.2.4. Conclusion on the Cytokine Concentration with Effective and Reproducible Pro-Inflammatory Effects

A concentration capable of inducing the desired pro-inflammatory cascades in chondrocytes needed to be chosen in order to proceed with the following studies aiming to evaluate the anti-inflammatory and anti-proteolytic activity of the loaded nanodelivery systems, and to establish a pro-inflammatory microenvironment in COPLA® Scaffolds.

As such, taking into consideration all the results collected, IL-1β at 100 ng/mL was selected as an adequate stimulus, essentially because it was not toxic to the cultured cells, was the one where the higher production of IL-1β is suggested, and was also able to stimulating chondrocytes to produce identifiable amounts of TNF-α and substantial of IL-6. Additionally, this appeared to be the one that induced the lowest levels of sox9, collagen type II and aggrecan transcripts and leaded the cells to produce several MMPs and ADAMTS-4 and -5.

In summary, IL-1β stimulation with 100 ng/mL was able to cause a serious inflammatory reaction in hACs, showing to be the most effective condition in the establishment of a pro-inflammatory environment. To test the reproducibility of the effects induced by this condition, the number of experiments should be increased.

5.3. EVALUATION OF THE CHONDROPROTECTIVE EFFECTS OF IBUPROFEN-LOADED PLGA NANOPARTICLES

In these experiments, the possible chondroprotective effects of ibuprofen-loaded PLGA NPs in a pro-inflammatory microenvironment were evaluated three days after the treatment with those NPs. This is an appropriate approach as the targeting of pro-inflammatory cascades is considered an attractive and promising strategy to prevent the progression of articular cartilage damage [243].

Chondroprotective effects are related to the capacity of the loaded nanodelivery system to inhibit cartilage ECM degradation in this *in vitro* cultures of hACs.

5.3.1. Cytotoxicity Assessment

The possible cytotoxicity of ibuprofen-loaded NPs in hACs was studied first. The cytotoxicity of free drug and unloaded NPs was also assessed. These results were converted into cell viability values that are shown in Figure 30.

Based on the five independent conducted experiments, none of the tested conditions seems to be cytotoxic, as cell viability was maintained around 80% of the negative control (100% cell death).

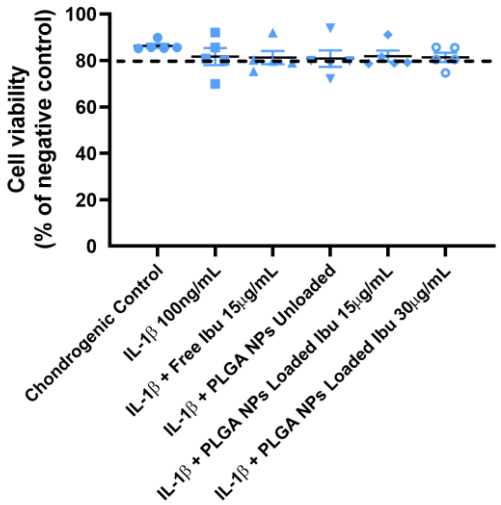

Figure 30 - Cell viability of 3D pellets aimed to test ibuprofen-loaded PLGA nanoparticles under a pro-inflammatory microenvironment. Results are presented as mean ± SEM; n = 5 replicates. Ibu – Ibuprofen; PLGA – Poly(Lactic-Co-Glycolic Acid); NPs – Nanoparticles.

5.3.2. Alcian Blue and Safranin-O Stainings

Regarding sGAG deposition revealed by alcian blue stainings, it seems to be clearly more intensified in the chondrogenic control than in the other tested conditions (Figure 31). Moreover, this ECM deposition seems to have decreased in the pro-inflammatory environment induced by 100 ng/mL of IL-1β and not being able to recover except when 15 μg/mL of ibuprofen-loaded PLGA NPs were added to the 3D pellets. In the condition where 30 μg/mL of ibuprofen-loaded PLGA NPs is tested, the staining seems to less blueish than in the other conditions.

As for the safranin-O stainings, coloration intensity is decreased in every treatment when compared to the one observed in the chondrogenic control (Figure 32), especially for 30 μg/mL of ibuprofen-loaded PLGA NPs.

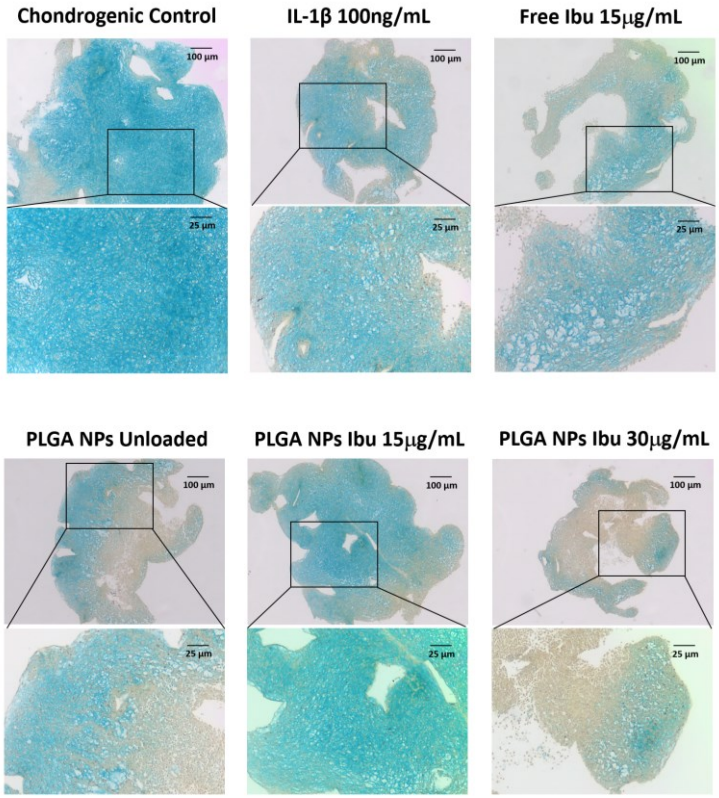

Figure 31 - Alcian blue histological stainings of 3D pellets aimed to test ibuprofen-loaded PLGA nanoparticles under a pro-inflammatory microenvironment. Scale bar of upper images = 100 μm; Scale bar of lower images = 25 μm. Ibu – Ibuprofen; PLGA – Poly(Lactic-Co-Glycolic Acid); NPs – Nanoparticles.

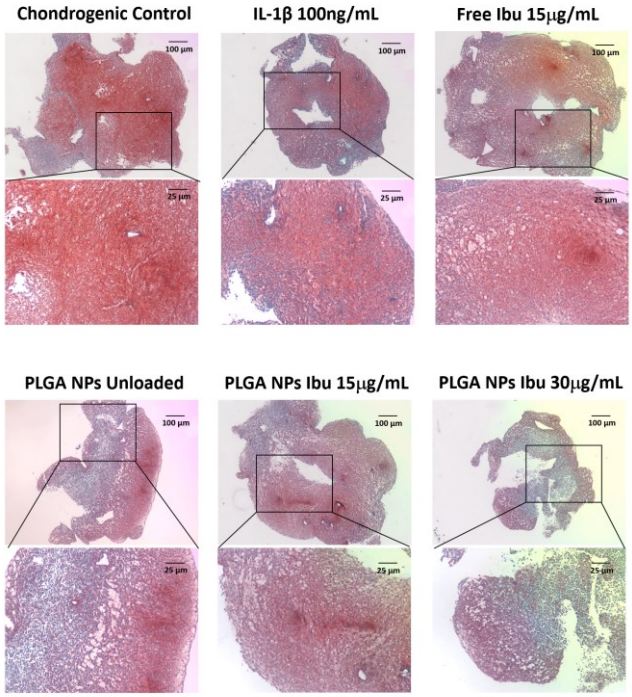

Figure 32 - Safranin-O histological stainings of 3D pellets aimed to test ibuprofen-loaded PLGA nanoparticles under a pro-inflammatory microenvironment. Scale bar of upper images = 100 μm; Scale bar of lower images = 25 μm. Ibu – Ibuprofen; PLGA – Poly(Lactic-Co-Glycolic Acid); NPs – Nanoparticles.

5.3.3. Immunohistochemical Staining of Type II Collagen and Aggrecan

As presented in Figure 33, the IL-1β stimulation seems to induce a reduction of both type II collagen and aggrecan in comparison with the chondrogenic control condition.

Concomitantly, the results in the treatment with of PLGA NPs loaded with 30 μg/mL of ibuprofen point towards a restoration of collagen expression to levels higher than the ones observed in the chondrogenic control, which proposes a chondrogenic capacity of this experimental condition as this capacity is associated with the ability to induce an increased anabolic activity.

In the case of aggrecan, the recovery of its expression is suggested when adding PLGA NPs loaded with 15 μg/mL of ibuprofen and also when adding ibuprofen free form at that same concentration, even though in a lesser extent.

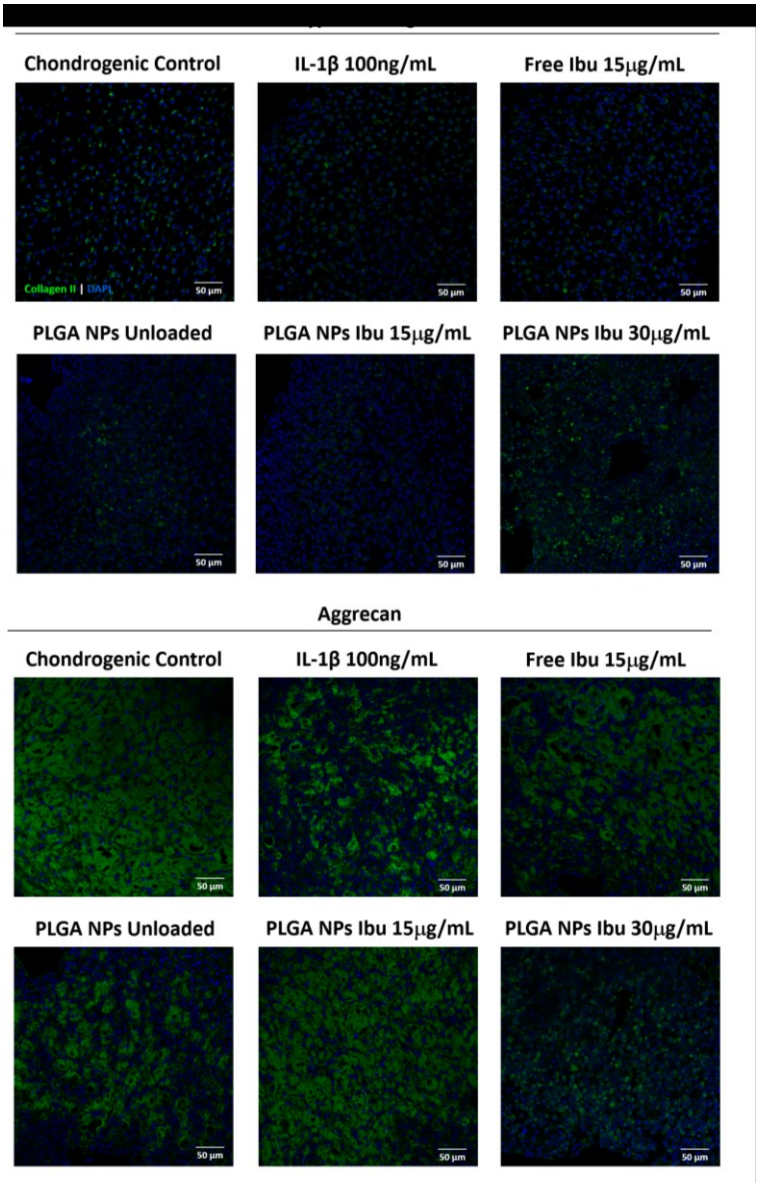

Figure 33 - Immunohistochemical staining of type II collagen (top panel) and aggrecan (bottom panel) in 3D pellets aimed to test ibuprofen-loaded PLGA nanoparticles under a pro-inflammatory microenvironment. Scale bar = 50 μm. Ibu – Ibuprofen; PLGA – Poly(Lactic-Co-Glycolic Acid); NPs – Nanoparticles.

5.3.4. Cytokine Profiling

The levels of IL-1β, TNF-α, IL-6 and IL-10 were evaluated in the experimental conditions in order to clarify the possible modulatory effect of ibuprofen-loaded NPs on the inflammatory reactivity of chondrocytes stimulated by 100 ng/mL of IL-1β.

However, for this and further experiments, these levels of TNF-α and IL-10 were found to be below the kit's detection limit and, thus, those results will not be presented.

Generally, although not statistically different, IL-1β synthesised levels seem to be lower in the chondrogenic control samples and to be maintained higher in the pro-inflammatory condition only with the IL-1β (100 ng/mL) and similarly in the remaining tested conditions (Figure 34 A).

The levels of IL-6 were null in chondrogenic control and were suggested to be consistently high not only in the pro-inflammatory condition alone but in the other conditions as well, namely when unloaded PLGA NPs were added to the pelleted chondrocytes under pro-inflammatory conditions (Figure 34 B).

This way, the treatment with ibuprofen-loaded NPs does not seem to have mitigated the release of both cytokines.

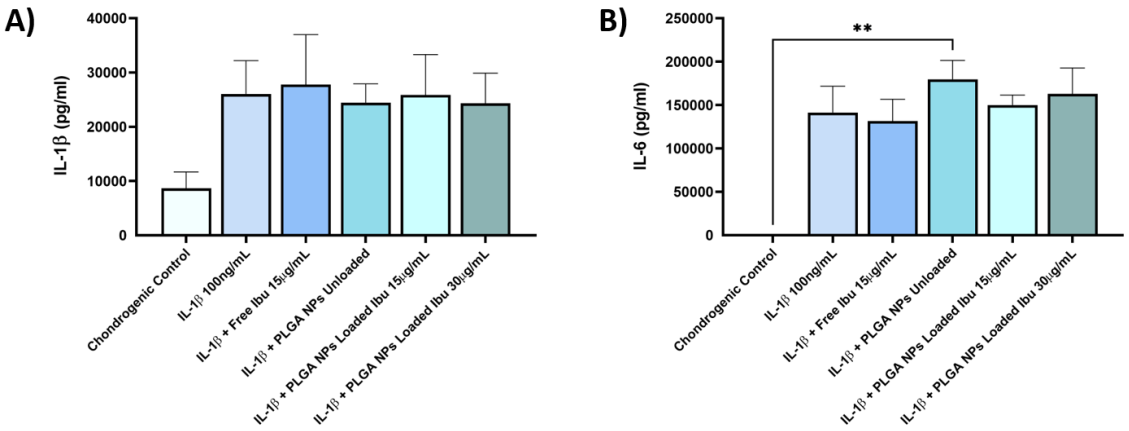

*Figure 34 - Levels of A) IL-1β; and B) IL-6 measured in the conditioned mediums of 3D pellets aimed to test ibuprofen-loaded PLGA nanoparticles under a pro-inflammatory microenvironment. Results are presented as mean + SEM; n = 5 replicates. ** p<0.01. Ibu – Ibuprofen; PLGA – Poly(Lactic-Co-Glycolic Acid); NPs – Nanoparticles.*

5.3.5. MMP Expression

MMP-1 and MMP-13 are collagenases and so degrade collagen fibers whereas MMP-9 degrades gelatins, being a gelatinase [68]. MMP-3 is a stromelysin able to destroy the structure of not only proteoglycans but also collagens and MMP-13 also has a role in degrading aggrecan [68, 82].

The exposure of pelleted hACs to the pro-inflammatory microenvironment induced by the 100 ng/mL of IL-1β is suggested to stimulate a trend towards an increase in MMP-3 and MMP-9 expression (Figure 35). This might justify the lower deposition of type II collagen previously observed in Figure 33 (top panel) and of proteoglycans

(Figure 32) in the pro-inflammatory condition in comparison to the chondrogenic control.

Importantly, MMP-1 seems to be far more transcribed in the conditions treated with unloaded PLGA NPs in comparison to the other remaining tested conditions (Figure 35 A).

In the case of MMP-13, its mRNA expression seems to be lower in the condition where PLGA NPs loaded with 30 μg/mL of ibuprofen were added to the 3D pellets (Figure 35 B). In addition, MMP-9 transcripts are suggested to also be reduced by the action of PLGA this concentration of loaded NPs, which is also verified for the MMP-3, the MMP with greatly higher levels of expression (Figure 35 D).

No statistically significant differences could be observed for any MMP mRNA expression between the different culture conditions, which might be a consequence of the low number of replicates. Therefore, it should be increased.

Overall, these low mRNA expression levels of collagen and gelatin-degrading proteinases in PLGA NPs loaded with 30 μg/mL of ibuprofen treatment seem to be in agreement with what was observed in the immunohistochemical staining of collagen for this condition, which seemed to be a chondrogenic inducer of this ECM component. However, these data should be carefully interpreted once these results are only about mRNA expression and not MMPs effective production and, therefore, further studies on the activity of these MMPs should be conducted. Even so, the deposition rate of type II collagen seems to be higher than its degrading rate, which highlights the possible dual role of this loaded concentration of NPs in both protecting collagen pro-inflammatory-induced destruction while also inducing its expression.

On the other hand, no direct associations between the results obtained for MMP-13 expression and the immunohistochemical stainings of aggrecan seem to be established. In order to obtain more reproducible and coherent results, the number of experiments should be increased.

These results were further explored by the evaluation of MMPs enzymatic activity by zymography.

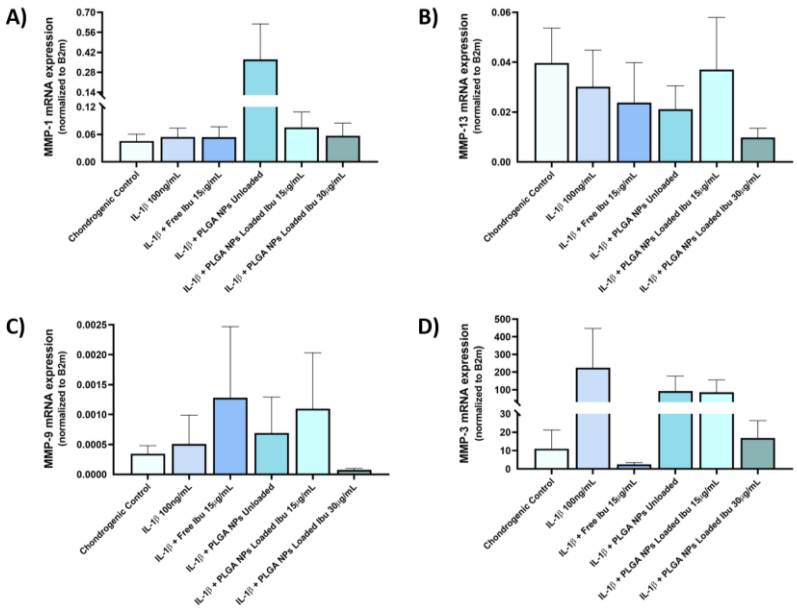

Figure 35 - mRNA expression levels of a) MMP-1; B) MMP-13; C) MMP-9; and D) MMP-3 in 3D pellets aimed to test ibuprofen-loaded PLGA nanoparticles under a pro-inflammatory microenvironment. Results are presented as mean + SEM; n = 5. Ibu – Ibuprofen; PLGA – Poly(Lactic-Co-Glycolic Acid); NPs – Nanoparticles.

5.3.6. Gelatin Zymography

To complement the data obtained for MMPs expression and to more effectively evaluate the potential anti-enzymatic activity of the tested ibuprofen-loaded PLGA NPs through the blockage of the prostaglandin-mediated production of MMPs [147], gelatin zymography was conducted using the samples' conditioned medium.

Although the employed gels were composed of gelatin and gelatinases (MMP-2 and MMP-9) were the MMPs more likely expected to be evaluated, the molecular weight of the detected bands seems to indicate that the pro and active MMP-3 forms were the ones degrading the gels (Figure 36 A).

Generally, pro-MMP-3 form seems to be in a higher amount than its active form in all samples (Figure 36). An increase of active form of MMP-3 was verified in the pro-inflammatory control compared to the chondrogenic one along with a subsequent decrease in the tested conditions (Figure 36 C), as also observed in Figure 35 D.

To prove and sustain these results and to confirm that the identified enzyme is MMP-3, MMP-3 activity quantification should be further carried out.

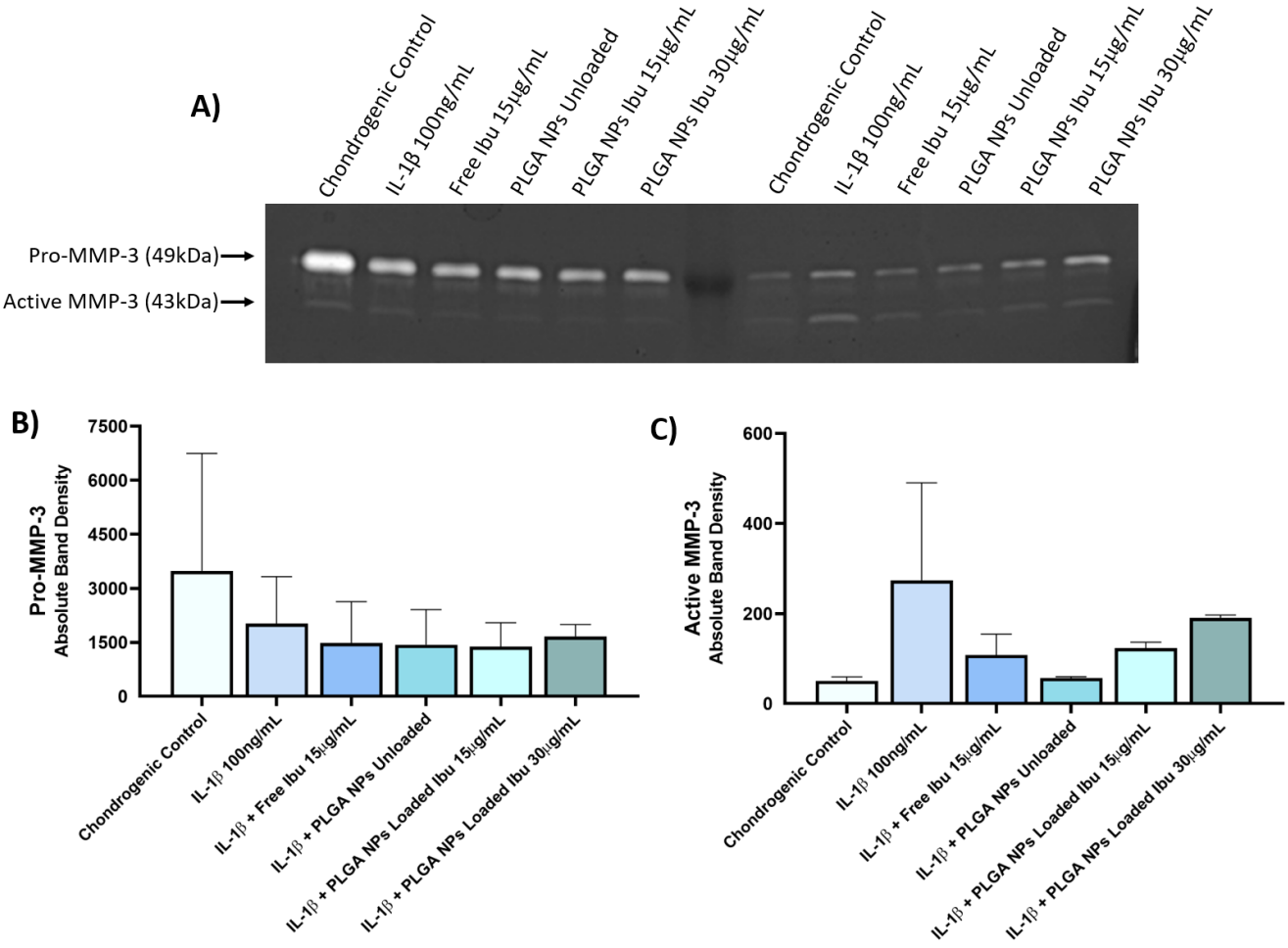

Figure 36 - MMP-3 enzyme activity for measured in the conditioned mediums of 3D pellets aimed to test ibuprofen-loaded PLGA nanoparticles under a pro-inflammatory microenvironment. A) Gelatin zymography gelatin results; B) Absolute band density for Pro-MMP-3; and C) Absolute band density for Active MMP-3 Results are presented as mean + SEM; n = 2 replicates. Ibu – Ibuprofen; PLGA – Poly(Lactic-Co-Glycolic Acid); NPs – Nanoparticles.

5.3.7. Evaluation of Pellet Areas

As shown in Figure 37, the pellet related to the chondrogenic control seems to be bigger than in the other conditions. After the areas decreased as a possible result of ECM degradation induced by 100 ng/mL of IL-1β condition, they appear to remain almost steady throughout the tested conditions.

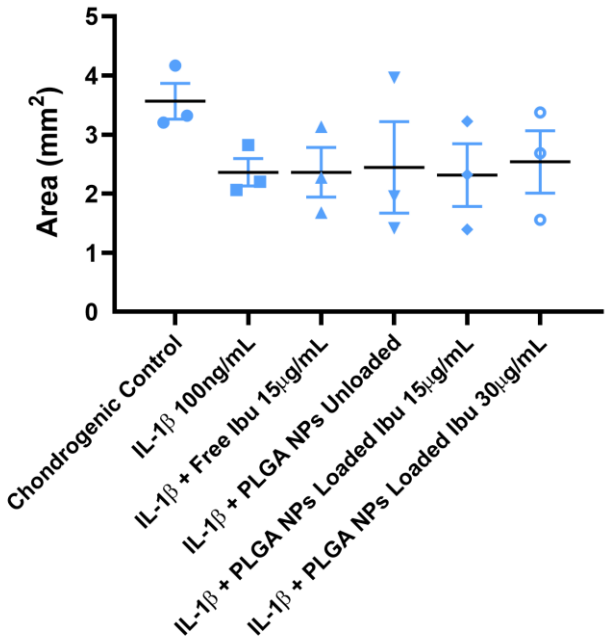

Figure 37 - Areas of 3D pellets aimed to test ibuprofen-loaded PLGA nanoparticles under a pro-inflammatory microenvironment. Results are presented as mean ± SEM; n = 3 replicates. Ibu – Ibuprofen; PLGA – Poly(Lactic-Co-Glycolic Acid); NPs – Nanoparticles.

5.3.8. Conclusion on the Ibuprofen-Loaded PLGA Nanoparticles Concentration with Reproducible Chondroprotective Effects

Through these early results, it is not yet possible to specify which concentration produces the best anti-inflammatory and anti-proteolytic effects. For that purpose, the number of experiments should be increased to further confirm these results and achieve statistically significant differences between the different conditions to assure they are reproducible.

However, these results clearly point out the potential chondroprotective and chondrogenic effects of ibuprofen-loaded PLGA NPs under a pro-inflammatory microenvironment, as they are not cytotoxic, generally induced a decrease in MMPs expression and a protection against ECM degradation. Moreover, the tested concentrations of 15 μg/mL and 30 μg/mL of loaded ibuprofen seem to be identified as chondroprotective and chondrogenic inducers, once the first restored the levels of aggrecan and the second exceeded the control in increasing the production of collagen II.

5.4. EVALUATION OF THE CHONDROPROTECTIVE EFFECTS OF IBUPROFEN-LOADED CH/PGA NANOPARTICLES

In these experiments, the potential chondroprotective effects of ibuprofen-loaded chitosan/PGA NPs under pro-inflammatory conditions were evaluated three days after the treatment with those NPs.

The capacities of these nanodelivery systems to inhibit cartilage ECM degradation in *in vitro* cultures of hACs were evaluated.

5.4.1. Cytotoxicity Assessment

The cytotoxicity results obtained for two independent experiment were converted into cell viability and are displayed in Figure 38. With a cell viability above 80% (of negative control), none of the tested conditions appear to be toxic for hACs.

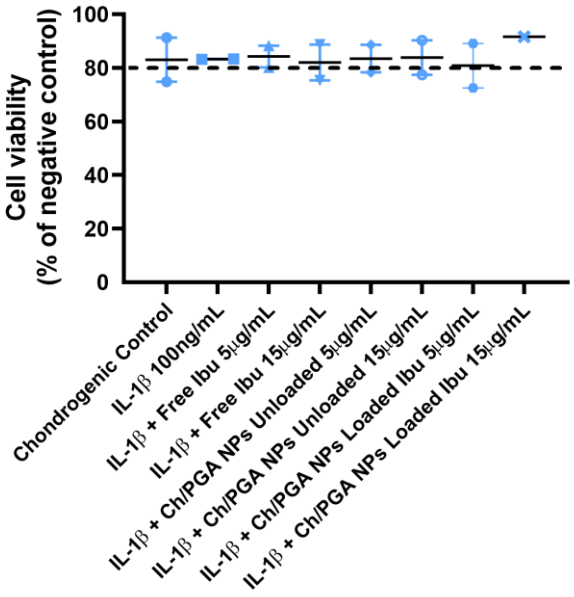

Figure 38 - Cell viability of 3D pellets aimed to test ibuprofen-loaded chitodan/PGA nanoparticles under a pro-inflammatory microenvironment. Results are presented as mean ± SEM; n = 2 replicates. Ibu – Ibuprofen; Ch – Chitosan; PGA – Polyglutamic Acid; NPs – Nanoparticles.

5.4.2. Alcian Blue and Safranin-O Stainings

Regarding alcian blue and safranin-O stainings that overall reflect ECM deposition in terms of sGAG and proteoglycans, it is clear that this deposition diminishes when hACs pellets are subjected to the pro-inflammatory microenvironment when compared to the chondrogenic control (Figure 39, Figure 40). This was also observed for the stained pellets of these conditions in the experiment regarding the treatment with PLGA NPs (Figure 31, Figure 32).

In Figure 39 sGAG deposition seems to be maintained the same as in the IL-1β treatment when pellets were under the treatment of unloaded NPs 5μg/mL and loaded NPs at both concentrations.

In Figure 40 proteoglycans deposition appears to be recovered more proximately to the normal conditions when ibuprofen free was added at 15 μg/mL. It looks like the deposition intensity verified in the pro-inflammatory control was maintained with the addition of ibuprofen at 5 μg/mL either in its free and loaded form.

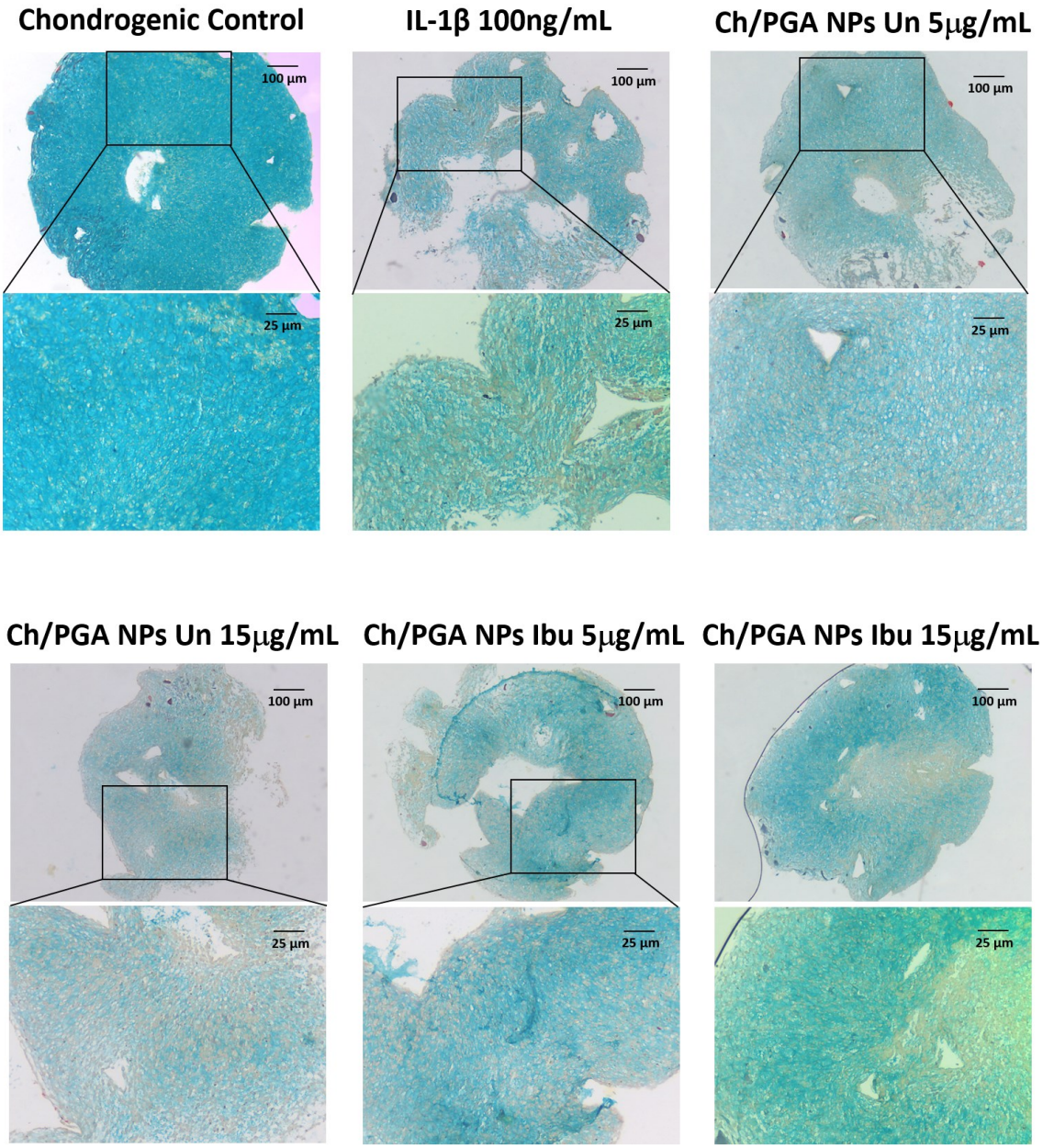

Figure 39 - Alcian blue histological stainings of 3D pellets aimed to test ibuprofen-loaded chitosan/PGA nanoparticles under a pro-inflammatory microenvironment. Scale bar of upper images = 100 μm; Scale bar of lower images = 25 μm. Ibu – Ibuprofen; Ch – Chitosan; PGA – Polyglutamic Acid; NPs – Nanoparticles; Un – Unloaded.

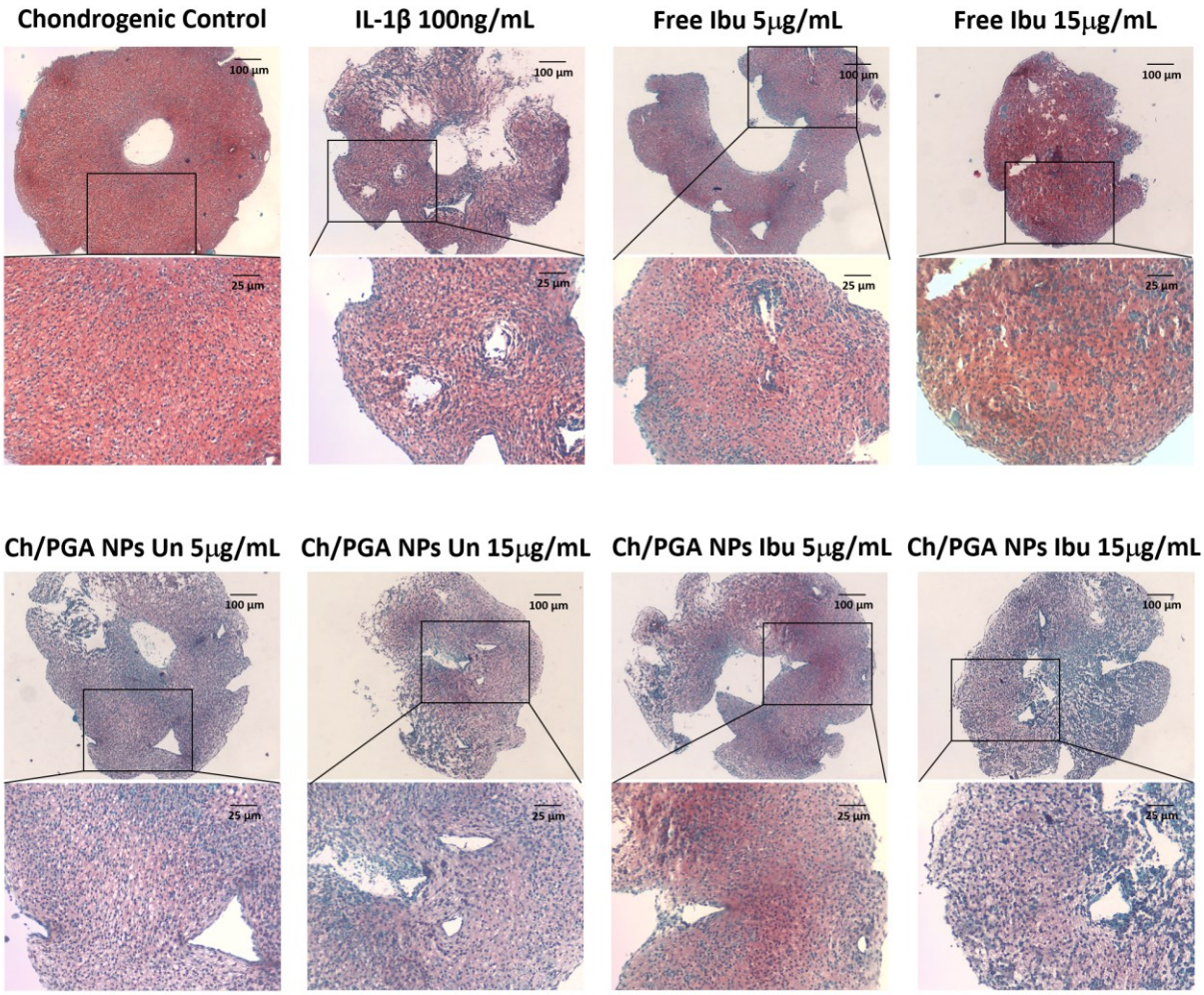

Figure 40 - Safranin-O histological stainings of 3D pellets aimed to test ibuprofen-loaded chitosan/PGA nanoparticles under a pro-inflammatory microenvironment. Scale bar of upper images = 100 μm; Scale bar of lower images = 25 μm. Ibu – Ibuprofen; Ch – Chitosan; PGA – Polyglutamic Acid; NPs – Nanoparticles; Un – Unloaded.

5.4.3. Immunohistochemical Staining of Type II Collagen and Aggrecan

Both collagen II and aggrecan expression showed to be reduced under the stimulation with IL-1β when compared to the chondrogenic control (Figure 41).

The treatments with free ibuprofen, unloaded and loaded chitosan/PGA NPs, all at the concentration of 15 μg/mL, seem to improve the expression levels of type II collagen. Overall, all the tested conditions of free drug, unloaded and loaded NPs appear to exert a beneficial impact on collagen expression.

As for the levels of aggrecan, they appear to be slightly increased with the treatment with 5 μg/mL of free ibuprofen and with both concentrations of unloaded NPs. This last observation is in agreement with chitosan feature of inducing chondrogenic phenotype [173]

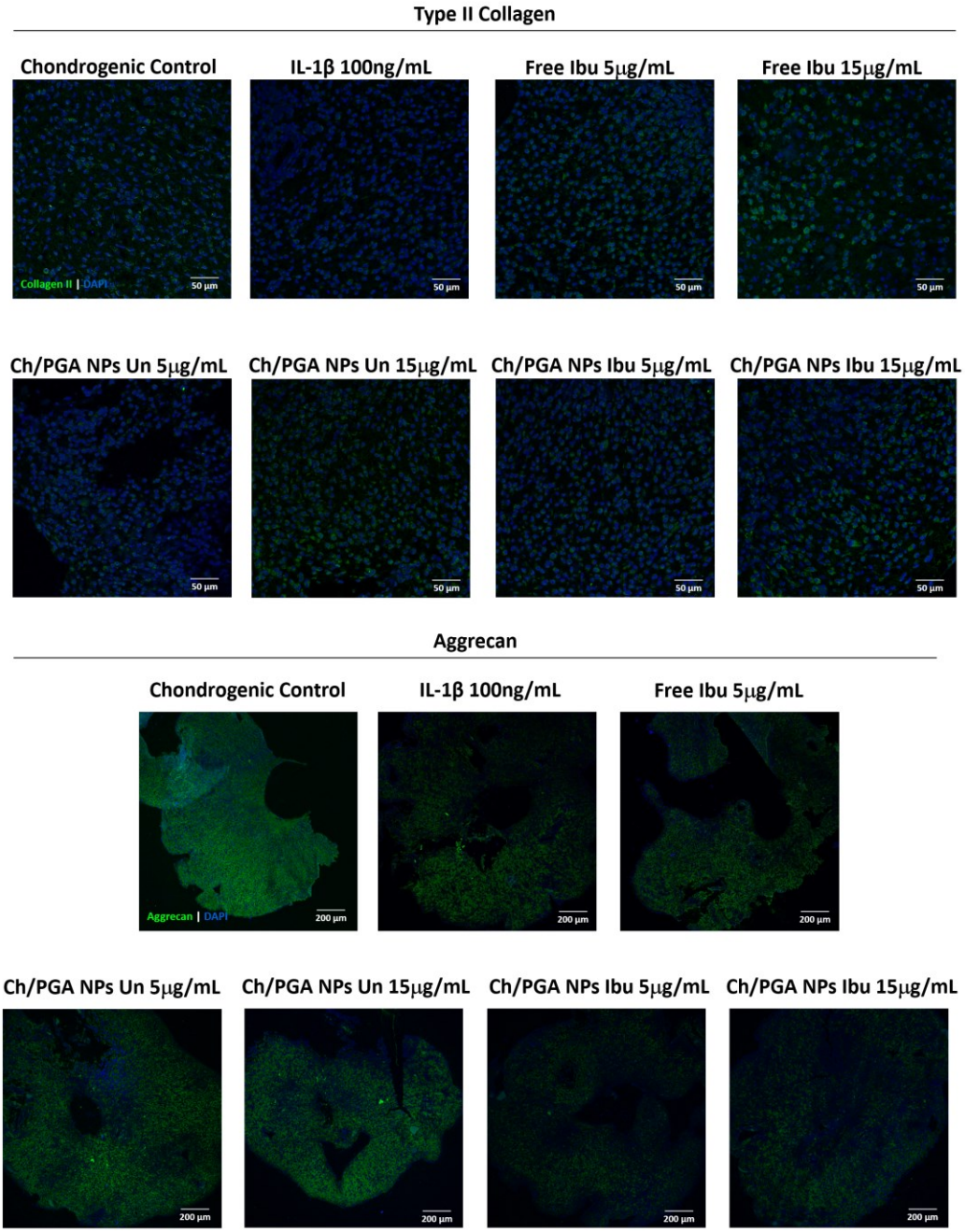

Figure 41 - Immunohistochemical staining of type II collagen (top panel) and aggrecan (bottom panel) in 3D pellets aimed to test ibuprofen-loaded chitosan/PGA nanoparticles under a pro-inflammatory microenvironment. Top panel scale bar = 50 μm; Bottom panel scale bar = 200 μm. Ibu – Ibuprofen; Ch – Chitosan; PGA – Polyglutamic Acid; NPs – Nanoparticles; Un – Unloaded.

5.4.4. Cytokine Profiling

Both IL-1β and IL-6 synthesis appear to be increased in the 100 ng/mL of IL-1β condition in comparison to the chondrogenic control, taking into consideration that no IL-6 was produced in this control (Figure 42)), although no statistically significant

changes were observed, which maybe due to the low number of performed experiments and to the variability between donors. IL-1β levels are suggested to be high in every other conditions, inclusively higher than in the pro-inflammatory control for unloaded NPs 15 μg/mL and for NPs loaded with 5 μg/mL of ibuprofen (Figure 42 A).

Regarding IL-6 production by hACs in the 3D pellet pro-inflammatory microenvironment, it seems to be decreased in all tested conditions with free ibuprofen, and loaded and unloaded NPs, especially in the loaded ones at the concentration 15 μg/mL of ibuprofen (Figure 42 B). The displayed data resulted from only two independent experiments, which means it needs to be further explored in future experiments.

As previously mentioned, the levels of TNF-α and IL-10 were found to be below the kit's detection limits.

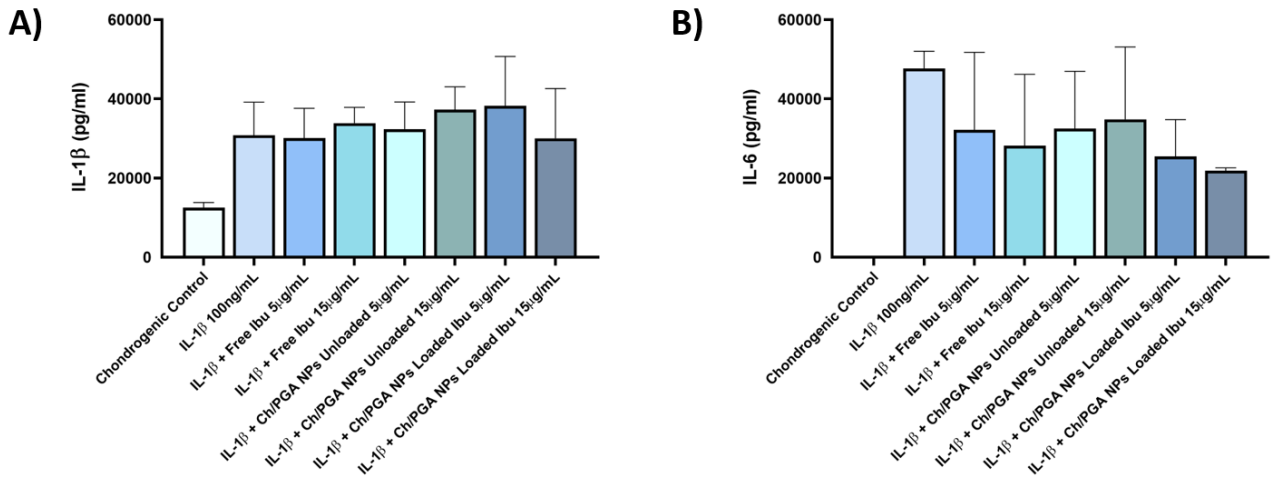

Figure 42 - Levels of A) IL-1β; and B) IL-6 measured in the conditioned mediums of 3D pellets aimed to test ibuprofen-loaded chitosan/PGA nanoparticles under a pro-inflammatory microenvironment. Results are presented as mean + SEM; n = 2 replicates. Ibu – Ibuprofen; Ch – Chitosan; PGA – Polyglutamic Acid; NPs – Nanoparticles; Un – Unloaded.

5.4.5. MMP Expression

The inhibitory effects of ibuprofen-loaded chitosan/PGA NPs on the expression of MMPs by hACS exposed to 100 ng/mL of IL-1β were evaluated. The results of two independent experiments are shown in Figure 43.

The obtained data appears to reveal that the treatment with NPs loaded with 15 μg/mL of ibuprofen may be inducing a trend toward decreased MMP-13 and MMP-9 transcripts (Figure 43 B, C) and MMP-3 seems to be the MMP more highly expressed in the tested conditions (Figure 43 D).

Overall, the analysis does not allow to clearly conclude any effect of the tested conditions on mRNA expression of MMPs. The number of experiments will be increased in order to reach reasoned conclusions.

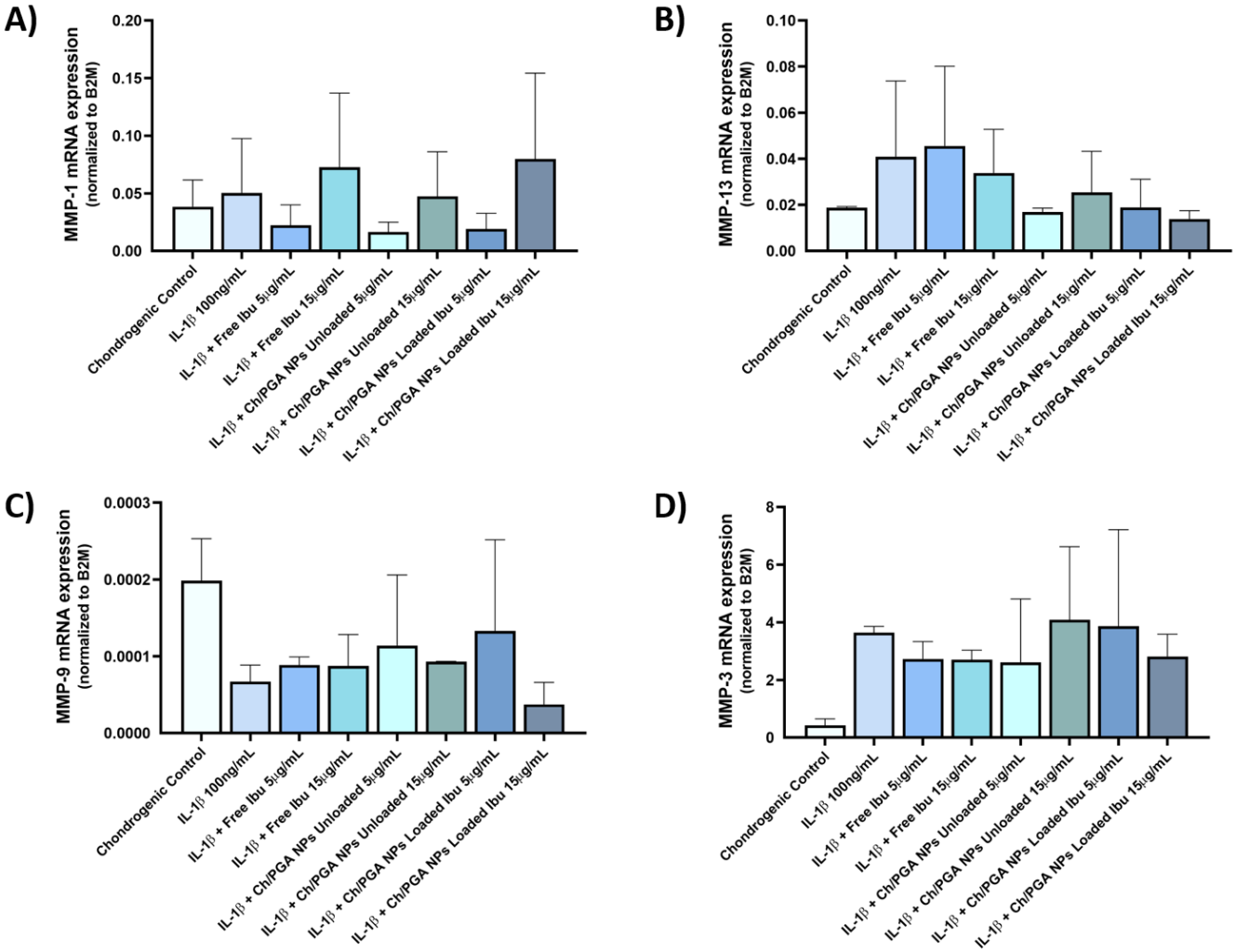

Figure 43 - mRNA expression levels of a) MMP-1; B) MMP-13; C) MMP-9; and D) MMP-3 in 3D pellets aimed to test ibuprofen-loaded chitosan/PGA nanoparticles under a pro-inflammatory microenvironment. Results are presented as mean + SEM; n = 2 replicates. Ibu – Ibuprofen; Ch – Chitosan; PGA – Polyglutamic Acid; NPs – Nanoparticles; Un – Unloaded.

5.4.6. Gelatin Zymography

In an attempt to complement the data obtained for MMPs expression and to more effectively evaluate the potential anti-enzymatic activity of the tested ibuprofen-loaded chitosan/PGA NPs, gelatin zymography was conducted using the samples' conditioned medium.

Although the employed gels were composed of gelatin and gelatinases (MMP-2 and MMP-9) were the MMPs more likely expected to be evaluated, the molecular weight of the detected bands seems to indicate that the pro and active MMP-3 forms were the ones degrading the gels (Figure 44).

It might be relevant to state the pro-MMP-3 form is higher in the chondrogenic control than in the pro-inflammatory condition (Figure 44 A) but that this situation is reverted in terms of MMP-3 active form (Figure 44 A), as expected.

Although the RT-qPCR results of MMP-3 synthesised transcripts does not show differences (Figure 43 D.), zymogram seems to indicate that every condition seemed to

be effective in reducing the activity of MMP-3 in the hACs 3D pellet exposed to the pro-inflammatory conditions (Figure 44).

To prove and sustain these results and to confirm that the identified enzyme is MMP-3, MMP-3 activity quantification will be further carried out.

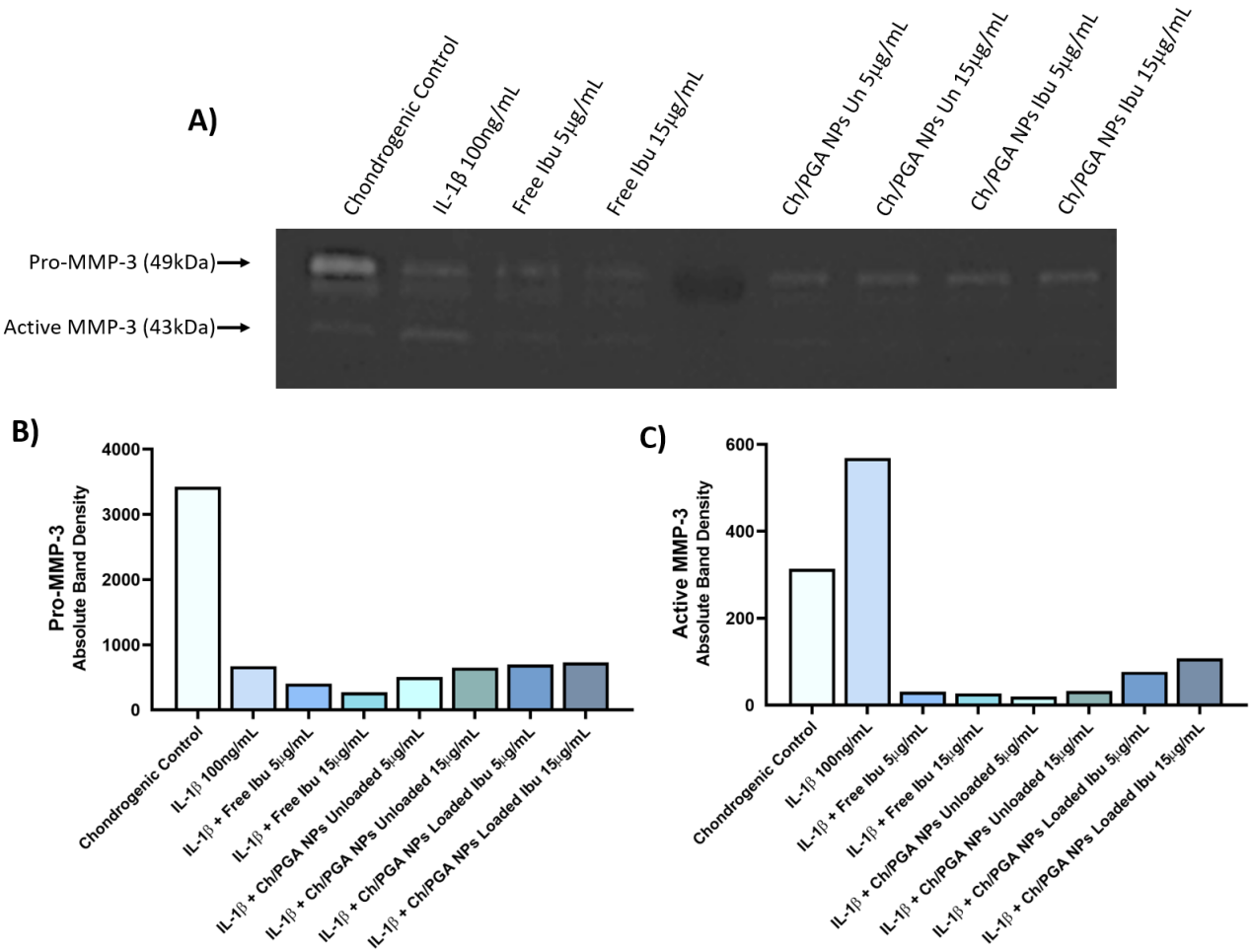

Figure 44 - MMP-3 enzyme activity for measured in the conditioned mediums of 3D pellets aimed to test ibuprofen-loaded chitosan/PGA nanoparticles under a pro-inflammatory microenvironment. A) Gelatin zymography gelatin results; B) Absolute band density for Pro-MMP-3; and C) Absolute band density for Active MMP-3 Results are presented as mean + SEM; n = 1 replicates. Ibu – Ibuprofen; Ch – Chitosan; PGA – Polyglutamic Acid; NPs – Nanoparticles; Un – Unloaded.

5.4.7. Evaluation of Pellet Areas

Pellets area seem to decrease from the ones treated only with chondrogenic medium and the ones where 100 ng/mL of IL-1β was added (Figure 45). The fact that non-significant differences can be achieved in the different areas measurements might be due to the low number of experiments and inter-donor variability. However, pellets from free ibuprofen 15 µg/mL, unloaded and loaded NPs at 5 µg/mL seem to present less area values, which can be either derived from a lower ECM deposition or a higher ECM degradation.

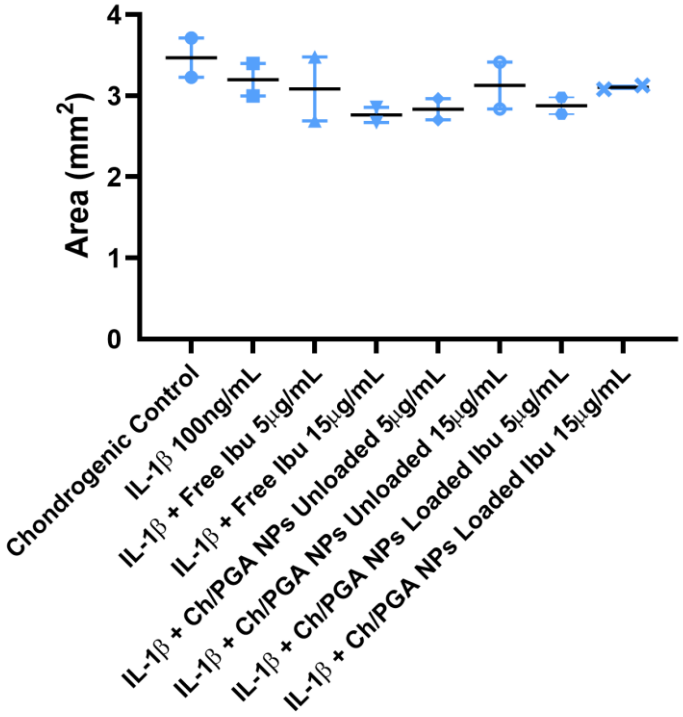

Figure 45 - Areas of 3D pellets aimed to test ibuprofen-loaded chitosan/PGA nanoparticles under a pro-inflammatory microenvironment. Results are presented as mean ± SEM; n = 2 replicates. Ibu – Ibuprofen; Ch – Chitosan; PGA – Polyglutamic Acid; NPs – Nanoparticles; Un – Unloaded.

5.4.8. Conclusion on the Ibuprofen-Loaded Ch/PGA Nanoparticles Concentration with Reproducible Chondroprotective Effects

Even though the collected data only refers to two independent experiments, it shows that the chitosan/PGA NPs are not cytotoxic for the hACs.

Additionally, results regarding pellets under the treatment of chitosan/PGA NPs loaded with 15 μg/mL of ibuprofen appear to show that these NPs have the ability to mitigate the chondrocytes' inflammatory reactivity (lower levels of IL-6 production), and to protect ECM from destruction (increased collagen II expression).

Further experiments need to be performed to confirm these results and advocate if they are reproducible.

5.4. EVALUATION OF THE EFFECTS OF BB-94-LOADED NANOEMULSIONS

In addition to try supressing IL-1β-induced inflammation by ibuprofen, another tested approach was to determine whether inhibiting the direct proteolysis of aggrecan or collagen or both would be effective in controlling the progression of cartilage matrix degradation in the established pro-inflammatory model of pelleted

hACs. As several enzymes are involved in the cartilage degradation, the targeting of several MMPs might be and effective tactic to protect ECM from that process [75].

This was attempted with the delivery of BB-94, a broad-spectrum inhibitor of several MMPs [73], to the cultured cells and assessments were performed three days after the treatment with those NEs. For this purpose, two different formulations were tested, as indicated in Table 1.

5.4.1. Cytotoxicity Assessment

Four independent experiments were simultaneously conducted with to evaluate the effects of BB-94-loaded NEs. The cytotoxicity results were converted into cell viability and are displayed in Figure 46.

Results reveal that the treatment with free BB-94 in the three evaluated concentrations (20, 40 and 100 nM) were not cytotoxic, but both unloaded and loaded NEs were cytotoxic to hACs. Particularly, the conditions where unloaded NEs corresponding to 40 nM (NEs lipid concentration of 2.5 mg/mL), and unloaded and loaded NEs of 100 nM (NEs lipid concentration of 6.25 mg/mL) induced a strong cytotoxicity, exhibiting a mean cell viability below 40% (of negative control).

It is of relevance to notice that in either unloaded and loaded NEs, cell viability appears to decrease with increasing concentration of NEs, which might indicate the cell death is related to the amount of NEs added.

Due to these high values, no further assessments were performed and a new formulation, where a lower concentration of NEs was needed to encapsulate the same amount of BB-94 (Table 1), was tested as an attempt to solve this problem.

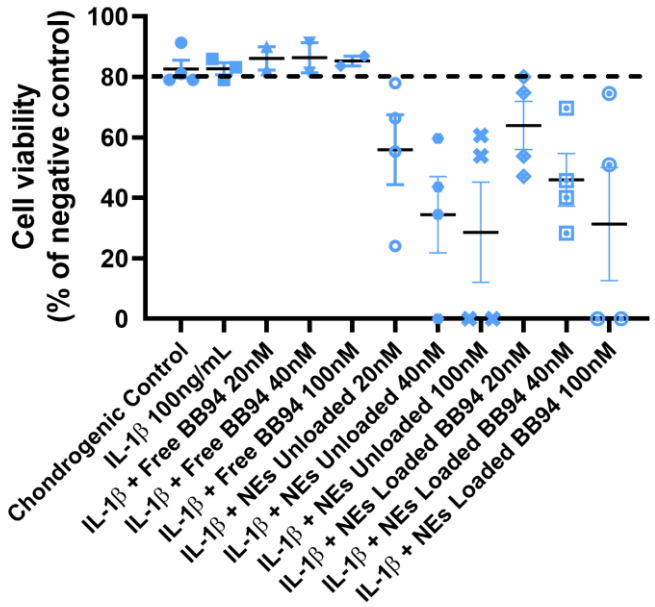

Figure 46 - Cell viability of 3D pellets aimed to test BB-94-loaded nanoemulsions under a pro-inflammatory microenvironment. Results are presented as mean ± SEM; n = 4 replicates. NEs – Nanoemulsions; BB94 – Batimastat.

For the newly developed formulation of NEs with increased drug loading (lipid concentration of 25, 50 and 125 μg/mL for the encapsulation of 20, 40 and 100 nM, respectively), two independent experiments were conducted simultaneously in order to evaluate if a lower concentration of NEs would lead to a reduction in cytotoxicity. The cytotoxicity results obtained for one independent experiment were converted into cell viability and are displayed in Figure 47.

By the obtained results it seems correct to affirm that the cytotoxicity issues were surpassed with the employment of this new formulation, once the overall cell viability results were above 80% (of negative control).

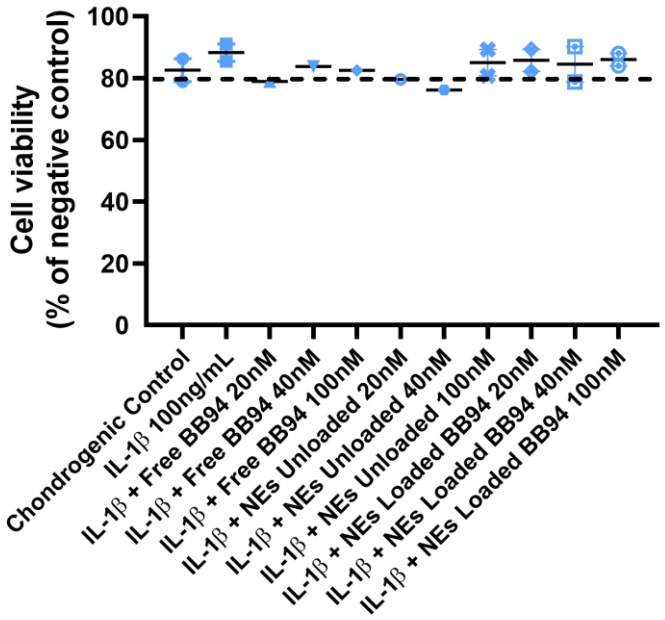

Figure 47 - Cell viability of 3D pellets aimed to test BB-94-loaded nanoemulsions under a pro-inflammatory microenvironment. Results are presented as mean ± SEM; n = 2 replicates. NEs – Nanoemulsions; BB94 – Batimastat.

5.4.2. Evaluation of Pellet Areas

As suggested in Figure 48, ECM deposition and destruction might be higher and lower, respectively, at the chondrogenic control condition and the other way around for the pro-inflammatory condition, once the pellets' areas drops from one condition to another.

The treatment with BB-94-loaded NEs at the three tested conditions appears not to induce an increase of pellet area when compared to the 100 ng/mL of IL-1β condition.

Further evaluations should be performed to assess the anti-proteolytic and chondrogenic activity of these NEs loaded with BB-94.

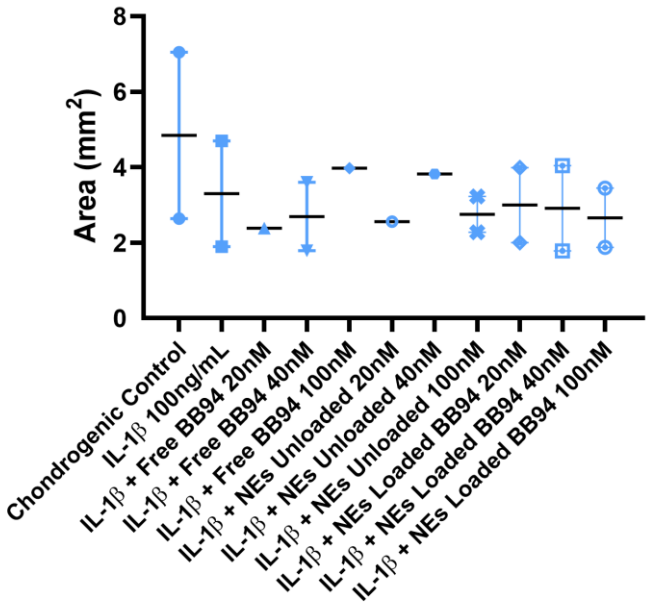

Figure 48 - Areas of 3D pellets aimed to test BB-94-loaded nanoemulsions under a pro-inflammatory microenvironment. Results are presented as mean ± SEM; n = 2 replicates. NEs – Nanoemulsions; BB94 – Batimastat.

5.5. EVALUATION OF THE EFFECTS OF TRICOMBINATORY NANOEMULSIONS

Due to the large number of different molecules involved in OA and cartilage lesions, a combination of anti-inflammatory and anti-proteolytic approaches seems to be required [71, 84]. As such, an approach to test the effect of the combined delivery of both ibuprofen and BB-94 was carried.

Besides these anti-inflammatory and anti-proteolytic compounds, nisin was also present in the formulation of tricombinatory NEs. Nisin is an antimicrobial peptide [251] included in the formulation with the aim of avoiding the development bacterial infections during COPLA® Scaffold implantation at the lesion sites. Assessments were performed three days after adding the tricombinatory NEs to the pellets.

5.5.1. Cytotoxicity Assay

For this formulation of NEs, two independent experiments were simultaneously conducted. The cytotoxicity results were converted into cell viability and are displayed in Figure 49.

Similarly to what was observed for the first formulation of BB-94-loaded NPs, both unloaded and loaded tricombinatory NEs appeared to be exerting a severe cytotoxicity in hACs. It is also noticeable that, in each group, the higher the concentration of NEs, the lower the cell viability levels.

A new formulation with a higher encapsulation of compounds in a lower concentration of NEs should be tested as an attempt to overcome this issue.

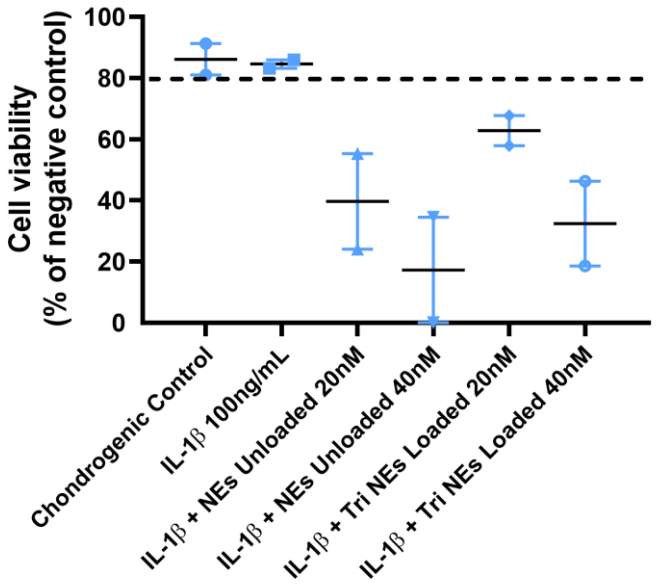

Figure 49 - Cell viability of 3D pellets aimed to test tricombinatory nanoemulsions under a pro-inflammatory microenvironment. Results are presented as mean ± SEM; n = 2 replicates. NEs – Nanoemulsions.

5.6. EVALUATION OF THE EFFECTS OF MUPIROCIN-LOADED NANOEMULSIONS

As nisin is unstable at physiologic pH [251], it was decided to test another antibacterial peptide, mupirocin [252], to further be incorporated in tricombinatory NEs. Assessments were performed three days after adding the tested conditions to the pellets.

5.6.1. Cytotoxicity Assessment

A concentration of this drug was tested, 1.2 μg/mL, which was the concentration that had the best anti-bacterial activity, and LDH assay was performed. The cytotoxicity results from one experiment were converted into cell viability and are shown in Figure 50.

Cytotoxicity analysis suggests that NEs are not toxic to the pelleted hACs, even though only one experiment was performed.

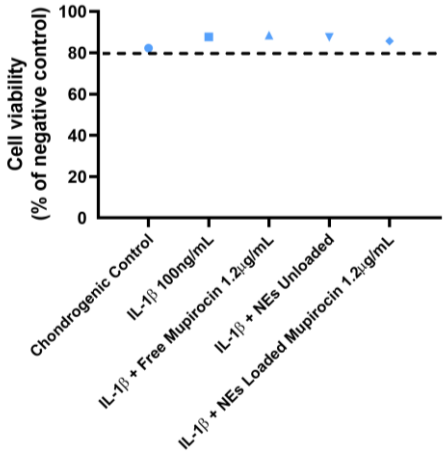

Figure 50 - Cell viability of 3D pellets aimed to test mupirocin-loaded nanoemulsions under a pro-inflammatory microenvironment. n = 1 replicate. NEs – Nanoemulsions.

5.6.2. Evaluation of Pellet Areas

Pellet seemed to be bigger in size in the chondrogenic condition, decreased in the pro-inflammatory condition and was not able to recover in the free, unloaded nor loaded condition (Figure 51).

Mupirocin is described to be able to reduce the up-regulated IL-6 levels induced by bacterial infections in skin [253], but these and other possible unknown effects in chondrocytes should be verified and tested through further assessments.

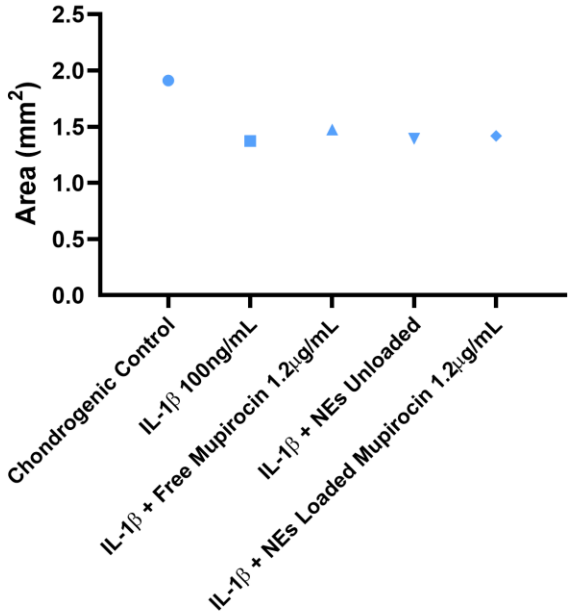

Figure 51 - Areas of 3D pellets aimed to test mupirocin-loaded nanoemulsions under a pro-inflammatory microenvironment. n = 1 replicate. NEs – Nanoemulsions.

5.7. EVALUATION OF THE CAPACITY OF COPLA® SCAFFOLDS TO SUPPORT HUMAN CHONDROCYTES' ADHESION, DIFFERENTIATION AND ECM PRODUCTION

Targeting the effect of a single cytokine at the systemic level, like IL-1β or TNF-α, might not be efficient in inducing a beneficial effect on cartilage destruction, as therapeutics are unable to penetrate the damaged joint [84]. This is the main reason why the local delivery of ibuprofen through biodegradable NPs is a favourable approach.

As for the blockage of MMPs activity with BB-94, its on site, sustained delivery by controlled-release NEs represents an asset in the treatment of cartilage lesions. Moreover, in comparison with other approaches, this avoids the complete inhibition of proteinases, which would reduce necessary remodelling and other cellular signalling pathways that involve these enzymes [144]. The complete inhibition of these enzymes is undesirable in the treatment of inflammatory conditions [144].

Altogether and collecting all the mentioned advantages, the implantation of the adjustable in shape and depth nanoenabled COPLA® Scaffolds at the defect sites to effectuate the local delivery of anti-inflammatory and anti-proteolytic compounds seems to be a promising approach, once cartilage lesions and OA may involve only limited areas of cartilage [254] and it may reduce drugs side effects while improving local half-life and concentration.

The local delivery provided by the ibuprofen-loaded NPs, BB-94-loaded NEs or tricombinatory NEs embedded in COPLA® Scaffolds should promote a reduction in the pro-inflammatory-induced cartilage loss, in order to maintain the normal biomechanical function of the affected joint [156].

While the experiments above related with the 3D pellet cultures aimed to obtain preliminary results on the evaluation of chondroprotective and chondrogenic effects of the loaded nanodelivery systems, the following experiments were set and evaluated in order to understand the effects of scaffolds *per se* in hACs and to establish a pro-inflammatory microenvironment in these biodegradable polymers.

First, the goal was to establish an adequate model of cell seeding on COPLA® Scaffolds, evaluate cell adhesion in these 3D porous structures, and assess their ability to promote chondrocytes' (re)differentiation (when cells were previously expanded) and chondrogenic potential. Two protocols were followed when seeding chondrocytes on scaffolds: one where hACs were previously expanded in 2D culture monolayers and another using hACs readily after their isolation from cartilage samples.

5.7.1. Cytotoxicity Assessment

5.7.1.1. Seeding with Previously Expanded Chondrocytes

In this approach, hACs were cultured on COPLA® Scaffolds for 28 days. The cytotoxicity results from one experiment were converted into cell viability. As demonstrated in Figure 52, the culture conditions only in chondrogenic medium were not cytotoxic to the cells throughout culture time.

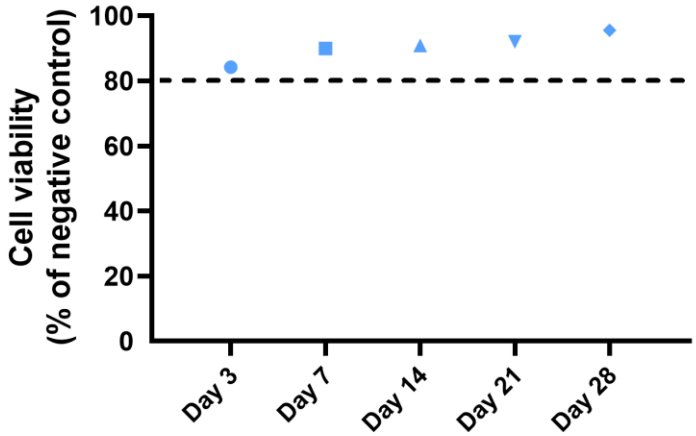

Figure 52 - Cell viability of previously expanded chondrocytes cultured on COPLA® Scaffolds for 28 days. n = 1 replicate.

5.7.1.2. Seeding with Readily Isolated Chondrocytes

In this approach, hACs were cultured on COPLA® Scaffolds for 14 days. The cytotoxicity results from two independent experiments were converted into cell viability. As shown in Figure 53, the culture conditions of already differentiated chondrocytes were not cytotoxic in the first three days of culture. At 7th and 14th days, these conditions induced only weak cytotoxicity in these fully differentiated hACs.

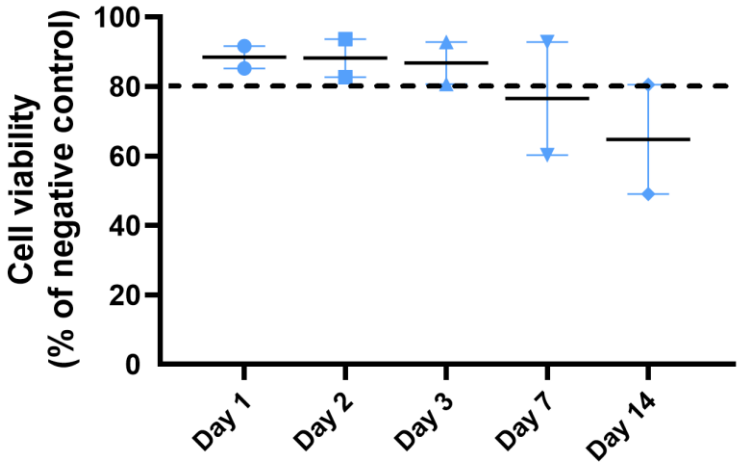

Figure 53 - Cell viability of readily isolated chondrocytes cultured on COPLA® Scaffolds for 14 days. Results are presented as mean ± SEM; n = 2 replicates.

5.7.2. Immunohistochemical Staining of Type II Collagen, Aggrecan and Actin

5.7.2.1. Seeding with Previously Expanded Chondrocytes

As expanded chondrocytes need a 3D environment to induce and support their native chondrogenic phenotype [26] and COPLA® Scaffold promotes that kind of environment, it is expected that pellets redifferentiate when cultured in these scaffolds. Immunohistochemical stainings are presented since day 3 until day 21 of culture (Figure 54).

Through the staining of actin filaments it is possible to notice that as soon as day 3, cells already start changing their morphology and rediferentiating into a more rounded shape (white arrows).

Both type II collagen and aggrecan deposition seems to increase from day 3 to day 7 but to decrease in longer timepoints. This initial increase might suggest that COPLA® Scaffold allows for hACs to redifferentiate.

As day 7 is suggested to be the timepoint where cartilage-specific markers deposition is more pronounced and cells are already regaining their native round morphology, IL-1β was only added after 7 days of differentiation to assure that cells were already reacquiring their native phenotype. This is coherent with the 7 days of differentiation defined in the 3D pellets model.

Moreover, cell adhesion in the COPLA® Scaffolds appears to be good, otherwise they would be washed out during medium changes.

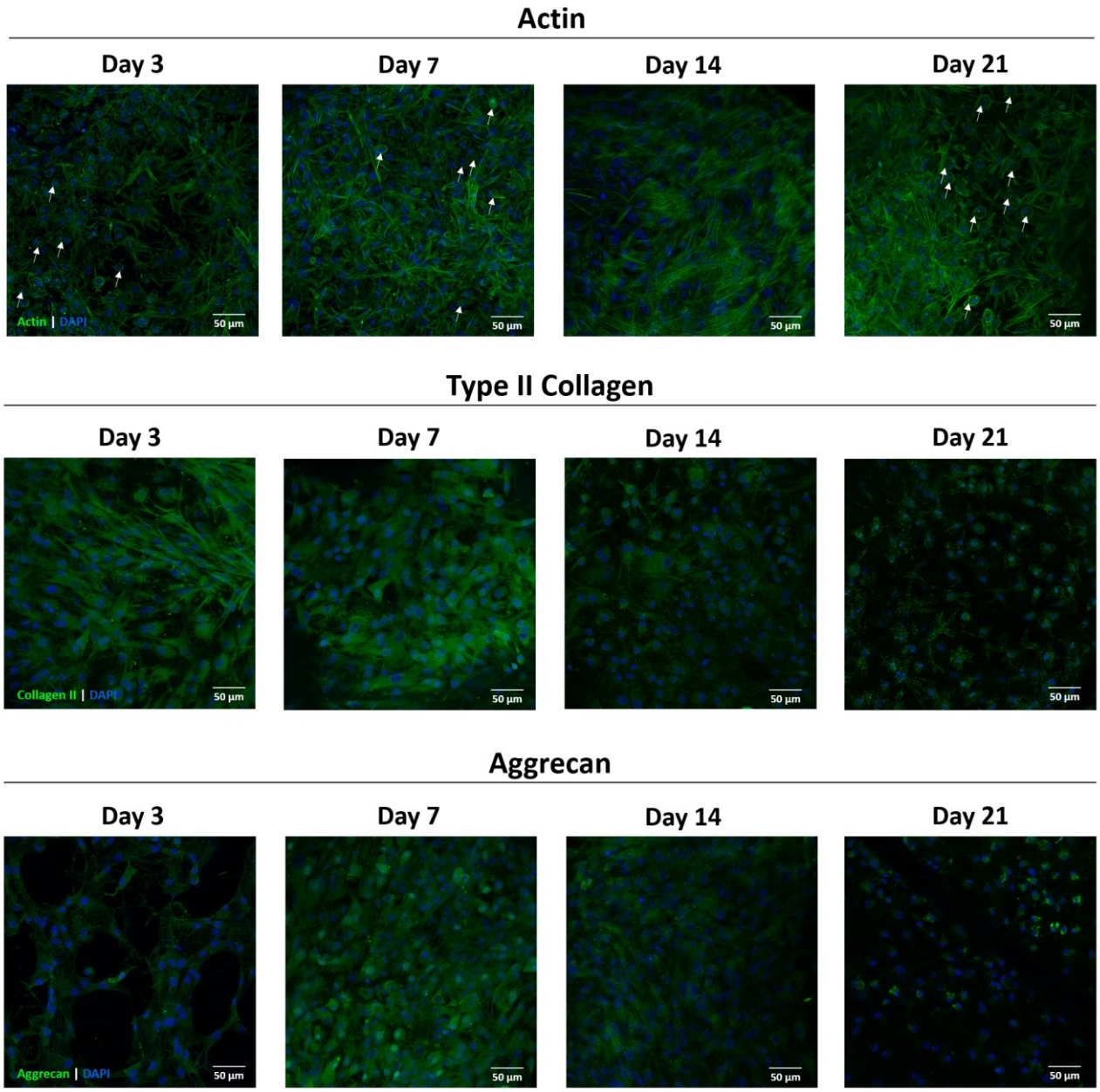

Figure 54 - Immunohistochemical staining of actin (top panel), type II collagen (middle panel) and aggrecan (bottom panel) in previously expanded chondrocytes cultured on COPLA® Scaffolds for 28 days. White arrows point to the cells with a rounded shape. Scale bar = 50 µm.

5.7.2.2. Seeding with Previously Expanded Versus Readily Isolated Chondrocytes

Images displayed in Figure 55 aim to enable a direct comparison of cell morphology between the two different seeding approaches at a specific timepoint.

A clear distinction in chondrocytes' morphology can be identified, essentially because, at day 3 of culture, in the directly seeded condition all fully differentiated chondrocytes are round in shape, whereas although in the previously expanded condition some were already showing that morphology, the vast majority of cells were still fibroblast-like-shaped.

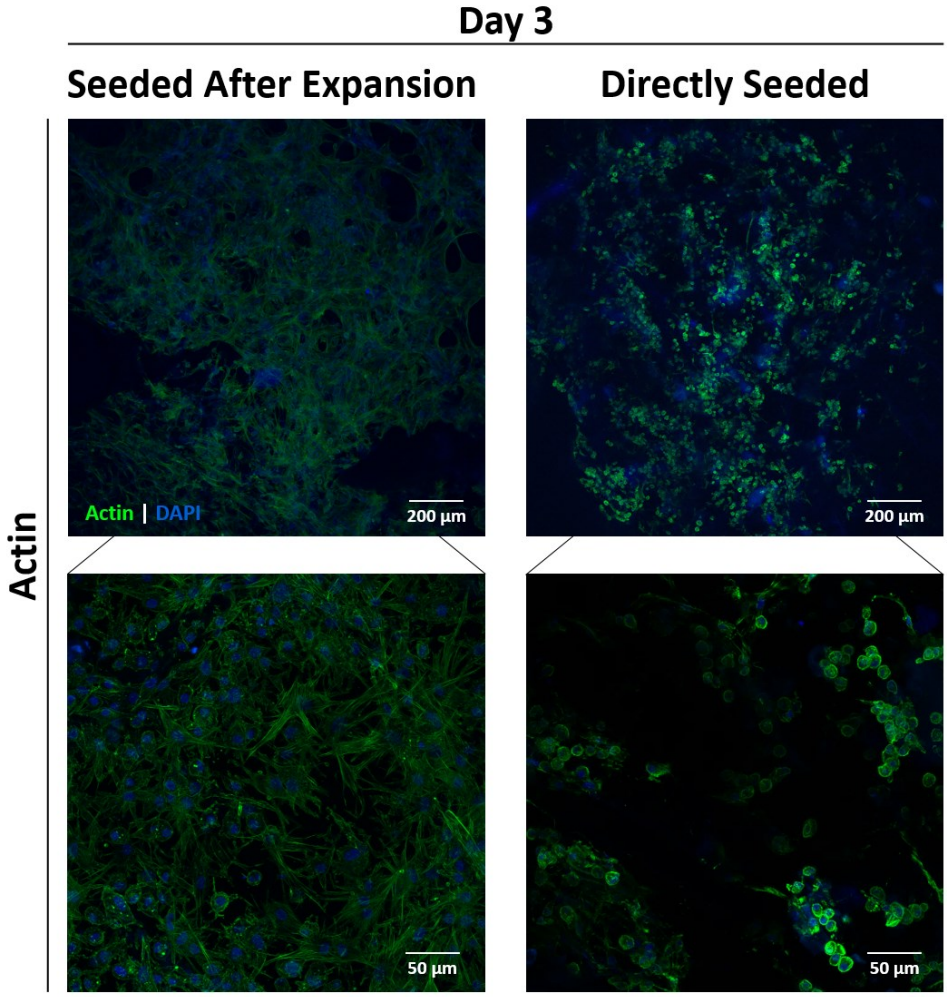

Figure 55 - Immunohistochemical staining of actin both in previously expanded chondrocytes (left) and in readily isolated chondrocytes (right) seeded on COPLA® Scaffolds at day 3 of culture. Top images scale bar = 200 µm; Bottom images scale bar = 50 µm.

5.8. ESTABLISHMENT OF A PRO-INFLAMMATORY MICROENVIRONMENT IN COPLA® SCAFFOLDS

As showed in the 3D pellet cultures, the 100 ng/mL of IL-1β added to the chondrogenic medium appears to be both the concentration and the cytokine that enables the most efficient establishment of a pro-inflammatory environment in hACs.

Considering those results, that was the condition used in COPLA® Scaffolds for such purpose.

5.8.1. Cytotoxicity Assessment

5.8.1.1. Seeding with Previously Expanded Chondrocytes

The cytotoxicity of the pro-inflammatory stimulus in hACs, cultured for 7 days on COPLA® Scaffolds after being expanded in 2D monolayers, was assessed 3 and 7 days after the addition of that stimulus.

The cytotoxicity results obtained for one independent experiment were converted into cell viability and are displayed in Figure 56Figure 26. The results confirm that the addition of 100 ng/mL did not induce cytotoxicity at day 3 nor at day 7 of culture.

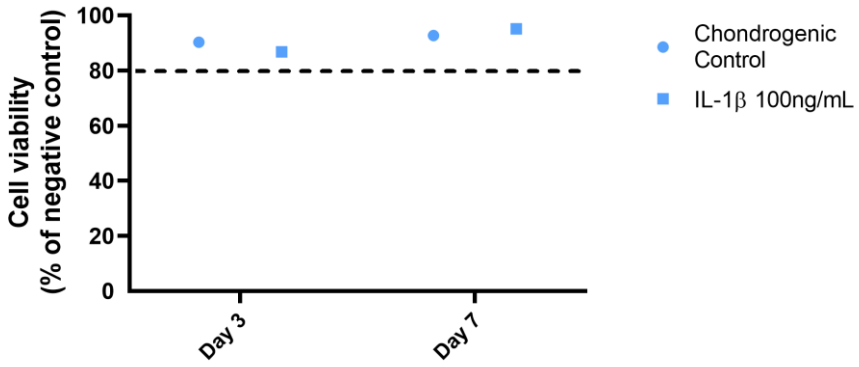

Figure 56 - Cell viability of previously expanded chondrocytes cultured on COPLA® Scaffolds 3 and 7 days after the addition of the pro-inflammatory stimulus. n = 1 replicate.

5.8.1.2. Seeding with Readily Isolated Chondrocytes

Regarding the hACs readily seeded after isolation, two different approaches were followed: one where the 100 ng/ml of IL-1β were directly added to the scaffold medium right after cell seeding and another where the 100 ng/ml of IL-1β were only added to the scaffold medium three hours after cell seeding was performed.

Afterwards, assessments were conducted 3, 7 and 14 days of culture under the pro-inflammatory microenvironment.

The cytotoxicity results obtained for two independent experiments were converted into cell viability and are shown in Figure 57Figure 26. At day 3, both conditions of pro-inflammatory microenvironment establishment showed weak cytotoxicity when compared to the non-toxic chondrogenic control.

At day 7, the addition of IL-1β to the chondrogenic medium seems to induce a weak cytotoxicity in hACs but they this weak effect was also happened in the chondrogenic control for this day (in agreement with Figure 53).

However, at day 14 of culture the mean cell viability is showed to increase above 80% (of the negative control) in the control and tested conditions. More experiments showed be performed in other to confirm these results.

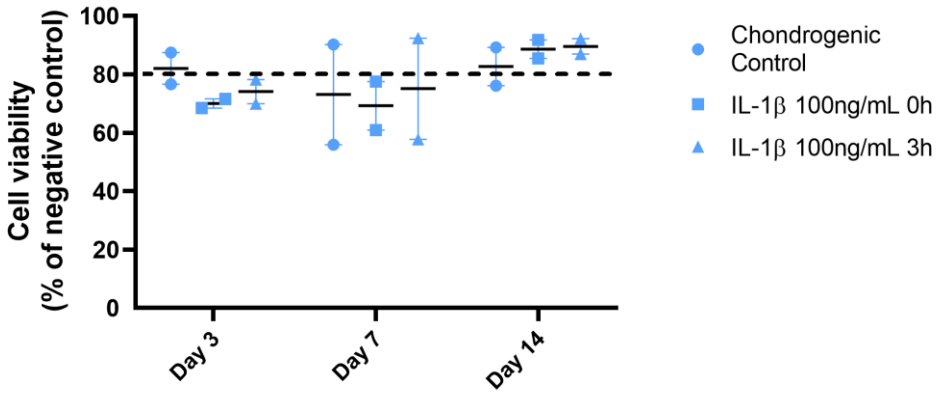

Figure 57 - Cell viability of readily isolated chondrocytes cultured on COPLA® Scaffolds 3, 7 and 14 days after the addition of the pro-inflammatory stimulus. Results are presented as mean ± SEM; n = 2 replicates.

5.8.2. Immunohistochemical Staining of Type II Collagen, Aggrecan and Actin

5.8.2.1. Seeding with Previously Expanded Chondrocytes

Actin and type II collagen were immunohistochemically stained in the scaffolds seeded with previously expanded chondrocytes cultured under 100 ng/mL of IL-1β influence and compared to the stainings obtained for the chondrogenic control (Figure 58). Actin fibers deposition reveal that, even though not as perceptible in day 7, IL-1β-stimulated cells maintain their shape at day 3 when compared to the control.

As for the deposition of type II collagen, it is shown to decrease in both timepoints under the pro-inflammatory microenvironment (as happened for the pellets, Figure 33 and Figure 41 top panels).

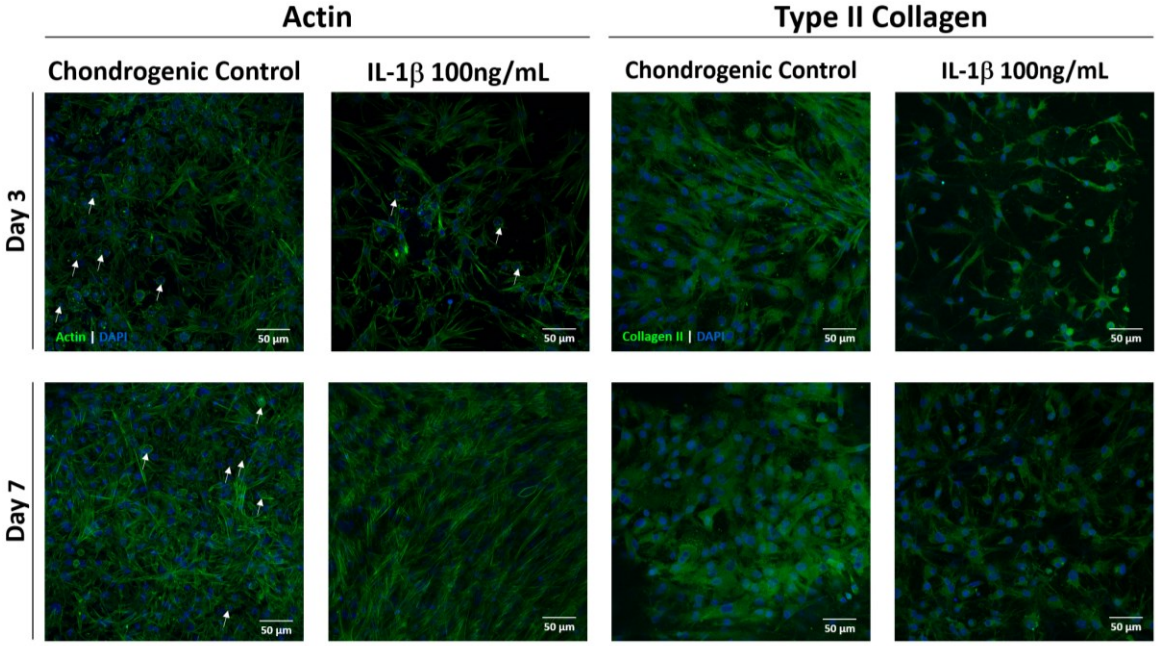

Figure 58 - Immunohistochemical staining of actin (right panel) and type II collagen (left panel) in previously expanded chondrocytes cultured on COPLA® Scaffolds 3 and 7 days after the addition of the pro-inflammatory stimulus. White arrows point to the cells with a rounded shape. Scale bar = 50 µm.

5.8.2.2. Seeding with Readily Isolated Chondrocytes

Actin, type II collagen and aggrecan were immunohistochemically stained in the scaffolds seeded with readily isolated hACs three days after the addition of 100 ng/mL of IL-1β, which was performed either 0 or 3 hours after seeding (Figure 59).

Actin deposition is more pronounced in the control condition than in the conditions of 0 and 3h of IL-1β addition after seeding, but in every condition the rounded cell morphology is evident.

As for the deposition of collagen type II, it appears to be more extended to the intercellular space in the control than in the pro-inflammatory conditions, where this ECM component seems to be more restricted to the boundaries of the chondrocytes. Additionally, a reduction in this deposition seems to be clearer in the addition of IL-1β 0h after seeding condition.

Regarding the deposition of aggrecan, it also appears to decrease in both treatments with IL-1β and to be more noticeable in the proximate surroundings of chondrocytes than in the intercellular space when compared to the chondrogenic control.

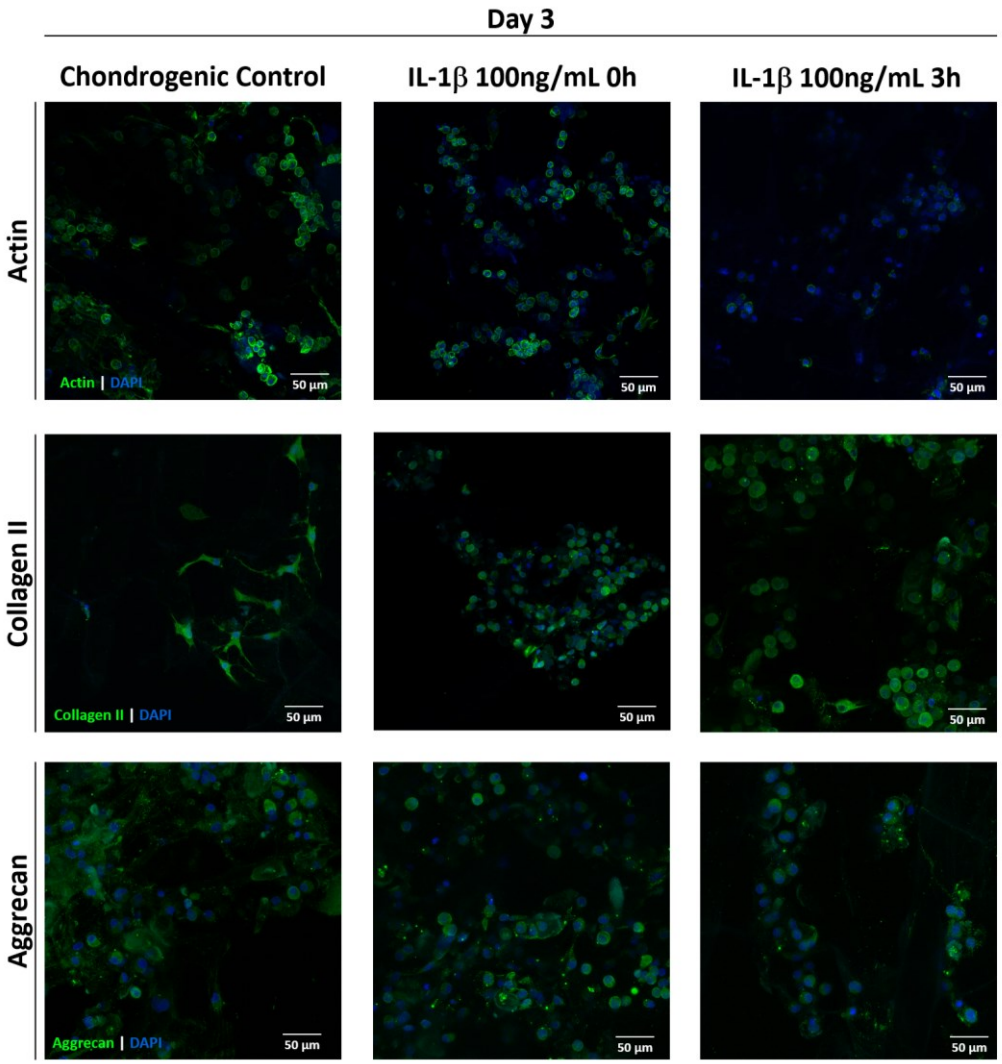

Figure 59 - Immunohistochemical staining of actin (top panel), type II collagen (middle panel) and aggrecan (bottom panel) in readily isolated chondrocytes cultured on COPLA® Scaffolds 3 days after the addition of the pro-inflammatory stimulus. Scale bar = 50 µm.

5.8.3. Cytokine Profiling

5.8.3.1. Seeding with Previously Expanded Chondrocytes

The IL-1β levels induced in previously expanded hACs were higher three days after the treatment with 100 ng/mL of IL-1β when compared to the chondrogenic control (Figure 60 A). However, at day 7, these synthesised levels were lower than in the chondrogenic control and also lower than the ones measured at the control condition where scaffolds were only cultured with chondrogenic medium and IL-1β and without cells (dashed line).

As for the production of IL-6, it was only detectable at day 3 after the pro-inflammatory treatment (Figure 60 B).

Altogether, these data point out to a possible capacity of COPLA® Scaffolds to induce a downregulation of the synthesis of these pro-inflammatory cytokines at day 7. Considering that IL-1β induces the production of IL-6 and that the signalling cascade of these two cytokines induce the synthesis of matrix-degrading MMPs [65, 73], lower levels of these cytokines will downregulate the production of MMPs and so decrease ECM degradation. In this way, this chondroprotective effect seems to be in agreement with the verified higher content of type II collagen at day 7 of pro-inflammatory treatment when compared to the day 3 (Figure 58).

The levels of TNF-α and IL-10 were found to be below the kit's detection limits.

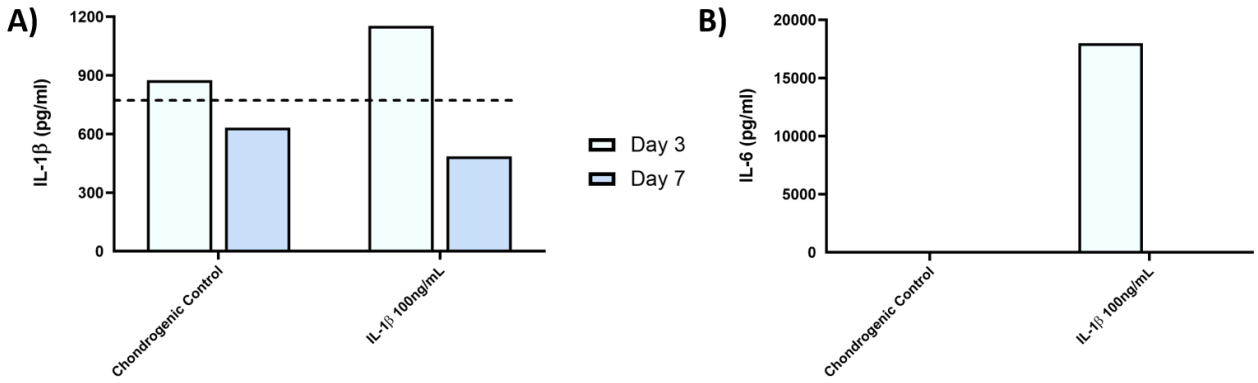

Figure 60 - Levels of A) IL-1β; and B) IL-6 measured in the conditioned mediums of previously expanded chondrocytes cultured on COPLA® Scaffolds 3 and 7 days after the addition of the pro-inflammatory stimulus. The dashed lines in graph A) mark the amount of IL-1β measured in the control where COPLA® Scaffolds were cultured under the pro-inflammatory microenvironment without the presence of cells. n = 1 replicate.

5.8.3.2. Seeding with Readily Isolated Chondrocytes

IL-6 levels measured in the conditioned medium of IL-1β-treated hACs were higher both in days 3 and 7, and either 0 and 3 hours after cell seeding, when compared to the chondrogenic control (Figure 61).

Although the synthesis of this cytokine was higher when culturing readily isolated chondrocytes than when culturing previously expanded chondrocytes (Figure 60 B), a trend towards diminishing IL-6 levels of production from day 3 to day 7 is also herein

verified both at the 0 and 3 hours conditions. Moreover, these levels were undetected at day 14 of treatment.

The levels of synthesised IL-1β were below the kit's detection limits. Overall, these results seem to corroborate the chondroprotective effect of COPLA® Scaffolds upon day 7 in inhibiting the production of pro-inflammatory cytokines, as suggested in Figure 60 for the expanded chondrocytes.

The levels of TNF-α and IL-10 were found to be below the kit's detection limits.

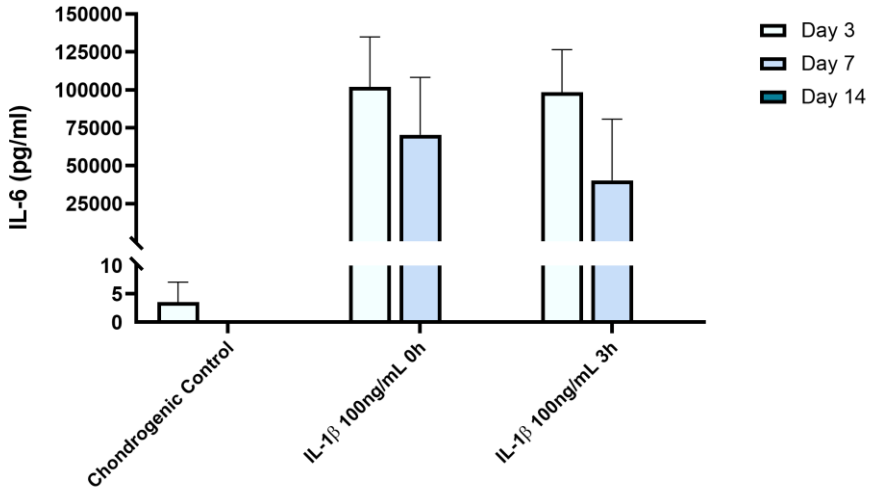

Figure 61 - Levels of IL-6 measured in the conditioned mediums of readily isolated chondrocytes cultured on COPLA® Scaffolds 3, 7 and 14 days after the addition of the pro-inflammatory stimulus. Results are presented as mean + SEM; n = 2 replicates.

5.8.3.3. Comparison between Culture on Pellets and on COPLA® Scaffolds

As both in pellets and in COPLA® Scaffolds seeded chondrocytes after monolayered expansion a period of 7 days of (re)differentiation preceded the treatment with 100 ng/mL of IL-1β and as the same cell density was cultured in both experimental conditions ($1x10^6$ cells/mL for pellets and $300x10^6$ cells in 300 μL), a direct comparison between cytokine levels seems to be appropriate.

In terms of IL-1β levels, they appear to be far more increased in hACs cultured in 3D pellets than in COPLA® Scaffolds (Figure 62 A). Moreover, after the addition of the pro-inflammatory stimulus the augmented synthesis of this cytokine seems to occur in a much higher extent in 3D pellets than in the scaffolds, when compared to each control.

As for the production of IL-6, its levels appear to be lower in hACs cultured in COPLA® Scaffolds after expansion than in 3D pellets (Figure 62 B), not only after the IL-1β treatment, but also in the chondrogenic control.

About these concentrations in the COPLA® Scaffolds seeded readily after isolation, IL-1β was not detected (Figure 62 A) and IL-6 is increased when they were treated with the pro-inflammatory stimulus in comparison to either hACs seeded in scaffolds after expansion and in 3D pellets (Figure 62 B). However, IL-6 is suggested to be downregulated in the chondrogenic control of this condition when compared to the 3D pellets.

Considering all the described observations, it seems that COPLA® Scaffolds might be exerting some anti-inflammatory intrinsic effect in hACs seeded under pro-inflammatory conditions.

To corroborate this data and to have a better understanding of this anti-inflammatory phenomenon, the number of replicates should be increased and further studies on MMPs production and activity should be carried out.

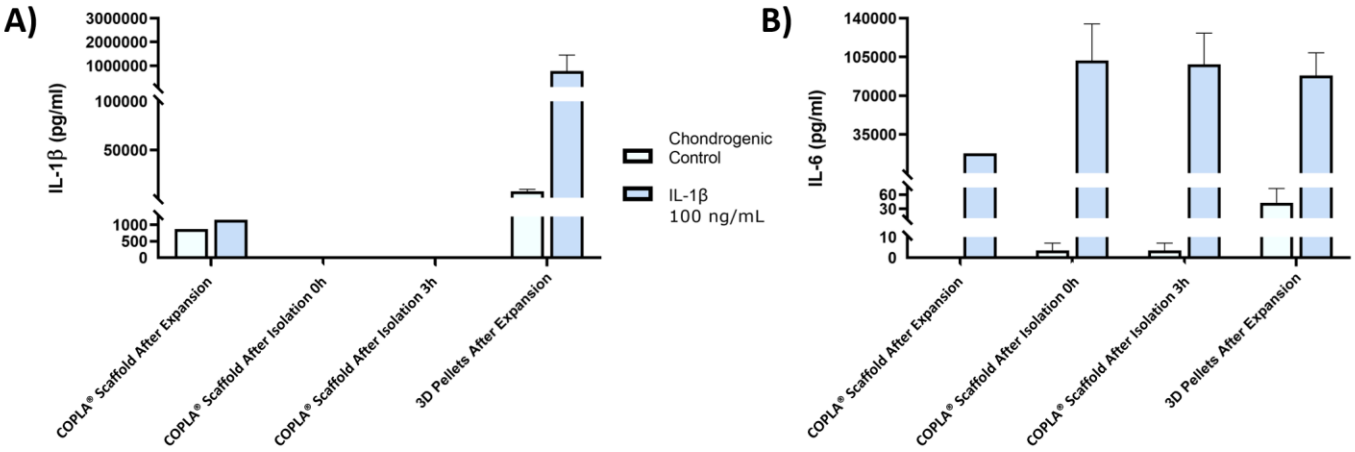

Figure 62 - Levels of A) IL-1β; and B) IL-6 measured in the conditioned mediums of chondrocytes cultured on COPLA® Scaffolds both after monolayer expansion and readily after isolation and in 3D pellets 3 and 7 days after the addition of the pro-inflammatory stimulus. n = 1 replicate for seeding in COPLA® Scaffold after expansion; n = 2 replicates for seeding in COPLA® Scaffold after isolation; n = 8 for 3D pellets.

6. CONCLUSIONS AND FUTURE DIRECTIONS

Lesions to the articular cartilage are highly frequent and tend to evolve towards bigger defects and OA, largely debilitating the life of people that once had active and healthy everyday routines.

Over the years, many conservative and surgical therapies have emerged, but none seems to correctly restore native cartilage composition and function.

COPLA® Scaffolds are biodegradable, meaning that after cell migration and adhesion to the 3D polymers and being degraded, it can support for the synthesis of newly ECM. Therefore, when nanoenabled with anti-inflammatory and anti-proteolytic delivery systems, these scaffolds may not only halt the progression of cartilage destruction but also allow the deposition of newly-formed ECM at the defect site. On top of this, the fact that COPLA® Scaffold's area can be customised for the lesion site is an attractive feature and a major breakthrough in tailored care for patients, as the drawbacks of current therapy approaches are highly dependent on the patients' age, the size and the location of the defects.

Overall, it is proposed that nanoenabled COPLA® Scaffolds will facilitate improved outcomes in patients while reducing unsuitable health care resources utilization, as in the case of TJA, once the current palliative approach of pain killers prescription or alternative injections intra-articular followed by joint replacement is often employed and largely inappropriate.

For such aim to be accomplished, the main goal of this study was to prove the chondroprotection induced by the nanodelivered administration of anti-inflammatory and anti-proteolytic compounds in *in vitro* cultured hACs, and the successful seeding of chondrocytes and pro-inflammatory microenvironment establishment in COPLA® Scaffolds.

The establishment of 3D pellet culture in hACs was successfully achieved and choosing the day 7 of culture supported the previous studies performed by this research group, being a timepoint where culture conditions were not toxic, and ECM deposition and mRNA expression of chondrogenic markers were observed.

Given the fact that the treatment with 100 ng/mL of IL-1β did not affect cell viability, and induced both the production of other pro-inflammatory cytokines and the expression ECM-degrading enzymes, an effective pro-inflammatory microenvironment was promoted.

Collectively, ibuprofen-loaded PLGA and chitosan/PLGA NPs, and the newly formulation of BB-94-loaded and mupirocin-loaded NEs were not cytotoxic to primary hACs in 3D pellet cultures. The tricombinatory NEs have shown to be toxic at the tested conditions, therefore ways of overcoming this issue should be looked for, namely by the similar approach followed in BB-94-loaded newly formulation, where

increased drug loading was reached to reduce the concentration of NEs added to the cultures.

Both 15 μg/mL and 30 μg/mL of loaded ibuprofen PLGA NPs showed to exert chondroprotective effects in the IL-1β-stimulated pro-inflammatory chondrocytes, proved by the observed trend towards a decrease in MMPs expression that might have made possible the increased detection of the deposition of the two main cartilage-specific markers, type II collagen and aggrecan.

Regarding the ibuprofen-loaded chitosan/PLGA NPS, the encapsulated concentration of 15 μg/mL seems to induce the most beneficial chondroprotective results, as lower levels of synthesised IL-6 and increased type II collagen deposition were achieved.

The number of replicates of the experiments should be increased in order to make a strongly based decision on which is the drug concentration for each delivery system that promotes the most strong and reproducible chondroprotective effect. Those concentrations should be further incorporated in COPLA® Scaffold.

Experiments with BB-94-loaded NEs and with mupirocin-loaded NEs, as well as with tricombinatory NEs, once the cytotoxicity issues are surpassed, should be continued.

Moreover, COPLA® Scaffolds successfully promoted hACs adhesion, redifferentiation (in the case of the seeding with previously expanded chondrocytes) and subsequent ECM production without cytotoxicity problems. Clear morphology changes were noticed between previously expanded primary hACs and the ones seed readily after isolation, have the last one rounded native shape.

For the hACs seeded after expansion in monolayers, day 7 was suggested to be the timepoint to be used in further experiments to treat cells with IL-1β stimulus.

Lastly, the pro-inflammatory microenvironment was successfully established in COPLA® Scaffolds and, when compared to the 3D pellets, it seems that empty COPLA® Scaffold might be exerting some anti-inflammatory effect by itself in hACs seeded under pro-inflammatory conditions.

As for future direction, after assessing the most adequate concentrations of NPs and NEs with the ability to inhibit cartilage ECM degradation in *in vitro* cultures of hACs, the role of COPLA® Scaffold's functionalization with those NPs and NEs in modulating inflammatory reactivity of those cultured cells should be evaluated.

After these *in vitro* assays are proved to be safe and effectively chondroprotective, in vivo studies must take place in order to evaluate the biosafety and the effectiveness of this approach in preventing cartilage degradation and restoring the original structure and function of damaged joints.

7. REFERENCES

1. DeLise, A., L. Fischer, and R. Tuan, *Cellular interactions and signaling in cartilage development.* Osteoarthritis and cartilage, 2000. **8**(5): p. 309-334 DOI: https://doi.org/10.1053/joca.1999.0306.
2. Kawakami, Y., J. Rodriguez-León, and J.C.I. Belmonte, *The role of TGFβs and Sox9 during limb chondrogenesis.* Current opinion in cell biology, 2006. **18**(6): p. 723-729 DOI: https://doi.org/10.1016/j.ceb.2006.10.007.
3. Tallheden, T., et al., *Human articular chondrocytes–plasticity and differentiation potential.* Cells Tissues Organs, 2006. **184**(2): p. 55-67 DOI: https://doi.org/10.1159/000098947.
4. Goldring, M.B., K. Tsuchimochi, and K. Ijiri, *The control of chondrogenesis.* Journal of cellular biochemistry, 2006. **97**(1): p. 33-44 DOI: https://doi.org/10.1002/jcb.20652.
5. Camarero-Espinosa, S., et al., *Articular cartilage: from formation to tissue engineering.* Biomaterials Science, 2016. **4**(5): p. 734-67 DOI: https://doi.org/10.1039/c6bm00068a.
6. Goldring, M.B., *Chondrogenesis, chondrocyte differentiation, and articular cartilage metabolism in health and osteoarthritis.* Ther Adv Musculoskelet Dis, 2012. **4**(4): p. 269-85 DOI: https://doi.org/10.1177/1759720x12448454.
7. Lefebvre, V. and M. Dvir-Ginzberg, *SOX9 and the many facets of its regulation in the chondrocyte lineage.* Connective Tissue Research, 2017. **58**(1): p. 2-14 DOI: https://doi.org/10.1080/03008207.2016.1183667.
8. Bertrand, J., et al., *Molecular mechanisms of cartilage remodelling in osteoarthritis.* The International Journal of Biochemistry & Cell Biology, 2010. **42**(10): p. 1594-1601 DOI: https://doi.org/10.1016/j.biocel.2010.06.022.
9. Mansour, J.M., *Biomechanics of cartilage*, in *Kinesiology: the mechanics and pathomechanics of human movement*. 2003. p. 69-83.
10. Pap, T. and A. Korb-Pap, *Cartilage damage in osteoarthritis and rheumatoid arthritis—two unequal siblings.* Nature Reviews Rheumatology, 2015. **11**(10): p. 606-615 DOI: https://doi.org/10.1038/nrrheum.2015.95.
11. Luo, Y., et al., *The minor collagens in articular cartilage.* Protein & cell, 2017. **8**(8): p. 560-572 DOI: https://doi.org/10.1007/s13238-017-0377-7.
12. Setton, L., *Reservoir drugs.* Nature Materials, 2008. **7**(3): p. 172-174 DOI: https://doi.org/10.1038/nmat2130.
13. Neil, K.M., J.P. Caron, and M.W. Orth, *The role of glucosamine and chondroitin sulfate in treatment for and prevention of osteoarthritis in animals.* J Am Vet Med Assoc, 2005. **226**(7): p. 1079-88 DOI: https://doi.org/10.2460/javma.2005.226.1079.
14. Ng, H.Y., K.-X.A. Lee, and Y.-F. Shen, *Articular cartilage: Structure, composition, injuries and repair.* JSM Bone and Joint Dis, 2017. **1**(2): p. 1010.
15. Carballo, C.B., et al., *Basic Science of Articular Cartilage.* Clin Sports Med, 2017. **36**(3): p. 413-425 DOI: https://doi.org/10.1016/j.csm.2017.02.001.

16. Sophia Fox, A.J., A. Bedi, and S.A. Rodeo, *The basic science of articular cartilage: structure, composition, and function.* Sports Health, 2009. **1**(6): p. 461-8 DOI: https://doi.org/10.1177/1941738109350438.
17. Burrage, P.S., K.S. Mix, and C.E. Brinckerhoff, *Matrix metalloproteinases: role in arthritis.* Front Biosci, 2006. **11**: p. 529-43 DOI: https://doi.org/10.2741/1817.
18. Gosset, M., et al., *Primary culture and phenotyping of murine chondrocytes.* Nat Protoc, 2008. **3**(8): p. 1253-60 DOI: http://doi.org/10.1038/nprot.2008.95.
19. Martin, I., et al., *Mammalian Chondrocytes Expanded in the Presence of Fibroblast Growth Factor 2 Maintain the Ability to Differentiate and Regenerate Three-Dimensional Cartilaginous Tissue.* Experimental Cell Research, 1999. **253**(2): p. 681-688 DOI: https://doi.org/10.1006/excr.1999.4708.
20. Demoor, M., et al., *Cartilage tissue engineering: molecular control of chondrocyte differentiation for proper cartilage matrix reconstruction.* Biochim Biophys Acta, 2014. **1840**(8): p. 2414-40 DOI: http://doi.org/10.1016/j.bbagen.2014.02.030.
21. Lotz, M. and R.F. Loeser, *Effects of aging on articular cartilage homeostasis.* Bone, 2012. **51**(2): p. 241-248 DOI: https://doi.org/10.1016/j.bone.2012.03.023.
22. Aida, Y., et al., *The effect of IL-1β on the expression of matrix metalloproteinases and tissue inhibitors of matrix metalloproteinases in human chondrocytes.* Life Sciences, 2005. **77**(25): p. 3210-3221 DOI: https://doi.org/10.1016/j.lfs.2005.05.052.
23. Tallheden, T., et al., *Phenotypic plasticity of human articular chondrocytes.* JBJS, 2003. **85**(suppl_2): p. 93-100 DOI: https://doi.org/10.2106/00004623-200300002-00012.
24. Duan, L., et al., *Cytokine networking of chondrocyte dedifferentiation in vitro and its implications for cell-based cartilage therapy.* American journal of translational research, 2015. **7**(2): p. 194-208.
25. Goldring, M.B., et al., *Roles of inflammatory and anabolic cytokines in cartilage metabolism: signals and multiple effectors converge upon MMP-13 regulation in osteoarthritis.* European cells & materials, 2011. **21**: p. 202-220 DOI: https://doi.org/10.22203/ecm.v021a16.
26. Schulze-Tanzil, G., *Activation and dedifferentiation of chondrocytes: implications in cartilage injury and repair.* Annals of Anatomy-Anatomischer Anzeiger, 2009. **191**(4): p. 325-338 DOI: https://doi.org/10.1016/j.aanat.2009.05.003.
27. Goldring, M.B. and K.B. Marcu, *Cartilage homeostasis in health and rheumatic diseases.* Arthritis research & therapy, 2009. **11**(3): p. 224 DOI: https://doi.org/10.1186/ar2592.
28. Grogan, S.P. and D.D. D'Lima, *Joint aging and chondrocyte cell death.* International journal of clinical rheumatology, 2010. **5**(2): p. 199-214 DOI: https://doi.org/10.2217/ijr.10.3.
29. Akkiraju, H. and A. Nohe, *Role of Chondrocytes in Cartilage Formation, Progression of Osteoarthritis and Cartilage Regeneration.* Journal of developmental biology, 2015. **3**(4): p. 177-192 DOI: https://doi.org/10.3390/jdb3040177.

30. Davies, R.L. and N.J. Kuiper, *Regenerative Medicine: A Review of the Evolution of Autologous Chondrocyte Implantation (ACI) Therapy.* Bioengineering, 2019. **6**(1): p. 22 DOI: https://doi.org/10.3390/bioengineering6010022.
31. Sharma, A.R., et al., *Interplay between cartilage and subchondral bone contributing to pathogenesis of osteoarthritis.* International journal of molecular sciences, 2013. **14**(10): p. 19805-19830 DOI: https://doi.org/10.3390/ijms141019805.
32. Baumann, C.A., et al., *Articular Cartilage: Structure and Restoration*, in *Joint Preservation of the Knee: A Clinical Casebook*, A.B. Yanke and B.J. Cole, Editors. 2019, Springer International Publishing: Cham. p. 3-24.
33. Bhosale, A.M. and J.B. Richardson, *Articular cartilage: structure, injuries and review of management.* British Medical Bulletin, 2008. **87**(1): p. 77-95 DOI: https://doi.org/10.1093/bmb/ldn025.
34. Lepage, S.I.M., et al., *Beyond Cartilage Repair: The Role of the Osteochondral Unit in Joint Health and Disease.* Tissue engineering. Part B, Reviews, 2019. **25**(2): p. 114-125 DOI: https://doi.org/10.1089/ten.TEB.2018.0122.
35. Ashraf, S., et al., *Regulation of senescence associated signaling mechanisms in chondrocytes for cartilage tissue regeneration.* Osteoarthritis and Cartilage, 2016. **24**(2): p. 196-205 DOI: https://doi.org/10.1016/j.joca.2015.07.008.
36. Gracitelli, G.C., et al., *Surgical interventions (microfracture, drilling, mosaicplasty, and allograft transplantation) for treating isolated cartilage defects of the knee in adults.* Cochrane Database of Systematic Reviews, 2016(9) DOI: https://doi.org/10.1002/14651858.CD010675.pub2.
37. Kraeutler, M.J., et al., *Biologic options for articular cartilage wear (platelet-rich plasma, stem cells, bone marrow aspirate concentrate).* Clinics in sports medicine, 2017. **36**(3): p. 457-468 DOI: https://doi.org/10.1016/j.csm.2017.02.004.
38. Tsumaki, N., M. Okada, and A. Yamashita, *iPS cell technologies and cartilage regeneration.* Bone, 2015. **70**: p. 48-54 DOI: https://doi.org/10.1016/j.bone.2014.07.011.
39. Sun, H.B., *Mechanical loading, cartilage degradation, and arthritis.* Annals of the New York Academy of Sciences, 2010. **1211**(1): p. 37-50 DOI: https://doi.org/10.1111/j.1749-6632.2010.05808.x.
40. C. Skelly, A., et al., *Osteochondral Allograft/Autograft Transplantation (OAT) - Health Technology Assessment* W.S.H.C. Authority, Editor. 2011: https://www.hca.wa.gov/.
41. Kwon, H., et al., *Surgical and tissue engineering strategies for articular cartilage and meniscus repair.* Nature Reviews Rheumatology, 2019. **15**(9): p. 550-570 DOI: https://doi.org/10.1038/s41584-019-0255-1.
42. Simon, T.M. and D.W. Jackson, *Articular cartilage: injury pathways and treatment options.* Sports medicine and arthroscopy review, 2006. **14**(3): p. 146-154 DOI: https://doi.org/10.1097/00132585-200609000-00006.
43. Redman, S.N., S.F. Oldfield, and C.W. Archer, *Current strategies for articular cartilage repair.* European Cells and Materials, 2005. **9**: p. 23-32; discussion 23-32 DOI: https://doi.org/10.22203/ecm.v009a04.

44. Robi, K., et al., *The physiology of sports injuries and repair processes.* Current issues in sports and exercise medicine, 2013: p. 43-86 DOI: https://doi.org/10.5772/54234.
45. Seo, S.-S., C.-W. Kim, and D.-W. Jung, *Management of focal chondral lesion in the knee joint.* Knee surgery & related research, 2011. **23**(4): p. 185-196 DOI: https://doi.org/10.5792/ksrr.2011.23.4.185.
46. Vogt, S. and A.B. Imhoff, *Injuries to the articular cartilage.* European Journal of Trauma, 2006. **32**(4): p. 325-331 DOI: https://doi.org/10.1007/s00068-006-6096-z.
47. Maldonado, M. and J. Nam, *The role of changes in extracellular matrix of cartilage in the presence of inflammation on the pathology of osteoarthritis.* BioMed research international, 2013. **2013**: p. 284873-284873 DOI: https://doi.org/10.1155/2013/284873.
48. Huang, B.J., J.C. Hu, and K.A. Athanasiou, *Cell-based tissue engineering strategies used in the clinical repair of articular cartilage.* Biomaterials, 2016. **98**: p. 1-22 DOI: https://doi.org/10.1016/j.biomaterials.2016.04.018.
49. Stone, A.V., et al., *Osteochondral allograft transplantation and osteochondral autograft transfer.* Operative Techniques in Sports Medicine, 2018. **26**(3): p. 183-188 DOI: https://doi.org/10.1053/j.otsm.2018.06.007.
50. Project, M. *Combining Technologies. Empowering Arthroscopy.* 2021 [cited 2021 10 June]; Available from: https://miracleproject.eu/.
51. Musumeci, G., M.A. Szychlinska, and A. Mobasheri, *Age-related degeneration of articular cartilage in the pathogenesis of osteoarthritis: molecular markers of senescent chondrocytes.* Histol Histopathol, 2015. **30**(1): p. 1-12 DOI: https://doi.org/10.14670/hh-30.1.
52. Pacifici, M., et al., *Cellular and molecular mechanisms of synovial joint and articular cartilage formation.* Annals of the New York Academy of Sciences, 2006. **1068**: p. 74 DOI: https://doi.org/10.1196/annals.1346.010.
53. Fusco, M., et al., *Degenerative Joint Diseases and Neuroinflammation.* Pain Pract, 2017. **17**(4): p. 522-532 DOI: https://doi.org/10.1111/papr.12551.
54. WHO, W.H.O. *Musculoskeletal conditions*. 2019 [cited 2021 25 April]; Available from: https://www.who.int/news-room/fact-sheets/detail/musculoskeletal-conditions.
55. Waller, D.G. and A.P. Sampson, *30 - Rheumatoid arthritis, other inflammatory arthritides and osteoarthritis*, in *Medical Pharmacology and Therapeutics (Fifth Edition)*, D.G. Waller and A.P. Sampson, Editors. 2018, Elsevier. p. 373-383.
56. Hsieh-Bonassera, N.D., et al., *Expansion and redifferentiation of chondrocytes from osteoarthritic cartilage: cells for human cartilage tissue engineering.* Tissue engineering. Part A, 2009. **15**(11): p. 3513-3523 DOI: http://doi.org/10.1089/ten.TEA.2008.0628.
57. Pizzorno, J.E., M.T. Murray, and H. Joiner-Bey, *58 - Osteoarthritis*, in *The Clinician's Handbook of Natural Medicine (Third Edition)*, J.E. Pizzorno, M.T. Murray, and H. Joiner-Bey, Editors. 2016, Churchill Livingstone: Edinburgh. p. 706-720.
58. James, S.L., et al., *Global, regional, and national incidence, prevalence, and years lived with disability for 354 diseases and injuries for 195 countries and territories, 1990–2017: a systematic analysis for the Global Burden of Disease*

Study 2017. The Lancet, 2018. **392**(10159): p. 1789-1858 DOI: https://doi.org/10.1016/S0140-6736(18)32279-7.
59. Litwic, A., et al., *Epidemiology and burden of osteoarthritis.* British Medical Bulletin, 2013. **105**(1): p. 185-199 DOI: https://doi.org/10.1093/bmb/lds038.
60. Medvedeva, E.V., et al., *Repair of damaged articular cartilage: current approaches and future directions.* International journal of molecular sciences, 2018. **19**(8): p. 2366 DOI: https://doi.org/10.3390/ijms19082366.
61. Wang, X., et al., *Identification of potential diagnostic gene biomarkers in patients with osteoarthritis.* Scientific Reports, 2020. **10**(1): p. 13591 DOI: https://doi.org/10.1038/s41598-020-70596-9.
62. Sandell, L.J. and T. Aigner, *Articular cartilage and changes in Arthritis: Cell biology of osteoarthritis.* Arthritis Research & Therapy, 2001. **3**(2): p. 107 DOI: https://doi.org/10.1186/ar148.
63. Amoako, A.O. and G.G.A. Pujalte, *Osteoarthritis in young, active, and athletic individuals.* Clinical medicine insights. Arthritis and musculoskeletal disorders, 2014. **7**: p. 27-32 DOI: https://doi.org/10.4137/CMAMD.S14386.
64. Tadman, J. and J. Hill, *The management of osteoarthritis and rheumatoid arthritis.* Nurs Times, 2005. **101**(2): p. 28-9.
65. Kapoor, M., et al., *Role of proinflammatory cytokines in the pathophysiology of osteoarthritis.* Nature Reviews Rheumatology, 2011. **7**(1): p. 33-42 DOI: https://doi.org/10.1038/nrrheum.2010.196.
66. Brown, S., S. Kumar, and B. Sharma, *Intra-articular targeting of nanomaterials for the treatment of osteoarthritis.* Acta Biomaterialia, 2019. **93**: p. 239-257 DOI: https://doi.org/10.1016/j.actbio.2019.03.010.
67. Pelletier, J.P., J. Martel-Pelletier, and S.B. Abramson, *Osteoarthritis, an inflammatory disease: potential implication for the selection of new therapeutic targets.* Arthritis Rheum, 2001. **44**(6): p. 1237-47 DOI: https://doi.org/10.1002/1529-0131(200106)44:6<1237::aid-art214>3.0.co;2-f.
68. Iannone, F. and G. Lapadula, *The pathophysiology of osteoarthritis.* Aging Clinical and Experimental Research, 2003. **15**(5): p. 364-372 DOI: https://doi.org/10.1007/BF03327357.
69. Troeberg, L. and H. Nagase, *Proteases involved in cartilage matrix degradation in osteoarthritis.* Biochimica et Biophysica Acta (BBA) - Proteins and Proteomics, 2012. **1824**(1): p. 133-145 DOI: https://doi.org/10.1016/j.bbapap.2011.06.020.
70. Daheshia, M. and J.Q. Yao, *The interleukin 1beta pathway in the pathogenesis of osteoarthritis.* J Rheumatol, 2008. **35**(12): p. 2306-12 DOI: https://doi.org/10.3899/jrheum.080346.
71. Chevalier, X., F. Eymard, and P. Richette, *Biologic agents in osteoarthritis: hopes and disappointments.* Nature Reviews Rheumatology, 2013. **9**(7): p. 400-10 DOI: https://doi.org/10.1038/nrrheum.2013.44.
72. Haseeb, A. and T.M. Haqqi, *Immunopathogenesis of osteoarthritis.* Clinical Immunology, 2013. **146**(3): p. 185-196 DOI: https://doi.org/10.1016/j.clim.2012.12.011.
73. Catterall, J.B. and T.E. Cawston, *Drugs in development: bisphosphonates and metalloproteinase inhibitors.* Arthritis Research & Therapy, 2003. **5**(1): p. 12-24 DOI: https://doi.org/10.1186/ar604.

74. Mehana, E.-S.E., A.F. Khafaga, and S.S. El-Blehi, *The role of matrix metalloproteinases in osteoarthritis pathogenesis: An updated review.* Life Sciences, 2019. **234**: p. 116786 DOI: https://doi.org/10.1016/j.lfs.2019.116786.
75. Murphy, G. and H. Nagase, *Reappraising metalloproteinases in rheumatoid arthritis and osteoarthritis: destruction or repair?* Nature Clinical Practice Rheumatology, 2008. **4**(3): p. 128-35 DOI: https://doi.org/10.1038/ncprheum0727.
76. Verma, P. and K. Dalal, *ADAMTS-4 and ADAMTS-5: key enzymes in osteoarthritis.* Journal of Cellular Biochemistry, 2011. **112**(12): p. 3507-14 DOI: https://doi.org/10.1002/jcb.23298.
77. Alaaeddine, N., et al., *Osteoarthritic synovial fibroblasts possess an increased level of tumor necrosis factor-receptor 55 (TNF-R55) that mediates biological activation by TNF-alpha.* J Rheumatol, 1997. **24**(10): p. 1985-94.
78. Westacott, C.I., et al., *Tumor necrosis factor-alpha receptor expression on chondrocytes isolated from human articular cartilage.* J Rheumatol, 1994. **21**(9): p. 1710-5.
79. Murphy, G. and M.H. Lee, *What are the roles of metalloproteinases in cartilage and bone damage?* Annals of the Rheumatic Diseases, 2005. **64**(suppl 4): p. iv44-iv47 DOI: https://doi.org/10.1136/ard.2005.042465.
80. Yamamoto, K., D. Wilkinson, and G. Bou-Gharios, *Targeting Dysregulation of Metalloproteinase Activity in Osteoarthritis.* Calcified Tissue International, 2020 DOI: https://doi.org/10.1007/s00223-020-00739-7.
81. Pelletier, J.-P., et al., *The protective effect of licofelone on experimental osteoarthritis is correlated with the downregulation of gene expression and protein synthesis of several major cartilage catabolic factors: MMP-13, cathepsin K and aggrecanases.* Arthritis Research & Therapy, 2005. **7**(5): p. R1091 DOI: https://doi.org/10.1186/ar1788.
82. Rose, B.J. and D.L. Kooyman, *A Tale of Two Joints: The Role of Matrix Metalloproteases in Cartilage Biology.* Disease markers, 2016. **2016**: p. 4895050-4895050 DOI: https://doi.org/10.1155/2016/4895050.
83. Klatt, A.R., et al., *A critical role for collagen II in cartilage matrix degradation: Collagen II induces pro-inflammatory cytokines and MMPs in primary human chondrocytes.* Journal of Orthopaedic Research, 2009. **27**(1): p. 65-70 DOI: https://doi.org/10.1002/jor.20716.
84. Robinson, W.H., et al., *Low-grade inflammation as a key mediator of the pathogenesis of osteoarthritis.* Nature Reviews Rheumatology, 2016. **12**(10): p. 580-592 DOI: 10.1038/nrrheum.2016.136.
85. Yang, C.Y., A. Chanalaris, and L. Troeberg, *ADAMTS and ADAM metalloproteinases in osteoarthritis - looking beyond the 'usual suspects'.* Osteoarthritis and cartilage, 2017. **25**(7): p. 1000-1009 DOI: https://doi.org/10.1016/j.joca.2017.02.791.
86. Wojdasiewicz, P., Ł.A. Poniatowski, and D. Szukiewicz, *The Role of Inflammatory and Anti-Inflammatory Cytokines in the Pathogenesis of Osteoarthritis.* Mediators of Inflammation, 2014. **2014**: p. 561459 DOI: https://doi.org/10.1155/2014/561459.

87. Katz, J.N., K.R. Arant, and R.F. Loeser, *Diagnosis and Treatment of Hip and Knee Osteoarthritis: A Review.* Journal of the American Medical Association, 2021. **325**(6): p. 568-578 DOI: https://doi.org/10.1001/jama.2020.22171.
88. Nakano, N., et al., *Outcomes of cartilage repair techniques for chondral injury in the hip—a systematic review.* International Orthopaedics, 2018. **42**(10): p. 2309-2322 DOI: https://doi.org/10.1007/s00264-018-3862-6.
89. Lespasio, M.J., et al., *Knee Osteoarthritis: A Primer.* Perm J, 2017. **21**: p. 16-183 DOI: https://doi.org/10.7812/tpp/16-183.
90. DeRogatis, M., et al., *Non-operative treatment options for knee osteoarthritis.* Annals of translational medicine, 2019. **7**(Suppl 7): p. S245-S245 DOI: https://doi.org/10.21037/atm.2019.06.68.
91. Poddar, S.K. and L. Widstrom, *Nonoperative Options for Management of Articular Cartilage Disease.* Clin Sports Med, 2017. **36**(3): p. 447-456 DOI: https://doi.org/10.1016/j.csm.2017.02.003.
92. Conaghan, P.G., et al., *Safety of Paracetamol in Osteoarthritis: What Does the Literature Say?* Drugs & Aging, 2019. **36**(1): p. 7-14 DOI: https://doi.org/10.1007/s40266-019-00658-9.
93. Leopoldino, A.O., et al., *Paracetamol versus placebo for knee and hip osteoarthritis.* Cochrane Database Syst Rev, 2019. **2**: p. Cd013273 DOI: https://doi.org/10.1002/14651858.cd013273.
94. Cooper, C., et al., *Safety of Oral Non-Selective Non-Steroidal Anti-Inflammatory Drugs in Osteoarthritis: What Does the Literature Say?* Drugs & aging, 2019. **36**(Suppl 1): p. 15-24 DOI: https://doi.org/10.1007/s40266-019-00660-1.
95. Kloppenburg, M. and F. Berenbaum, *Osteoarthritis year in review 2019: epidemiology and therapy.* Osteoarthritis and Cartilage, 2020. **28**(3): p. 242-248 DOI: https://doi.org/10.1016/j.joca.2020.01.002.
96. Abramson, S.B., *Do nonsteroidal anti-inflammatory drugs accelerate disease progression in osteoarthritis?* Nature Clinical Practice Rheumatology, 2006. **2**(6): p. 302-303 DOI: https://doi.org/10.1038/ncprheum0211.
97. Chahla, J., et al., *Bone Marrow Aspirate Concentrate Harvesting and Processing Technique.* Arthroscopy techniques, 2017. **6**(2): p. e441-e445 DOI: https://doi.org/10.1016/j.eats.2016.10.024.
98. Damia, E., et al., *Adipose-Derived Mesenchymal Stem Cells: Are They a Good Therapeutic Strategy for Osteoarthritis?* International journal of molecular sciences, 2018. **19**(7): p. 1926 DOI: https://doi.org/10.3390/ijms19071926.
99. Jones, I.A., R.C. Togashi, and C. Thomas Vangsness, Jr., *The Economics and Regulation of PRP in the Evolving Field of Orthopedic Biologics.* Current reviews in musculoskeletal medicine, 2018. **11**(4): p. 558-565 DOI: https://doi.org/10.1007/s12178-018-9514-z.
100. Themistocleous, G.S., et al., *Effectiveness of a single intra-articular bone marrow aspirate concentrate (BMAC) injection in patients with grade 3 and 4 knee osteoarthritis.* Heliyon, 2018. **4**(10): p. e00871-e00871 DOI: https://doi.org/10.1016/j.heliyon.2018.e00871.
101. McAlindon, T.E., et al., *Effect of Intra-articular Triamcinolone vs Saline on Knee Cartilage Volume and Pain in Patients With Knee Osteoarthritis: A Randomized Clinical Trial.* Jama, 2017. **317**(19): p. 1967-1975 DOI: https://doi.org/10.1001/jama.2017.5283.

102. Saltzman, B.M., et al., *Chapter 9 - Preserving the Articulating Surface of the Knee*, in *Biologics in Orthopaedic Surgery*, A.D. Mazzocca and A.D. Lindsay, Editors. 2019, Mica Haley: Philadelphia. p. 85-100.
103. AAOS, A.A.O.O.S., *Treatment Of Osteoarthritis Of The Knee Evidence-Based Guideline*. 2013, American Academy of Orthopaedic Surgeons.
104. AAOS, A.A.O.O.S., *Management Of Osteoarthritis Of The Hip Evidence-Based Clinical Practice Guideline*. 2017, American Academy of Orthopaedic Surgeons.
105. Kolasinski, S.L., et al., *2019 American College of Rheumatology/Arthritis Foundation Guideline for the Management of Osteoarthritis of the Hand, Hip, and Knee.* Arthritis Care Res (Hoboken), 2020. **72**(2): p. 149-162 DOI: https://doi.org/10.1002/acr.24131.
106. Khan, M., et al., *Management of osteoarthritis of the knee in younger patients.* CMAJ: Canadian Medical Association Journal, 2018. **190**(3): p. E72 DOI: https://doi.org/10.1503/cmaj.170696.
107. Erickson, B.J., S.M. Strickland, and A.H. Gomoll, *Indications, Techniques, Outcomes for Matrix-Induced Autologous Chondrocyte Implantation (MACI).* Operative Techniques in Sports Medicine, 2018. **26**(3): p. 175-182 DOI: https://doi.org/10.1053/j.otsm.2018.06.002.
108. Price, A.J., et al., *Knee replacement.* The Lancet, 2018. **392**(10158): p. 1672-1682 DOI: https://doi.org/10.1016/S0140-6736(18)32344-4.
109. Lespasio, M.J., et al., *Hip Osteoarthritis: A Primer.* The Permanente journal, 2018. **22**: p. 17-084 DOI: https://doi.org/10.7812/TPP/17-084.
110. Rönn, K., et al., *Current surgical treatment of knee osteoarthritis.* Arthritis, 2011. **2011**: p. 454873-454873 DOI: https://doi.org/10.1155/2011/454873.
111. Tarafder, S. and C. Lee, *Synovial Joint: In Situ Regeneration of Osteochondral and Fibrocartilaginous Tissues by Homing of Endogenous Cells*, in *In Situ Tissue Regeneration*. 2016, Elsevier. p. 253-273.
112. Segal, N.A., J.A. Buckwalter, and A. Amendola, *Other surgical techniques for osteoarthritis.* Best Practice & Research Clinical Rheumatology, 2006. **20**(1): p. 155-176 DOI: https://doi.org/10.1016/j.berh.2005.09.009.
113. Jones, K.J., et al., *Comparative Effectiveness of Cartilage Repair With Respect to the Minimal Clinically Important Difference.* Am J Sports Med, 2019. **47**(13): p. 3284-3293 DOI: https://doi.org/10.1177/0363546518824552.
114. Wang, C., et al., *Cryogenic 3D printing of heterogeneous scaffolds with gradient mechanical strengths and spatial delivery of osteogenic peptide/TGF-beta1 for osteochondral tissue regeneration.* Biofabrication, 2020. **12**(2): p. 025030 DOI: https://doi.org/10.1088/1758-5090/ab7ab5.
115. Farr, J., et al., *Clinical cartilage restoration: evolution and overview.* Clinical orthopaedics and related research, 2011. **469**(10): p. 2696-2705 DOI: https://doi.org/10.1007/s11999-010-1764-z.
116. Yen, Y.-M., et al., *Treatment of osteoarthritis of the knee with microfracture and rehabilitation.* Medicine & Science in Sports & Exercise, 2008. **40**(2): p. 200-205 DOI: https://doi.org/10.1249/mss.0b013e31815cb212.
117. Berta, A., et al., *Clinical experiences with cartilage repair techniques: outcomes, indications, contraindications and rehabilitation.* Eklem Hastalik Cerrahisi, 2015. **26**(2): p. 84-96 DOI: https://doi.org/10.5606/ehc.2015.19.

118. Gobbi, A., G. Karnatzikos, and A. Kumar, *Long-term results after microfracture treatment for full-thickness knee chondral lesions in athletes.* Knee Surgery, Sports Traumatology, Arthroscopy, 2014. **22**(9): p. 1986-1996 DOI: https://doi.org/10.1007/s00167-013-2676-8.
119. Goyal, D., et al., *Evidence-based status of microfracture technique: a systematic review of level I and II studies.* Arthroscopy: The Journal of Arthroscopic & Related Surgery, 2013. **29**(9): p. 1579-1588 DOI: https://doi.org/10.1016/j.arthro.2013.05.027.
120. Weber, A.E., et al., *Clinical Outcomes After Microfracture of the Knee: Midterm Follow-up.* Orthopaedic journal of sports medicine, 2018. **6**(2): p. 2325967117753572-2325967117753572 DOI: https://doi.org/10.1177/2325967117753572.
121. Pisanu, G., et al., *Large Osteochondral Allografts of the Knee: Surgical Technique and Indications.* Joints, 2018. **6**(1): p. 42-53 DOI: https://doi.org/10.1055/s-0038-1636925.
122. Solheim, E., et al., *Results at 10 to 14years after osteochondral autografting (mosaicplasty) in articular cartilage defects in the knee.* The Knee, 2013. **20**(4): p. 287-290 DOI: https://doi.org/10.1016/j.knee.2013.01.001.
123. Filardo, G., et al., *Arthroscopic mosaicplasty: long-term outcome and joint degeneration progression.* Knee, 2015. **22**(1): p. 36-40 DOI: https://doi.org/10.1016/j.knee.2014.10.001.
124. Bugbee, W.D., et al., *Osteochondral allograft transplantation in cartilage repair: Graft storage paradigm, translational models, and clinical applications.* J Orthop Res, 2016. **34**(1): p. 31-8 DOI: https://doi.org/10.1002/jor.22998.
125. Gross, A.E., N. Shasha, and P. Aubin, *Long-term followup of the use of fresh osteochondral allografts for posttraumatic knee defects.* Clin Orthop Relat Res, 2005(435): p. 79-87 DOI: https://doi.org/10.1097/01.blo.0000165845.21735.05.
126. Raz, G., et al., *39 – MEAN 20 YEARS FOLLOW UP FOR DISTAL FEMUR FRESH OSTEOCHONDRAL ALLOGRAFTED PATIENTS – PROSPECTIVE STUDY.* Orthopaedic Proceedings, 2011. **93-B**(SUPP_IV): p. 559-560 DOI: 10.1302/0301-620X.93BSUPP_IV.0930559e.
127. Mistry, H., et al., *The cost-effectiveness of osteochondral allograft transplantation in the knee.* Knee surgery, sports traumatology, arthroscopy : official journal of the ESSKA, 2019. **27**(6): p. 1739-1753 DOI: https://doi.org/10.1007/s00167-019-05392-8.
128. Raz, G., et al., *Distal Femoral Fresh Osteochondral Allografts: Follow-up at a Mean of Twenty-two Years.* J Bone Joint Surg Am, 2014. **96**(13): p. 1101-1107 DOI: 10.2106/jbjs.m.00769.
129. Carey, J.L., et al., *Autologous Chondrocyte Implantation as Treatment for Unsalvageable Osteochondritis Dissecans: 10- to 25-Year Follow-up.* Am J Sports Med, 2020. **48**(5): p. 1134-1140 DOI: https://doi.org/10.1177/0363546520908588.
130. Ogura, T., et al., *A 20-Year Follow-up After First-Generation Autologous Chondrocyte Implantation.* Am J Sports Med, 2017. **45**(12): p. 2751-2761 DOI: https://doi.org/10.1177/0363546517716631.

131. Peterson, L., et al., *Autologous chondrocyte implantation: a long-term follow-up.* Am J Sports Med, 2010. **38**(6): p. 1117-24 DOI: https://doi.org/10.1177/0363546509357915.
132. Berruto, M., et al., *Long-term follow-up evaluation of autologous chondrocyte implantation for symptomatic cartilage lesions of the knee: A single-centre prospective study.* Injury, 2017. **48**(10): p. 2230-2234 DOI: https://doi.org/10.1016/j.injury.2017.08.005.
133. Clair, B.L., A.R. Johnson, and T. Howard, *Cartilage repair: current and emerging options in treatment.* Foot Ankle Spec, 2009. **2**(4): p. 179-88 DOI: https://doi.org/10.1177/1938640009342272.
134. Tuan, R.S., A.F. Chen, and B.A. Klatt, *Cartilage regeneration.* The Journal of the American Academy of Orthopaedic Surgeons, 2013. **21**(5): p. 303-311 DOI: https://doi.org/10.5435/JAAOS-21-05-303.
135. Akgun, I., et al., *Matrix-induced autologous mesenchymal stem cell implantation versus matrix-induced autologous chondrocyte implantation in the treatment of chondral defects of the knee: a 2-year randomized study.* Archives of Orthopaedic and Trauma Surgery, 2015. **135**(2): p. 251-263 DOI: https://doi.org/10.1007/s00402-014-2136-z.
136. Genovese, E., et al., *Matrix-induced autologous chondrocyte implantation of the knee: mid-term and long-term follow-up by MR arthrography.* Skeletal Radiology, 2011. **40**(1): p. 47-56 DOI: https://doi.org/10.1007/s00256-010-0939-8.
137. Mancini, D. and A. Fontana, *Five-year results of arthroscopic techniques for the treatment of acetabular chondral lesions in femoroacetabular impingement.* International Orthopaedics, 2014. **38**(10): p. 2057-64 DOI: https://doi.org/10.1007/s00264-014-2403-1.
138. Basad, E., et al., *Matrix-induced autologous chondrocyte implantation (MACI) in the knee: clinical outcomes and challenges.* Knee Surg Sports Traumatol Arthrosc, 2015. **23**(12): p. 3729-35 DOI: https://doi.org/10.1007/s00167-014-3295-8.
139. Behrens, P., et al., *Matrix-associated autologous chondrocyte transplantation/implantation (MACT/MACI)--5-year follow-up.* Knee, 2006. **13**(3): p. 194-202 DOI: https://doi.org/10.1016/j.knee.2006.02.012.
140. Vijayan, S., et al., *Autologous chondrocyte implantation for osteochondral lesions in the knee using a bilayer collagen membrane and bone graft: a two- to eight-year follow-up study.* J Bone Joint Surg Br, 2012. **94**(4): p. 488-92 DOI: https://doi.org/10.1302/0301-620x.94b4.27117.
141. Gille, J., et al., *Matrix-Associated Autologous Chondrocyte Implantation: A Clinical Follow-Up at 15 Years.* Cartilage, 2016. **7**(4): p. 309-315 DOI: https://doi.org/10.1177/1947603516638901.
142. Latourte, A., M. Kloppenburg, and P. Richette, *Emerging pharmaceutical therapies for osteoarthritis.* Nature Reviews Rheumatology, 2020. **16**(12): p. 673-688 DOI: https://doi.org/10.1038/s41584-020-00518-6.
143. Oo, W.M., et al., *Disease-modifying drugs in osteoarthritis: current understanding and future therapeutics.* Expert Opinion on Emerging Drugs, 2018. **23**(4): p. 331-347 DOI: https://doi.org/10.1080/14728214.2018.1547706.

144. Clutterbuck, A.L., et al., *Targeting matrix metalloproteinases in inflammatory conditions.* Current Drug Targets, 2009. **10**(12): p. 1245-54 DOI: https://doi.org/10.2174/138945009789753264.
145. Persson, M.S.M., et al., *Conventional and biologic disease-modifying anti-rheumatic drugs for osteoarthritis: a meta-analysis of randomized controlled trials.* Rheumatology (Oxford), 2018. **57**(10): p. 1830-1837 DOI: https://doi.org/10.1093/rheumatology/key131.
146. Cohen, S.B., et al., *A randomized, double-blind study of AMG 108 (a fully human monoclonal antibody to IL-1R1) in patients with osteoarthritis of the knee.* Arthritis Research & Therapy, 2011. **13**(4): p. R125-R125 DOI: https://doi.org/10.1186/ar3430.
147. Adatia, A., K.D. Rainsford, and W.F. Kean, *Osteoarthritis of the knee and hip. Part II: therapy with ibuprofen and a review of clinical trials.* J Pharm Pharmacol, 2012. **64**(5): p. 626-36 DOI: 10.1111/j.2042-7158.2012.01456.x.
148. Li, R., et al., *Ibuprofen attenuates interleukin-1β-induced inflammation and actin reorganization via modulation of RhoA signaling in rabbit chondrocytes.* Acta Biochimica et Biophysica Sinica (Shanghai), 2019. **51**(10): p. 1026-1033 DOI: 10.1093/abbs/gmz101.
149. Mansouri, M., H. Reza Pouretedal, and V. Vosoughi, *Preparation and Characterization of Ibuprofen Nanoparticles by using Solvent/ Antisolvent Precipitation.* The Open Conference Proceedings Journal, 2011. **2**: p. 88-94 DOI: https://doi.org/10.2174/2210289201102010088.
150. Gallelli, L., et al., *The effects of nonsteroidal anti-inflammatory drugs on clinical outcomes, synovial fluid cytokine concentration and signal transduction pathways in knee osteoarthritis. A randomized open label trial.* Osteoarthritis and Cartilage, 2013. **21**(9): p. 1400-1408 DOI: https://doi.org/10.1016/j.joca.2013.06.026.
151. Sun, F., Y. Zhang, and Q. Li, *Therapeutic mechanisms of ibuprofen, prednisone and betamethasone in osteoarthritis.* Molecular Medicine Reports, 2017. **15**(2): p. 981-987 DOI: https://doi.org/10.3892/mmr.2016.6068.
152. Rogerson, F.M., *Cartilage matrix degradation: an appropriate therapeutic target in osteoarthritis.* Therapy, 2010. **7**: p. 579+.
153. Raeeszadeh-Sarmazdeh, M., L.D. Do, and B.G. Hritz, *Metalloproteinases and Their Inhibitors: Potential for the Development of New Therapeutics.* Cells, 2020. **9**(5) DOI: https://doi.org/10.3390/cells9051313.
154. Peterson, J.T., *The importance of estimating the therapeutic index in the development of matrix metalloproteinase inhibitors.* Cardiovascular Research, 2006. **69**(3): p. 677-687 DOI: https://doi.org/10.1016/j.cardiores.2005.11.032.
155. Li, N.G., et al., *New hope for the treatment of osteoarthritis through selective inhibition of MMP-13.* Curr Med Chem, 2011. **18**(7): p. 977-1001 DOI: https://doi.org/10.2174/092986711794940905.
156. Christopher, B.L. and J.F. Amanda, *Is Cartilage Matrix Breakdown an Appropriate Therapeutic Target in Osteoarthritis – Insights from Studies of Aggrecan and Collagen Proteolysis?* Current Drug Targets, 2010. **11**(5): p. 561-575 DOI: http://dx.doi.org/10.2174/138945010791011956.

157. Wojtowicz-Praga, S.M., R.B. Dickson, and M.J. Hawkins, *Matrix metalloproteinase inhibitors.* Invest New Drugs, 1997. **15**(1): p. 61-75 DOI: https://doi.org/10.1023/a:1005722729132.
158. Laronha, H., et al., *Challenges in Matrix Metalloproteinases Inhibition.* Biomolecules, 2020. **10**(5): p. 717 DOI: https://doi.org/10.3390/biom10050717.
159. Vandenbroucke, R.E. and C. Libert, *Is there new hope for therapeutic matrix metalloproteinase inhibition?* Nature Reviews Drug Discovery, 2014. **13**(12): p. 904-927 DOI: https://doi.org/10.1038/nrd4390.
160. Liu-Bryan, R. and R. Terkeltaub, *Emerging regulators of the inflammatory process in osteoarthritis.* Nature Reviews Rheumatology, 2015. **11**(1): p. 35-44 DOI: 10.1038/nrrheum.2014.162.
161. Kim, S., et al., *Cationic PLGA/Eudragit RL nanoparticles for increasing retention time in synovial cavity after intra-articular injection in knee joint.* International Journal of Nanomedicine 2015. **10**(1): p. 5263-5271 DOI: https://doi.org/10.2147/IJN.S88363.
162. Kou, L., et al., *Biomaterial-engineered intra-articular drug delivery systems for osteoarthritis therapy.* Drug Delivery, 2019. **26**(1): p. 870-885 DOI: https://doi.org/10.1080/10717544.2019.1660434.
163. Mohammadinejad, R., et al., *Nanotechnological Strategies for Osteoarthritis Diagnosis, Monitoring, Clinical Management, and Regenerative Medicine: Recent Advances and Future Opportunities.* Current Rheumatology Reports, 2020. **22**(4): p. 12 DOI: https://doi.org/10.1007/s11926-020-0884-z.
164. Zhou, Y., et al., *In vivo anti-apoptosis activity of novel berberine-loaded chitosan nanoparticles effectively ameliorates osteoarthritis.* International Immunopharmacology, 2015. **28**(1): p. 34-43 DOI: https://doi.org/10.1016/j.intimp.2015.05.014.
165. Zhang, Z. and G. Huang, *Micro- and Nano-Carrier Mediated Intra-Articular Drug Delivery Systems for the Treatment of Osteoarthritis.* Journal of Nanotechnology, 2012. **2012**: p. 748909 DOI: https://doi.org/10.1155/2012/748909.
166. Dinarvand, R., et al., *Polylactide-co-glycolide nanoparticles for controlled delivery of anticancer agents.* International Journal of Nanomedicine, 2011. **6**: p. 877-95 DOI: https://doi.org/10.2147/ijn.s18905.
167. Mota, A.H., et al., *Combination of hyaluronic acid and PLGA particles as hybrid systems for viscosupplementation in osteoarthritis.* International Journal of Pharmaceutics, 2019. **559**: p. 13-22 DOI: https://doi.org/10.1016/j.ijpharm.2019.01.017.
168. Elsaid, K.A., et al., *Intra-articular interleukin-1 receptor antagonist (IL1-ra) microspheres for posttraumatic osteoarthritis: in vitro biological activity and in vivo disease modifying effect.* Journal of Experimental Orthopaedics, 2016. **3**(1): p. 18 DOI: https://doi.org/10.1186/s40634-016-0054-4.
169. Sah, E. and H. Sah, *Recent Trends in Preparation of Poly(lactide-co-glycolide) Nanoparticles by Mixing Polymeric Organic Solution with Antisolvent.* Journal of Nanomaterials, 2015. **2015**: p. 794601 DOI: https://doi.org/10.1155/2015/794601.
170. Bonelli, P., et al., *Ibuprofen delivered by poly(lactic-co-glycolic acid) (PLGA) nanoparticles to human gastric cancer cells exerts antiproliferative activity at*

very low concentrations. International Journal of Nanomedicine, 2012. **7**: p. 5683-91 DOI: https://doi.org/10.2147/ijn.s34723.
171. Yurtdaş-Kırımlıoğlu, G., Ş. Görgülü, and M.S. Berkman, *Novel approaches to cancer therapy with ibuprofen-loaded Eudragit® RS 100 and/or octadecylamine-modified PLGA nanoparticles by assessment of their effects on apoptosis.* Drug Development and Industrial Pharmacy, 2020. **46**(7): p. 1133-1149 DOI: https://doi.org/10.1080/03639045.2020.1776319.
172. Lu, H.-D., et al., *Novel hyaluronic acid–chitosan nanoparticles as non-viral gene delivery vectors targeting osteoarthritis.* International Journal of Pharmaceutics, 2011. **420**(2): p. 358-365 DOI: https://doi.org/10.1016/j.ijpharm.2011.08.046.
173. Sultankulov, B., et al., *Progress in the Development of Chitosan-Based Biomaterials for Tissue Engineering and Regenerative Medicine.* Biomolecules, 2019. **9**(9): p. 470 DOI: https://doi.org/10.3390/biom9090470.
174. Haaparanta, A.M., et al., *Preparation and characterization of collagen/PLA, chitosan/PLA, and collagen/chitosan/PLA hybrid scaffolds for cartilage tissue engineering.* Journal of Materials Science: Materials in Medicine, 2014. **25**(4): p. 1129-36 DOI: https://doi.org/10.1007/s10856-013-5129-5.
175. Chen, Q., et al., *Carboxymethyl-chitosan protects rabbit chondrocytes from interleukin-1beta-induced apoptosis.* European Journal of Pharmacology, 2006. **541**(1-2): p. 1-8 DOI: https://doi.org/10.1016/j.ejphar.2006.03.044.
176. Yuan, Z., et al., *Chitosan-graft-β-cyclodextrin nanoparticles as a carrier for controlled drug release.* International Journal of Pharmaceutics, 2013. **446**(1-2): p. 191-8 DOI: https://doi.org/10.1016/j.ijpharm.2013.02.024.
177. Park, S.-B., et al., *Poly(glutamic acid): Production, composites, and medical applications of the next-generation biopolymer.* Progress in Polymer Science, 2021. **113**: p. 101341 DOI: https://doi.org/10.1016/j.progpolymsci.2020.101341.
178. Antunes, J.C., et al., *Poly(γ-Glutamic Acid) as an Exogenous Promoter of Chondrogenic Differentiation of Human Mesenchymal Stem/Stromal Cells.* Tissue Engineering Part A, 2015. **21**(11-12): p. 1869-85 DOI: https://doi.org/10.1089/ten.TEA.2014.0386.
179. Teixeira, G.Q., et al., *Anti-inflammatory Chitosan/Poly-γ-glutamic acid nanoparticles control inflammation while remodeling extracellular matrix in degenerated intervertebral disc.* Acta Biomaterialia, 2016. **42**: p. 168-179 DOI: https://doi.org/10.1016/j.actbio.2016.06.013.
180. Jaiswal, M., R. Dudhe, and P.K. Sharma, *Nanoemulsion: an advanced mode of drug delivery system.* 3 Biotech, 2015. **5**(2): p. 123-127 DOI: https://www.doi.org/10.1007/s13205-014-0214-0.
181. Pathak, K., S. Pattnaik, and K. Swain, *Chapter 13 - Application of Nanoemulsions in Drug Delivery*, in *Nanoemulsions*, S.M. Jafari and D.J. McClements, Editors. 2018, Academic Press. p. 415-433.
182. Borrelli, J.J., et al., *Understanding Articular Cartilage Injury and Potential Treatments.* Journal of Orthopaedic Trauma, 2019. **33**: p. S6-S12 DOI: https://doi.org/10.1097/bot.0000000000001472.
183. Farokhi, M., et al., *Alginate Based Scaffolds for Cartilage Tissue Engineering: A Review.* International Journal of Polymeric Materials and Polymeric

Biomaterials, 2020. **69**(4): p. 230-247 DOI: https://doi.org/10.1080/00914037.2018.1562924.
184. Park, K.-S., et al., *Versatile effects of magnesium hydroxide nanoparticles in PLGA scaffold–mediated chondrogenesis.* Acta Biomaterialia, 2018. **73**: p. 204-216 DOI: https://doi.org/10.1016/j.actbio.2018.04.022.
185. Moutos, F.T. and F. Guilak, *Composite scaffolds for cartilage tissue engineering.* Biorheology, 2008. **45**: p. 501-512 DOI: https://doi.org/10.3233/BIR-2008-0491.
186. Muhonen, V., et al., *Articular cartilage repair with recombinant human type II collagen/polylactide scaffold in a preliminary porcine study.* Journal of Orthopaedic Research, 2016. **34**(5): p. 745-753 DOI: https://doi.org/10.1002/jor.23099.
187. Yu, F., et al., *Mechanism research on a bioactive resveratrol- PLA-gelatin porous nano-scaffold in promoting the repair of cartilage defect.* International Journal of Nanomedicine, 2018. **13**: p. 7845-7858 DOI: https://doi.org/10.2147/ijn.s181855.
188. Sun, X., et al., *Collagen-based porous scaffolds containing PLGA microspheres for controlled kartogenin release in cartilage tissue engineering.* Artificial Cells, Nanomedicine, and Biotechnology, 2018. **46**(8): p. 1957-1966 DOI: https://doi.org/10.1080/21691401.2017.1397000.
189. Szychlinska, M.A., et al., *Functional Biomolecule Delivery Systems and Bioengineering in Cartilage Regeneration.* Current Pharmaceutical Biotechnology, 2019. **20**(1): p. 32-46 DOI: http://dx.doi.org/10.2174/1389201020666190206202048.
190. Tyler, B., et al., *Polylactic acid (PLA) controlled delivery carriers for biomedical applications.* Advanced Drug Delivery Reviews, 2016. **107**: p. 163-175 DOI: https://doi.org/10.1016/j.addr.2016.06.018.
191. Jeevitha, D. and K. Amarnath, *Chitosan/PLA nanoparticles as a novel carrier for the delivery of anthraquinone: Synthesis, characterization and in vitro cytotoxicity evaluation.* Colloids and Surfaces B: Biointerfaces, 2013. **101**: p. 126-134 DOI: https://doi.org/10.1016/j.colsurfb.2012.06.019.
192. Healthcare, A. *COPLA®*. [cited 2021 2 June]; Available from: https://askelhealthcare.com/products.
193. Cidetec, R. *COPLA® Scaffold – Already a solution for veterinary patients, moving towards human use*. 2019 [cited 2021 2 June]; Available from: https://restoreproject.eu/copla-scaffold-already-a-solution-for-veterinary-patients-moving-towards-human-use/.
194. Healthcare, A. *Animal health*. [cited 2021 2 June]; Available from: https://askelhealthcare.com/animal-health.
195. Merkely, G., J. Ackermann, and C. Lattermann, *Articular Cartilage Defects: Incidence, Diagnosis, and Natural History.* Operative Techniques in Sports Medicine, 2018. **26**(3): p. 156-161 DOI: https://doi.org/10.1053/j.otsm.2018.06.008.
196. Bliddal, H. and R. Christensen, *The treatment and prevention of knee osteoarthritis: a tool for clinical decision-making.* Expert Opin Pharmacother, 2009. **10**(11): p. 1793-804 DOI: https://doi.org/10.1517/14656560903018911.
197. Minas, T., et al., *The John Insall Award: a minimum 10-year outcome study of autologous chondrocyte implantation.* Clinical Orthopaedics and Related

Research®, 2014. **472**(1): p. 41-51 DOI: https://doi.org/10.1007/s11999-013-3146-9.
198. WHO, W.H.O. *Chronic diseases and health promotion*. [cited 2021 24 May]; Available from: https://www.who.int/chp/topics/rheumatic/en/.
199. Hao, H.Q., et al., *Cartilage oligomeric matrix protein, C-terminal cross-linking telopeptide of type II collagen, and matrix metalloproteinase-3 as biomarkers for knee and hip osteoarthritis (OA) diagnosis: a systematic review and meta-analysis.* Osteoarthritis and Cartilage, 2019. **27**(5): p. 726-736 DOI: https://doi.org/10.1016/j.joca.2018.10.009.
200. Xie, F., et al., *Economic and Humanistic Burden of Osteoarthritis: A Systematic Review of Large Sample Studies.* PharmacoEconomics, 2016. **34**(11): p. 1087-1100 DOI: https://doi.org/10.1007/s40273-016-0424-x.
201. Hiligsmann, M. and J. Reginster, *The economic weight of osteoarthritis in Europe.* Medicographia, 2013. **35**(1): p. 197-202.
202. Schreurs, B.W. and G. Hannink, *Total joint arthroplasty in younger patients: heading for trouble?* The Lancet, 2017. **389**(10077): p. 1374-1375 DOI: https://doi.org/10.1016/S0140-6736(17)30190-3.
203. Kim, K.T., et al., *Causes of failure after total knee arthroplasty in osteoarthritis patients 55 years of age or younger.* Knee surgery & related research, 2014. **26**(1): p. 13-19 DOI: https://doi.org/10.5792/ksrr.2014.26.1.13.
204. Ting, N.T. and C.J. Della Valle, *Diagnosis of Periprosthetic Joint Infection—An Algorithm-Based Approach.* The Journal of Arthroplasty, 2017. **32**(7): p. 2047-2050 DOI: https://doi.org/10.1016/j.arth.2017.02.070.
205. Pivec, R., et al., *Hip arthroplasty.* Lancet, 2012. **380**(9855): p. 1768-77 DOI: https://doi.org/10.1016/s0140-6736(12)60607-2.
206. Artroplastias, R.P.d. *Hospitais/Estatísticas*. 2021 [cited 2021 31 May]; Available from: http://www.rpa.spot.pt/Main-Sections/Hospitals.aspx.
207. Kurtz, S., et al., *Projections of primary and revision hip and knee arthroplasty in the United States from 2005 to 2030.* J Bone Joint Surg Am, 2007. **89**(4): p. 780-5 DOI: https://doi.org/10.2106/jbjs.f.00222.
208. Ackerman, I.N., et al., *The substantial personal burden experienced by younger people with hip or knee osteoarthritis.* Osteoarthritis and Cartilage, 2015. **23**(8): p. 1276-1284 DOI: https://doi.org/10.1016/j.joca.2015.04.008.
209. Babur, B.K., et al., *The Interplay between Chondrocyte Redifferentiation Pellet Size and Oxygen Concentration.* PLOS ONE, 2013. **8**(3): p. e58865 DOI: https://doi.org/10.1371/journal.pone.0058865.
210. McClurg, O., R. Tinson, and L. Troeberg, *Targeting Cartilage Degradation in Osteoarthritis.* Pharmaceuticals (Basel), 2021. **14**(2) DOI: https://doi.org/10.3390/ph14020126.
211. Antunes, J.C., et al., *Poly(γ-Glutamic Acid) as an Exogenous Promoter of Chondrogenic Differentiation of Human Mesenchymal Stem/Stromal Cells.* Tissue Eng Part A, 2015. **21**(11-12): p. 1869-85 DOI: http://doi.org/10.1089/ten.TEA.2014.0386.
212. Isyar, M., et al., *A practical way to prepare primer human chondrocyte culture.* Journal of orthopaedics, 2016. **13**(3): p. 162-167 DOI: https://doi.org/10.1016/j.jor.2016.03.008.

213. Centola, M., et al., *An improved cartilage digestion method for research and clinical applications.* Tissue Eng Part C Methods, 2015. **21**(4): p. 394-403 DOI: https://www.doi.org/10.1089/ten.TEC.2014.0393.
214. Lin, Z., et al., *Gene expression profiles of human chondrocytes during passaged monolayer cultivation.* Journal of orthopaedic research : official publication of the Orthopaedic Research Society, 2008. **26**(9): p. 1230-1237 DOI: https://doi.org/10.1002/jor.20523.
215. Corporation, P. *CytoTox 96® Non-Radioactive Cytotoxicity Assay Technical Bulletin*. 2016; Available from: https://worldwide.promega.com/-/media/files/resources/protocols/technical-bulletins/0/cytotox-96-nonradioactive-cytotoxicity-assay-protocol.pdf?la=en.
216. NanoDrop Technologies, I. *260/280 and 260/230 Ratios - Technical Support Bulletin*. 2007; Available from: https://www.bio.davidson.edu/projects/gcat/protocols/NanoDrop_tip.pdf.
217. Farrokhi, A., et al., *Appropriate reference gene selection for real-time PCR data normalization during rat mesenchymal stem cell differentiation.* Cell Mol Biol, 2012. **58**(Suppl): p. OL1660-OL1670.
218. Barbero, A., et al., *Age related changes in human articular chondrocyte yield, proliferation and post-expansion chondrogenic capacity.* Osteoarthritis and Cartilage, 2004. **12**(6): p. 476-484 DOI: https://doi.org/10.1016/j.joca.2004.02.010.
219. Heidari, M., et al., *In vitro human chondrocyte culture; a modified protocol.* Middle-East J Sci Res, 2011. **9**(1): p. 102-109.
220. Muhammad, S.A., et al., *Optimization of Protocol for Isolation of Chondrocytes from Human Articular Cartilage.* CARTILAGE, 2019: p. 1947603519876333 DOI: https://doi.org/10.1177/1947603519876333.
221. Caron, M.M.J., et al., *Redifferentiation of dedifferentiated human articular chondrocytes: comparison of 2D and 3D cultures.* Osteoarthritis and Cartilage, 2012. **20**(10): p. 1170-1178 DOI: https://doi.org/10.1016/j.joca.2012.06.016.
222. Kisiday, J.D., *Expansion of Chondrocytes for Cartilage Tissue Engineering: A Review of Chondrocyte Dedifferentiation and Redifferentiation as a Function of Growth in Expansion Culture.* Regenerative Medicine Frontiers, 2020. **2**(1): p. e200002 DOI: http://doi.org/10.20900/rmf20200002.
223. Gouttenoire, J., et al., *BMP-2 and TGF-beta1 differentially control expression of type II procollagen and alpha 10 and alpha 11 integrins in mouse chondrocytes.* European journal of cell biology, 2010. **89**(4): p. 307-314 DOI: 10.1016/j.ejcb.2009.10.018.
224. Barbero, A., et al., *Plasticity of clonal populations of dedifferentiated adult human articular chondrocytes.* Arthritis & Rheumatism, 2003. **48**(5): p. 1315-1325 DOI: https://doi.org/10.1002/art.10950.
225. Jakob, M., et al., *Specific growth factors during the expansion and redifferentiation of adult human articular chondrocytes enhance chondrogenesis and cartilaginous tissue formation in vitro.* Journal of Cellular Biochemistry, 2001. **81**(2): p. 368-377 DOI: https://doi.org/10.1002/1097-4644(20010501)81:2<368::AID-JCB1051>3.0.CO;2-J.

226. Ma, B., et al., *Gene expression profiling of dedifferentiated human articular chondrocytes in monolayer culture.* Osteoarthritis and Cartilage, 2013. **21**(4): p. 599-603 DOI: https://doi.org/10.1016/j.joca.2013.01.014.
227. Evans, C.H. and H.I. Georgescu, *Observations on the senescence of cells derived from articular cartilage.* Mech Ageing Dev, 1983. **22**(2): p. 179-91 DOI: https://doi.org/10.1016/0047-6374(83)90111-2
228. Brandl, A., et al., *Influence of the growth factors PDGF-BB, TGF-β1 and bFGF on the replicative aging of human articular chondrocytes during in vitro expansion.* Journal of Orthopaedic Research, 2010. **28**(3): p. 354-360 DOI: http://doi.org/10.1002/jor.21007.
229. Charlier, E., et al., *Chondrocyte dedifferentiation and osteoarthritis (OA).* Biochem Pharmacol, 2019. **165**: p. 49-65 DOI: http://doi.org/10.1016/j.bcp.2019.02.036.
230. Huang, B.J., J.C. Hu, and K.A. Athanasiou, *Effects of passage number and post-expansion aggregate culture on tissue engineered, self-assembled neocartilage.* Acta Biomaterialia, 2016. **43**: p. 150-159 DOI: https://doi.org/10.1016/j.actbio.2016.07.044.
231. Aigner, T., et al., *Mechanisms of disease: role of chondrocytes in the pathogenesis of osteoarthritis--structure, chaos and senescence.* Nat Clin Pract Rheumatol, 2007. **3**(7): p. 391-9 DOI: https://doi.org/10.1038/ncprheum0534.
232. Grigull, N.P., et al., *Chondrogenic Potential of Pellet Culture Compared to High-Density Culture on a Bacterial Cellulose Hydrogel.* International journal of molecular sciences, 2020. **21**(8): p. 2785 DOI: 10.3390/ijms21082785.
233. Liu, X., et al., *Role of insulin-transferrin-selenium in auricular chondrocyte proliferation and engineered cartilage formation in vitro.* International journal of molecular sciences, 2014. **15**(1): p. 1525-1537 DOI: 10.3390/ijms15011525.
234. Scientific, T.F. *Insulin-Transferrin-Selenium Supplement*. 2014; Available from: https://assets.thermofisher.com/TFS-Assets/LSG/manuals/2672.pdf.
235. Zamani, S., et al., *Assessment of TGF-β3 on production of aggrecan by human articular chondrocytes in pellet culture system.* Advanced biomedical research, 2014. **3**: p. 54-54 DOI: http://doi.org/10.4103/2277-9175.125799.
236. Scientific, T. *DMEM, high glucose*. [cited 2021 20 June]; Available from: https://www.thermofisher.com/order/catalog/product/11965084#/11965084.
237. ISO, I., *10993–5: 2009 Biological evaluation of medical devices—part 5: tests for in vitro cytotoxicity.* International Organization for Standardization, Geneva, 2009.
238. Horobin, R., *Educational guide special stains H&E. 2.* Carpinteria, CA, 2010.
239. Wall, A. and T. Board, *Chemical basis for the histological use of safranin O in the study of articular cartilage*, in *Classic papers in orthopaedics*. 2014, Springer. p. 433-435.
240. Dexheimer, V., S. Frank, and W. Richter, *Proliferation as a requirement for in vitro chondrogenesis of human mesenchymal stem cells.* Stem Cells Dev, 2012. **21**(12): p. 2160-9 DOI: 10.1089/scd.2011.0670.
241. Chen, X., et al., *Juglanin inhibits IL-1β-induced inflammation in human chondrocytes.* Artificial Cells, Nanomedicine, and Biotechnology, 2019. **47**(1): p. 3614-3620 DOI: https://doi.org/10.1080/21691401.2019.1657877.

242. Hosseinzadeh, A., et al., *Protective Effect of Ginger (Zingiber officinale Roscoe) Extract against Oxidative Stress and Mitochondrial Apoptosis Induced by Interleukin-1β in Cultured Chondrocytes.* Cells Tissues Organs, 2017. **204**(5-6): p. 241-250 DOI: https://doi.org/10.1159/000479789.
243. Wu, C.-C., et al., *Evaluation of the post-treatment anti-inflammatory capacity of osteoarthritic chondrocytes: An in vitro study using baicalein.* Regenerative Therapy, 2020. **14**: p. 177-183 DOI: https://doi.org/10.1016/j.reth.2020.02.002.
244. Caramés, B., et al., *Differential effects of tumor necrosis factor-α and interleukin-1β on cell death in human articular chondrocytes.* Osteoarthritis and Cartilage, 2008. **16**(6): p. 715-722 DOI: https://doi.org/10.1016/j.joca.2007.10.006.
245. López-Armada, M.J., et al., *Cytokines, tumor necrosis factor-α and interleukin-1β, differentially regulate apoptosis in osteoarthritis cultured human chondrocytes.* Osteoarthritis and Cartilage, 2006. **14**(7): p. 660-669 DOI: https://doi.org/10.1016/j.joca.2006.01.005.
246. Schuerwegh, A.J., et al., *Influence of pro-inflammatory (IL-1α, IL-6, TNF-α, IFN-γ) and anti-inflammatory (IL-4) cytokines on chondrocyte function.* Osteoarthritis and Cartilage, 2003. **11**(9): p. 681-687 DOI: https://doi.org/10.1016/S1063-4584(03)00156-0.
247. Li, X., et al., *Morphological, Immunocytochemical, and Biochemical Studies of Rat Costal Chondrocytes Exposed to IL-1β and TGF-β1.* Journal of Healthcare Engineering, 2017. **2017**: p. 9747264 DOI: https://doi.org/10.1155/2017/9747264.
248. Yang, G., et al., *Polydatin reduces IL-1β-induced chondrocytes apoptosis and inflammatory response via p38 MAPK signaling pathway in a rat model of osteoarthritis.* International Journal of Clinical and Experimental Medicine, 2017. **10**: p. 2263-2273.
249. Fan, Z., et al., *Activation of interleukin-1 signaling cascades in normal and osteoarthritic articular cartilage.* The American journal of pathology, 2007. **171**(3): p. 938-946 DOI: 10.2353/ajpath.2007.061083.
250. Little, C.B., et al., *Cytokine induced metalloproteinase expression and activity does not correlate with focal susceptibility of articular cartilage to degeneration.* Osteoarthritis Cartilage, 2005. **13**(2): p. 162-70 DOI: 10.1016/j.joca.2004.10.014.
251. Kelly, N.A., et al., *Solvent extraction of bacteriocins from model solutions and fermentation broths.* Journal of Chemical Technology & Biotechnology, 2000. **75**(9): p. 777-784 DOI: https://doi.org/10.1002/1097-4660(200009)75:9<777::AID-JCTB290>3.0.CO;2-0.
252. Pfalzgraff, A., K. Brandenburg, and G. Weindl, *Antimicrobial Peptides and Their Therapeutic Potential for Bacterial Skin Infections and Wounds.* Frontiers in Pharmacology, 2018. **9**(281) DOI: https://doi.org/10.3389/fphar.2018.00281.
253. Thangamani, S., et al., *Antibacterial activity and therapeutic efficacy of Fl-P(R)P(R)P(L)-5, a cationic amphiphilic polyproline helix, in a mouse model of staphylococcal skin infection.* Drug design, development and therapy, 2015. **9**: p. 5749-5754 DOI: https://doi.org/10.2147/DDDT.S94505.

254. Nieminen, H.J., et al., *Localized delivery of compounds into articular cartilage by using high-intensity focused ultrasound.* Scientific Reports, 2019. **9**(1): p. 15937 DOI: https://doi.org/10.1038/s41598-019-52012-z.

8. SUPPLEMENTARY INFORMATION

Annex 1

Table 3 – Information about the formulations of the tested nanoparticles and nanoemulsions. NPs – Nanoparticles; NEs – Nanoemulsions; PLGA – Poly(Lactic-Co-Glycolic Acid); Ch – Chitosan; PGA – Polyglutamic Acid; BB-94 – Batimastat.

NANOCARRIER	DRUG	STOCK SOLUTION	MANUFACTURER
PLGA NPS	IBUPROFEN	**10 mg/mL** of **NPs** with **1.5 mg/mL** of **ibuprofen** encapsulated	INEB
CHITOSAN NPS	IBUPROFEN	**300 μg/mL** of **NPs** with **0.5 mg/mL** of **ibuprofen** encapsulated	INEB
NES	BB-94 (FORMULATION 1)	**100 mg/mL** of **NEs** with **0.76 μg/mL** of **BB-94** encapsulated	CIDETEC
	BB-94 (FORMULATION 2)	**50 mg/mL** of **NEs** with **19 μg/mL** of **BB-94** encapsulated	
	IBUPROFEN, BB-94, NISIN	**100 mg/mL** of **NEs** with **1.2 mg/mL** of **ibuprofen**, **0.76 μg/mL** of **BB-94** and **6 mg/mL** of **nisin** incorporated	
	MUPIROCIN	**50 mg/mL** of **NEs** with **6 mg/mL** of **mupirocin** encapsulated	

Annex 2

This annex refer to an abstract selected for poster presentation at the 31st Conference of the European Society for Biomaterials (ESB2021), which will take place in September 5-9, 2021.

Chondroprotective effects of ibuprofen-loaded PLGA nanoparticles in a pro-inflammatory condition

Cecília J. Alves [1,2]; Alexandra Freitas[1,2,3]; Marina Couto [1,2,3]; Beatriz Sousa[1,2,3]; Daniela P. Vasconcelos [1,2]; Catarina L. Pereira [1,2]; Bruno Sarmento [1,2,4]; Raquel Gonçalves [1,2,3] and Meriem Lamghari [1,2,5]

1 - i3S – Instituto de Inovação e Investigação em Saúde, Universidade do Porto, Rua Alfredo Allen, 208, 4200-125 Porto, Portugal
2 - INEB – Instituto de Engenharia Biomédica, Rua Alfredo Allen, 208, 4200-125 Porto, Portugal
3 - ICBAS- Instituto Ciências Biomédicas Abel Salazar, Universidade do Porto, Rua Jorge de Viterbo Ferreira 228, 4050-313 Porto, Portugal
4 - CESPU- Instituto de Investigação e Formação Avançada em Ciências e Tecnologias da Saúde, Rua Central de Gandra, 1317, 4585-116 Gandra, Portugal

Traumatic chondral lesions are common in the young and active population, and if left untreated can evolve towards osteoarthritis. The inflammatory response initiated as a consequence of tissue damage imposes a major challenge in cartilage repair. The released pro-inflammatory factors induce a shift in chondrocytes activity towards a catabolic metabolism and promote further cartilage degradation (1-2). Several anti-inflammatory drugs have been proved to mitigate the deleterious effects of inflammation on cartilage (2), and we propose the use of Poly(lactic-co-glycolic acid) (PLGA) nanoparticles loaded with ibuprofen as a strategy to delivered locally an anti-inflammatory treatment.

In this work, we aimed to evaluate the chondroprotective and chondrogenic effects of the ibuprofen-loaded PLGA nanoparticles. To achieved this, human chondrocytes cultured as 3D pellets under an inflammatory condition (stimulation with 100ng/mL of IL-1β), were treated with PLGA nanoparticles loaded with 15 or 30 μg/mL of ibuprofen. Effects on the chondrocyte activity were assessed at day 3 of exposure.

The results show that nanoparticles loaded with 15 and 30 μg/mL of ibuprofen induce, under inflammatory conditions, a decrease in the IL-1β release and mRNA expression levels of metalloprotease, such as MMP1 and MMP8, at day 3 and 7 after the addition of ibuprofen-loaded nanoparticles. Moreover, data from the immunohistochemical analysis showed higher expression of collagen type II and aggrecan 3 days after treatment.

Altogether the obtained data suggest that treatment with ibuprofen-loaded PLGA nanoparticles mitigates the chondrocytes' pro-inflammatory response and extracellular matrix degradation activity induced in an inflammation scenario.

Acknowledgements

This study was supported by European Union´s Horizon 2020 research and innovation program under grant agreement number 814558 project RESTORE.

References:

1. van der Kraan PM. The Interaction between Joint Inflammation and Cartilage Repair." Tissue Eng Regen Med 16(4): 327-334, 2019.
2. Zhang Y, Pizzute T, Pei M. Anti-inflammatory strategies in cartilage repair. Tissue Eng Part B Rev 20(6): 655-668, 2014.